CRISTALOGRAFIA BIOLÓGICA

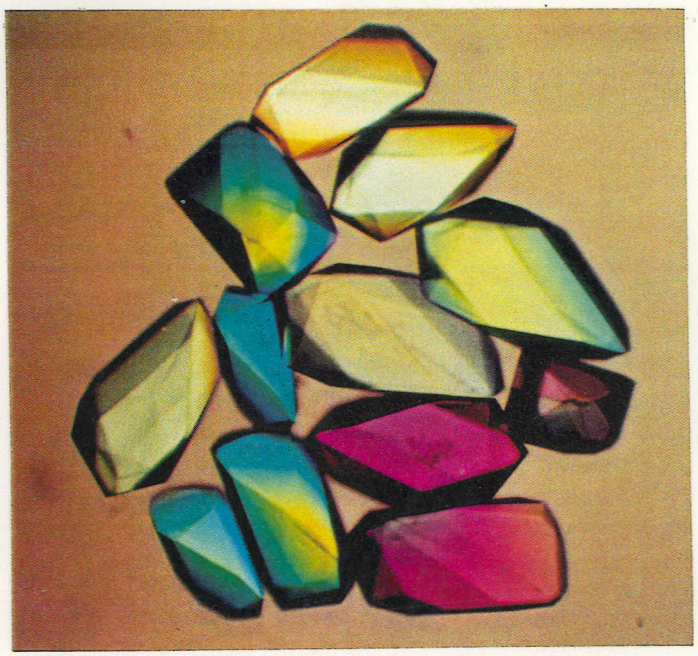

Texto que sistematiza o trabalho científico do candidato para a obtenção do título de Livre Docência

OK.
USP / IFQSC / SBI
8-2-001008

Prof.Dr. Glaucius Oliva

Departamento de Física e Ciência dos Materiais
Instituto de Física e Química de São Carlos
UNIVERSIDADE DE SÃO PAULO

Agosto, 1993

SERVIÇO DE BIBLIOTECA E INFORMAÇÃO - IFQSC
FÍSICA

ÍNDICE

Agradecimentos . . . . . -3-

I. Introdução . . . . . -4-

II. Glucosamina-6-Fosfato Deaminase . . . . . -7-

II.1 Introdução . . . . . -7-

II.2 Cristalização, caracterização dos cristais, coleta de dados de difração por monocristais da proteína nativa e determinação da simetria não-cristalográfica. Trabalho publicado no *Journal of Molecular Biology* -8-

II.3 Preparação de Derivados Isomorfos de Átomos Pesados . . . . . -15-

II.4 Interpretação do Mapa de Densidade Eletrônica . . . . . -23-

III. Proteína Sérica Humana Componente P de Amilóide . . . . . -28-

III.1 Introdução . . . . . -28-

III.2 Trabalhos publicados no *Journal of Molecular Biology*, *Journal of Crystal Growth*, capítulo no livro *Acute Phase Proteins in the Acute Phase Response* e trabalho submetido à *Nature* . . . . . -29-

IV. Métodos em Cristalografia de Proteínas . . . . . -81-

IV.1 Introdução . . . . . -81-

IV.2 Trabalho publicado no *Journal of Applied Crystallography* . . . . . -82-

V. Proteínas de Armazenamento em Sementes: Coixinas . . . . . -87-

V.1 Introdução . . . . . -87-

V.2 Trabalho publicado em *Proteins: Structure Function and Evolution.* -89-

VI. Estruturas de Moléculas Pequenas . . . . . -102-

VI.1 Introdução . . . . . -102-

VI.2 Complexos de Rutênio com Potenciais Propriedades Anti-tumorais. Trabalhos publicados em *Inorganica Chimica Acta* (2 trabalhos publicados, 1 submetido), *Journal of Coordination Chemistry* (2 trabalhos aceitos), *Polyhedron* (submetido) . . . . . -104-

VI.3 Outras estruturas. Trabalhos em *Inorganica Chimica Acta* (1 publicado e 2 submetidos) e *Acta Crystallographica* (7 trabalhos publicados) . . . . . -141-

Agradecimentos

Pela característica interdisciplinar da área de Cristalografia, o trabalho científico descrito neste texto envolve colaboração com diversos participantes nos projetos apresentados. A todos os co-autores dos trabalhos compreendidos nesta resenha, meus sinceros agradecimentos. Em especial gostaria de agradecer aos colegas do Grupo de Cristalografia Prof. Eduardo Castellano e Profª Yvonne Mascarenhas pela inestimável colaboração e estímulo e particularmente ao Prof. Richard Garratt, que conosco aceitou o desafio de estabelecer um laboratório de Cristalografia de Proteínas no Brasil. Durante estes anos pudemos contar com o apoio dos pesquisadores associados a nosso grupo Drª Ignez Caracelli do CENARGEN/EMBRAPA, Prof. Eduardo Horjales da Universidad de la República, Uruguai, e Prof.Júlio Zukerman-Schpector da Universidade Federal de São Carlos, aos quais agradeço também.

Com especial carinho gostaria de agradecer a todos os alunos do Grupo de Cristalografia, que em nós confiaram quando de sua escolha de orientação, e sem os quais este trabalho não poderia ter sido realizado.

Também é fundamental agradecer aos colegas Maria Helena B. de Carvalho, José Geraldo Catarino, José Augusto da Rocha e Wanda Draghetta P. de Jesus pelo inestimável apoio técnico, paciência e presteza no atendimento de nossos projetos.

Finalmente, agradeço a minha esposa Lívia e filhos Maria Amélia e Ciro pelo apoio, incentivo e sobretudo paciência e compreensão pelas frequentes horas de ausência familiar decorrentes da atividade científica.

I. Introdução

Os fenômenos da natureza associados à Vida constituem talvez a última grande fronteira do conhecimento humano ainda em grande parte intocada pela Física. A alta complexidade associada aos organismos biológicos é certamente a razão principal pela qual as chamadas Ciências da Vida adotaram, ao longo de sua história, uma abordagem sistêmica na descrição e análise dos problemas envolvidos. Este panorama modificou-se drasticamente nos últimos anos, com o florescimento de novas técnicas experimentais tanto físicas quanto bioquímicas e biológicas, que permitem a interação sistemática e racional com a Matéria Viva. O ímpeto para esta nova abordagem da pesquisa biológica deve-se ao reconhecimento universal de que a chave para o entendimento da biologia encontra-se nas estruturas moleculares e supramoleculares dos sistemas vivos. Por vários séculos os assim chamados "filósofos naturais" buscaram a compreensão do comportamento e função na forma que podia ser observada com a visão comum. Mais recentemente com o advento dos microscópios ópticos e, neste século, com o microscópio eletrônico, a pesquisa estendeu-se ao domínio da organização celular e subcelular. Hoje em dia, com as cada vez mais sofisticadas ferramentas da Física, esta visão alcança os níveis de moléculas e átomos.

Observa-se assim uma gradual transição da Biologia Clássica para a Biologia Molecular, na completa acepção desta denominação, qual seja a Ciência da Vida à nível molecular que busca entender os fenômenos biológicos na escala atômica.

Dentre as váriadas ferramentas da Física que possibilitam o conhecimento em detalhe das estruturas das moléculas da vida a nível atômico, a técnica de Difração de Raios-X por monocristais destes materiais tem tido papel preponderante. Até a presente data, a quase totalidade da informação acumulada sobre o arranjo tridimensional de átomos em proteínas, ácidos nucleicos (DNA e RNA) e vírus foi obtida através de métodos cristalográficos.

Cerca de 60 anos se passaram desde que os primeiros monocristais de proteínas foram obtidos por Sumner (enzima ureasa) e Northrop & Herriot (pepsina, tripsina e quimotripsina). Depois disso, foram necessários 30 anos até ser produzido, por técnicas de difração de raios-X, o primeiro mapa de densidade eletrônica à baixa resolução de uma proteína, a mioglobina de baleia (Kendrew et al., 1958, Nature, **181**, 662), logo seguido pelo mapa à baixa resolução da hemoglobina (Perutz et al., 1960, Nature, **185**, 416), feito que valeu o Prêmio Nobel à estes autores. Desde então cerca de 800 estruturas de proteínas foram determinadas a média

e alta resolução e a informação estrutural acumulada até o momento é a responsável maior pelo nosso entendimento presente das bases moleculares da atividade biológica.

Pela qualidade e precisão dos resultados obtidos, a Cristalografia de Proteínas tornou-se central para a Enzimologia, a Biologia Molecular e a Imunologia, devido à sua capacidade única de produzir modelos estruturais detalhados de macromoléculas, em termos das coordenadas de seus átomos. Além disso, quando combinada com os recentes desenvolvimentos na caracterização e produção de novas proteínas por técnicas de recombinação do DNA e engenharia genética, a Cristalografia de Proteínas juntamente com as técnicas de predição de estruturas e computação gráfica molecular, são as ferramentas básicas para a análise racional do desenvolvimento de novas drogas e vacinas, bem como para a engenharia de proteínas inéditas.

A importância da informação estrutural sobre macromoléculas, como a obtida por difração de raios-X em monocristais, é enfatizada pelo crescente interesse na área, acompanhado por um espetacular aumento no investimento de recursos que os governos dos países do primeiro mundo, através de seus órgãos financiadores de pesquisas e de suas instituições de pesquisa e acadêmicas, juntamente com todas as grandes indústrias químicas, farmacológicas e de biotecnologia, tem feito. Sem dúvida os próximos anos assistirão a uma explosão nas aplicações da biotecnologia nas áreas médica, tecnológica e industrial, talvez comparável apenas à grande explosão nas aplicações da micro-eletrônica na presente década.

Todas as indústrias farmacêuticas, biotecnológicas e de química fina têm hoje laboratórios próprios de Cristalografia de Macromoléculas, e cada vez mais as informações estruturais obtidas nestes laboratórios vêm sendo tratadas com sigilo industrial. Países que se distanciarem muito dos avanços que ora se fazem neste ramo do conhecimento correm o risco de se tornarem dependentes em áreas estratégicas como a produção de alimentos, de materiais e processos industriais especiais.

Dentro deste contexto se insere o trabalho que esta Introdução vem a preceder. Apresentamos, de forma sistematizada, o resultado do trabalho que desenvolvemos nos últimos cinco anos, período em que nos propusemos a estabelecer, no Departamento de Física e Ciência dos Materiais do IFQSC/USP, o primeiro laboratório na América Latina com competência, recursos humanos e equipamentos, para fazer pesquisa competitiva em Cristalografia de Proteínas e Biologia Estrutural.

No Capítulo II é descrito nosso trabalho com a enzima Glucosamina-6-Fosfato Deaminase, da bactéria *Escherichia coli*, a primeira proteína cristalizada no Brasil, e cuja estrutura tridimensional, completamente determinada em nosso laboratório pela técnica de substituição isomorfa de átomos pesados, está em fase final de refinamento.

No Capítulo III apresentamos os trabalhos relativos à determinação da estrutura da proteína sérica humana denominada Componente P de Amilóide, um pentâmero de peso molecular 123000 daltons. Esta proteína sérica apresenta singular afinidade de ligação à cromatina, deslocando seletivamente a histona H1. Também está associada a doenças como Amiloidose e Doença de Alzheimer. Esta proteína foi cristalizada e sua análise estrutural iniciada durante meu doutoramento no Birkbeck College, University of London. Continuamos a colaborar com o grupo do Prof. Tom Blundell neste projeto e o resultado foi a completa determinação da estrutura, apresentada pelo manuscrito submetido à publicação na revista *Nature*.

No Capítulo IV é apresentado um trabalho desenvolvido na área de Metodologia na determinação de estruturas de proteínas por difração de Raios-X. Este trabalho propõe uma nova ferramenta para a aplicação do método de substituição molecular a qual resultou, em desenvolvimentos posteriores por um dos co-autores do trabalho, no estabelecimento de um conjunto de programas computacionais que constituem o estado da arte na determinação de estruturas de novas proteínas nos casos em que há proteínas homólogas com estrutura conhecida.

No Capítulo V é abordado um problema de interesse à biotecnologia na agricultura, com o estudo estrutural de proteínas de reserva de sementes de plantas. Em particular é descrito o trabalho de modelagem molecular de proteínas do tipo Prolaminas da semente de Coix, um membro da família do milho e sorgo.

No capítulo VI são apresentados diversos trabalhos de determinação de estruturas de moléculas pequenas, várias das quais com interesse biológico e farmacológico. Em particular algumas estruturas de complexos de rutênio com potencias propriedades antitumorais são descritas.

II. Glucosamina-6-fosfato Deaminase

Neste capítulo descrevemos a cristalização e determinação estrutural da enzima Glucosamina-6-Fosfato Deaminase de *Escherichia coli*. Esta enzima, cujas características e interesse são descritos abaixo, resultou ser a primeira proteína inédita cristalizada no Brasil. As amostras de proteína purificada foram fornecidas pelo Prof. Mario Calcagno, da Universidade Nacional Autônoma do México, e posteriormente cristalizadas e estudadas cristalograficamente em nosso laboratório. A estrutura foi determinada pelo método clássico da Substituição Isomorfa de Átomos Pesados. Os mapas de densidade eletrônica obtidos permitiram a identificação do caminho da cadeia principal e da maioria das cadeias laterais. A seguir apresentamos suscintamente os principais resultados que levaram à determinação da estrutura. O refinamento completo à alta resolução do modelo estrutural está em andamento e será discutido quando da defesa oral deste trabalho.

A completa determinação desta estrutura implicou no desenvolvimento de competência em todas as etapas críticas na técnica cristalográfica: processos bioquímicos de preparação, caracterização e análise de proteínas; cristalização de amostras biológicas; coleta e processamento dos dados de difração; preparação e análise de derivados isomorfos de átomos pesados; cálculo de fases dos fatores de estrutura; interpretação dos mapas de densidade eletrônica; refinamento da estrutura a alta resolução.

II.1 Introdução

Em muitas espécies, amino-açúcares tem uma função específica tanto como unidade estrutural quanto como fonte de energia. Amino-açúcares são componentes essenciais das paredes celulares e dos lipo-polissacarídeos e, na ausência de amino-açúcares exógenos no meio, é induzida a expressão de glucosamina sintetase para sintetizar glucosamina (GlcN) a partir de glutamina e D-frutose-6-fosfato (Fru6P). Por outro lado o crescimento bacteriano na presença de amino-açúcares como N-acetil-glucosamina (GlcNac) e GlcN induz a expressão das enzimas necessárias para o seu metabolismo à Fru6P e daí à via glicolítica (White, 1968; Plumbridge, 1991).

Glucosamina-6-fosfato deaminase catalisa a conversão reversível de D-glucosamina-6-fosfato (GlcN6P) em D-fructose-6-fosfato (Fru6P) e amônia. A reação catalisada é uma

isomerização tipo aldose-cetona acoplada com uma aminação-deaminação, o chamado rearranjo de Amadori (Hodge, 1955). A enzima, que tem sido identificada em vários outros microorganismos e tecidos animais (Noltmann, 1972), quando purificada de *Escherichia coli* B (EC 5.3.1.10) resulta ser um homopolímero hexamérico com subunidades de 29.7kDa, exibindo uma intensa cooperatividade homotrópica modulada por (GlcNAc6P) (Calcagno *et al.*, 1984; Altamirano *et al.*, 1987). O gene que codifica a glucosamina-6-fosfato deaminase foi identificado, clonado e sequenciado (Rogers *et al.*, 1988; Plumbridge 1989) e uma linhagem que sobre-produz a enzima foi obtida por Altamirano *et al.* (1991). Uma busca na base de dados de sequências **OWL** (Bleasby & Wootton, 1990) (34000 entradas), mostrou que não existe homologia significativa com qualquer outra família de proteínas conhecida. A previsão da estrutura secundária baseada na sequência de aminoácidos e apoiada por espectroscopia de dicroismo circular (Altamirano *et al.*, 1991), sugere que a enzima possui uma estrutura α/ß dominante. Dos quatro resíduos Cys na sequência, dois são tituláveis com a enzima no seu estado nativo e outro com a cadeia aberta pela presença de SDS. O quarto resíduo Cys é exposto só sob condições de redução, o que levou aos autores que estudaram a caracterização bioquímica da proteína a sugerir a presença de uma ponte dissulfeto entre cadeias (Altamirano *et al.*, 1992), resultado este não confirmado pelos nossos estudos cristalográficos.

II.2 Cristalização, caracterização dos cristais, coleta de dados de difração por monocristais da proteína nativa e determinação da simetria não-cristalográfica. Publicação no *Journal of Molecular Biology.*

Estes resultados estão apresentados no trabalho a seguir. A Figura II.1 mostra alguns cristais de glucosamina-6-fosfato deaminase.

HORJALES,E., ALTAMIRANO,A.A., CALCAGNO,M., DAUTER,Z., WILSON,K, GARRATT,R.C and **OLIVA, G.**

"Crystallization and Preliminary Crystallographic Studies of Glucosamine-6-Phosphate Deaminase from *Escherichia coli* K12."

J.Mol.Biol., **226**, 1283-1286, 1992.

Figura II.1 Cristais de Glucosamina-6-fosfato deaminase.

De acordo com as políticas editoriais, este artigo não pode ser depositado em repositório de acesso aberto. Para acesso ao artigo completo entre em contato com o(a) autor(a) ou com o Serviço de Biblioteca e Informação IFSC - USP (bib@ifsc.usp.br)

HORJALES, E.; ALTAMIRANO, M. M.; CALCAGNO, M. L.; DAUTER, Z.; WILSON, K.; GARRATT, R. C.; OLIVA, G. Crystallization and preliminary crystallographic studies of glucosamine-6-phosphate deaminase from *Escherichia coli* K12. **Journal of Molecular Biology**, New York, v.226, p.1283-6, 1992

II.3 Preparação de Derivados Isomorfos de Átomos Pesados.

O mais importante e frutífero método desenvolvido para a solução do problema das fases na determinação de estruturas macromoleculares por difração de raios-X é o método da Substituição Isomorfa Múltipla (**MIR**). Inicialmente proposto por Perutz e colaboradores na determinação da estrutura da hemoglobina (Green *et al.*, 1954), o método MIR tem sido utilizado para resolver a maioria das estruturas de proteínas determinadas cristalograficamente.

O método consiste na introdução de átomos pesados na matriz cristalina. Os átomos pesados deveriam idealmente substituir um grupo "leve", usualmente uma molécula de solvente, sem introduzir modificações significativas na estrutura da própria proteína. Esta ligação deve ser específica de forma que os átomos pesados liguem-se identicamente em todas as moléculas de proteína do cristal.

O processo de determinação de fases dos fatores de estrutura da proteína nativa à partir das amplitudes de difração dos cristais nativo e derivados está resumido na Figura II.2 abaixo. Sejam $\mathbf{F_P}$ e $\mathbf{F_{PH}}$ os fatores de estrutura complexos dos cristais de proteína nativa e derivado isomorfo para uma dada reflexão **hkl** e $\mathbf{F_H}$ a contribuição dos átomos pesados ao espalhamento. O relacionamento entre estas grandezas complexas, expresso pela igualdade $\mathbf{F_{PH} = F_P + F_H}$, está representado no diagrama de Argand da Figura II.2.

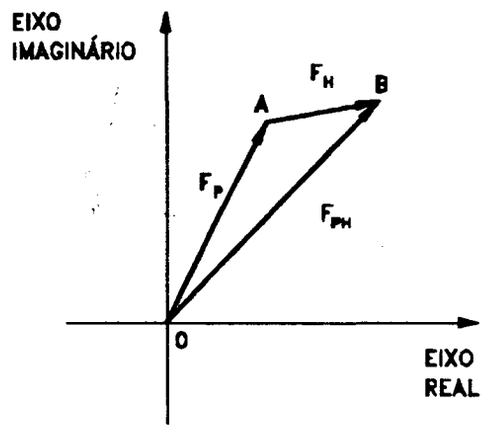

Figura II.2 Relação entre os vetores $\mathbf{F_P}$, $\mathbf{F_{PH}}$ e $\mathbf{F_H}$ para uma dada reflexão (o "triângulo de fases") (Blundell & Johnson, 1976).

Tendo medido as amplitudes F_P e F_{PH} em experimentos de difração e supondo possível a determinação das posições dos átomos pesados na cela unitária do cristal (i.e., $\mathbf{F_H}$ pode ser calculado em módulo e fase) então a construção gráfica representada na Figura II.3 pode ser utilizada para a determinação das fases dos fatores de estrutura da proteína nativa α_P. A ambiguidade resultante na determinação de α_P (vetores OG e OH na Figura II.3 são soluções possíveis) pode ser resolvida se um segundo derivado isomorfo for utilizado, como mostrado na Figura II.4. Uma descrição completa do método da Substituição Isomorfa Múltipla encontra-se no livro texto de Blundell & Johnson (1976).

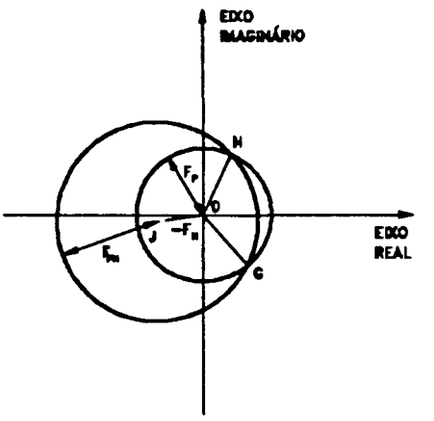

Figura II.3 A construção de Harker para a determinação de fases pelo método de Substituição Isomorfa Simples.

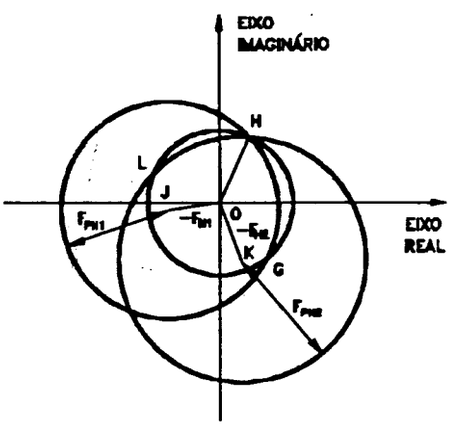

Figura II.4 A construção de Harker para a determinação de fases pelo método de Substituição Isomorfa Múltipla com dois derivados.

Devido à falta de homologia da Glucosamina-6-fosfato deaminase com qualquer outra família de proteínas conhecida, a resolução da estrutura molecular foi realizada pelo método de Substituição Isomorfa Múltipla.

A preparação de derivados isomorfos de átomos pesados se faz pela técnica de difusão em solução: cristais de proteína nativa previamente obtidos são acondicionados em soluções identicas à solução de cristalização à qual se adiciona o composto de átomo pesado desejado, como representado na Figura II.5 abaixo.

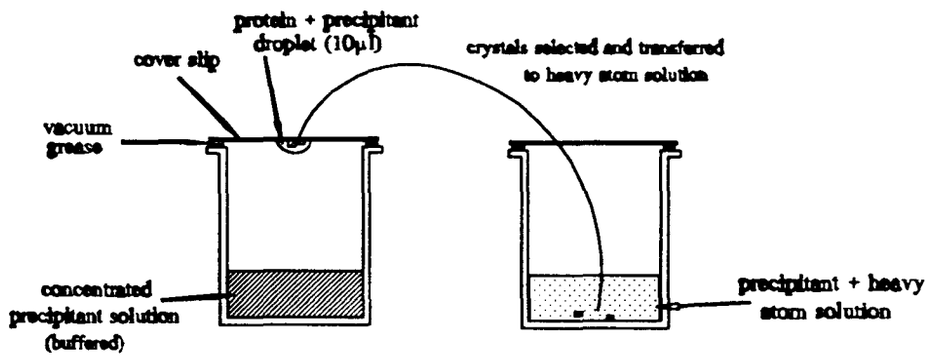

Figura II.5 Representação esquemática do método de preparação de derivados isomorfos pela técnica de difusão em solução.

Pela natureza do empacotamento cristalino de macromoléculas, canais de solvente se formam ao longo do cristal, os quais constituem o caminho pelo qual a difusão se processa. Cadeias laterais de aminoácidos polares frequentemente encontram-se expostas aos canais de solvente e, em casos favoráveis, apresentam configuração espacial que favorece a ligação específica de átomos pesados. Encontrar o átomo pesado ideal para a preparação dos derivados isomorfos implica numa busca sistemática com o procedimento cíclico representado na Figura II.6.

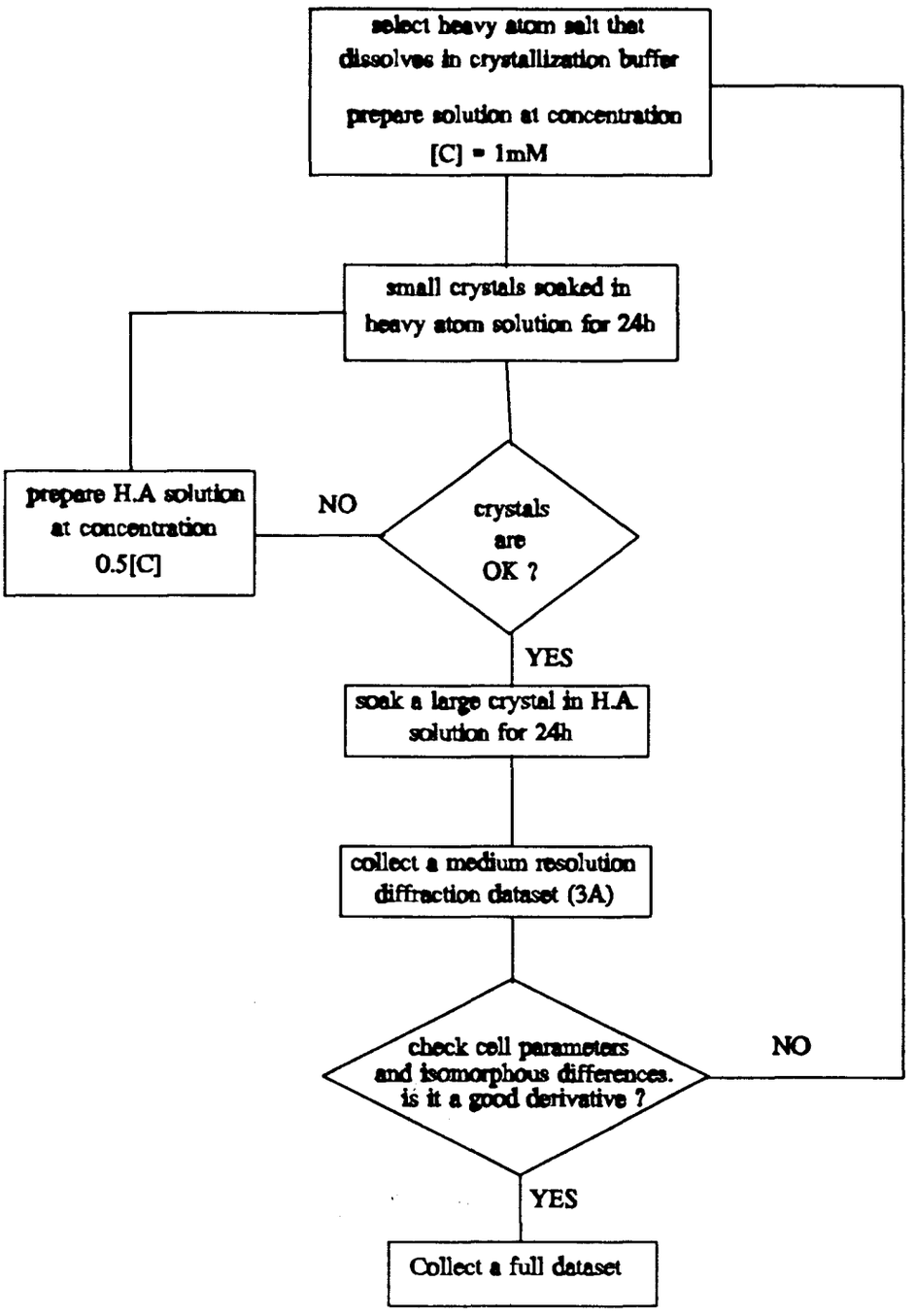

Figura II.6 Procedimento cíclico para a busca sistemática de derivados isomorfos de átomos pesados de cristais de proteínas.

Seguindo o procedimento acima foram obtidos dois derivados, com os compostos K_2PtCl_4 Mersalyl. As condições ideais estão sumarizadas na tabela abaixo.

	Tetracloro-platinato de potássio	Mersalyl
Fórmula química	K_2PtCl_4	$C_{13}H_{17}HgNO_6$
Concentração	1 mM	0.1 mM
Tempo de Difusão	48h	24h
Temperatura	18 °C	18 °C
Solução tampão	Fosfato de Na/K 1.2M	Fosfato de Na/K 1.2M
pH	8.2	8.2

Todas as coletas de dados de difração, tanto à baixa resolução durante o procedimento de busca sistemática quanto a coleta de dados final à alta resolução foram realizadas no sistema de difração de raios-X para proteínas equipado com gerador de anôdo rotatório e detetor de área com placa de imagens adquirido com apoio de projeto PADCT/SBIO e instalado em nosso laboratório em Dezembro/1992. Este sistema faz uso de um novo tipo de detetor de área para raios-X baseado na capacidade das chamadas Placas de Imagens (Fuji Photo Film, Ltd.) de armazenar intensidades de raios-X como imagens latentes na forma de centros de cor (Takahashi *et al.*, 1984; Takahashi *et al.*, 1985; Amemyia *et al.*, 1987). Estes são o resultado do aprisionamento de elétrons excitados em cristais de $BaFBr:Eu^{2+}$, como indicado na a estrutura de bandas de energia associada ao mecanismo de Luminescência Foto-estimulada nestes cristais, representada na Figura II.7. Por absorção de raios-X ou radiação UV, parte dos íons Eu^{+2} são excitados a Eu^{+3} e elétrons são liberados para a banda de condução, sendo então aprisionados em centros F^+. Por irradiação por luz visível, estes elétrons são novamente liberados para a banda de condução, retornando então ao estado de íons Eu^{+3}, os quais decaem para íons Eu^{+2} excitados produzindo a luminescência. As imagens armazenadas são assim lidas por varredura da placa com um laser de He-Ne. A luminescência estimulada resultante, na cor azul, tem intensidade proporcional ao número de fótons de raios-X absorvidos (Figura II.8). O instrumento é caracterizado por uma alta

eficiência quântica, faixa dinâmica linear e ruído intrínseco muito pequeno, o que o torna ideal para a coleta de dados de cristais de proteínas.

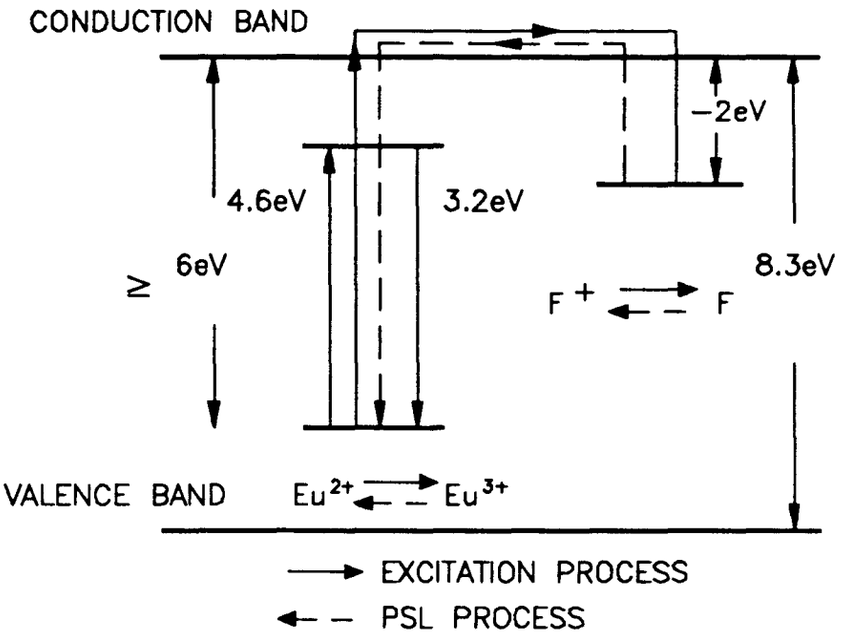

Figura II.7. O mecanismo de luminescência fotoestimulada em BaFBr:Eu^{2+}.

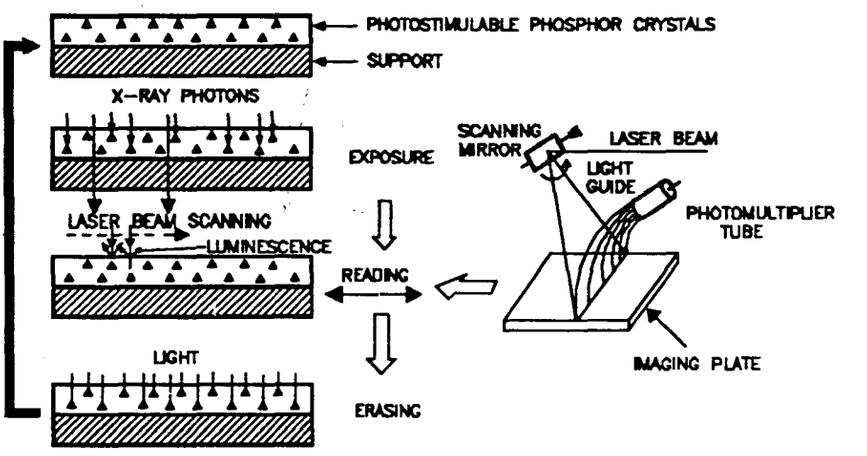

Figura II.8 Representação esquemática do processo de registro da imagem, leitura e regeneração de uma placa de imagens.

A Figura II.9 mostra uma representação esquemática do sistema RAXIS-IIC instalado no nosso laboratório. A configuração padrão utiliza um goniômetro de um único círculo (eixo ϕ) para orientação do cristal. O arranjo com duas placas de imagens permite a exposição e leitura simultâneas. As duas placas são conectadas através de um mecanismo na base do instrumento de forma que quando uma placa é movida em posição para a coleta de dados, a segunda placa é posicionada para ser lida com o conjunto laser/fotomultiplicadora. O arranjo óptico do sistema de leitura é usado tanto para irradiar a placa de imagens com a luz do laser de He-Ne quanto para coletar a luz proveniente da luminescência fotoestimulada. A luminescência emitida por incidência do feixe de laser é convertida em um sinal analógico por um tubo fotomultiplicador. Ao final de cada leitura, a imagem é completamente apagada pela exposição à luz visível intensa. A placa pode então ser utilizada novamente para coletar um novo espectro de difração. O processo completo é controlado automaticamente por um computador e as imagens, inicialmente armazenadas no microcomputador de controle, são transferidas para uma estação gráfica de alta resolução para posterior processamento e análise.

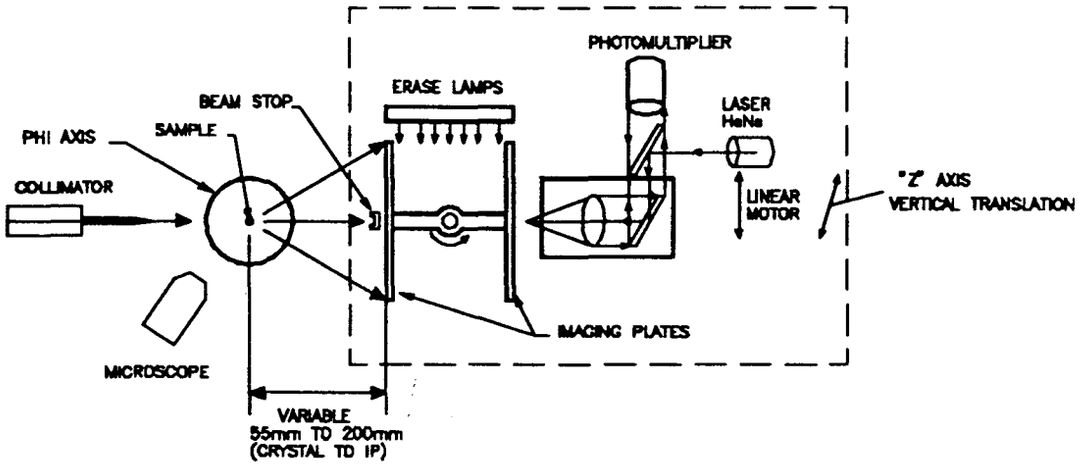

Figura II.9 O sistema Rigaku RAXIS-IIC para coleta de dados de difração de raios-X com detetor de placas de imagens.

Um sumário com os resultados das coletas finais de dados de difração de raios-X de cristais dos derivados isomorfos de K_2PtCl_4 e Mersalyl encontra-se na tabela abaixo.

	Tetracloro platinato de potássio (II)	Mersalyl
Máxima Resolução	2.5Å	3.0Å
Indice de concordância interno	8.2%	≈ 9%
Reflexões Medidas	51,818	-
Reflexões Independentes	22,611	10,327
Completeza dos dados	95.5 %	74.0 %
Diferenças Isomorfas Médias	26.8 %	16.3 %

As posições dos átomos pesados foram determinadas por métodos de superposição de vetores e mapas de Fourier Diferença cruzados. O refinamento dos átomos pesados foi feito no espaço de Patterson utilizando-se somente as diferenças isomorfas. Os parâmetros finais encontrados foram (em coordenadas fracionárias):

	Ocupação	X	Y	Z	B (Å²)
HG	0.4121	0.4953	0.1284	0.0207	20.00
HG	0.4608	0.1787	0.1195	0.0534	20.00
HG	0.2059	0.2124	0.1425	0.0641	20.00
HG	0.2553	0.6197	0.3392	0.0499	20.00
HG	0.2156	0.5181	0.1581	0.0103	20.00
PT	0.7135	0.1101	0.0616	0.1587	20.00
PT	0.6748	0.5744	0.2375	0.1176	20.00
PT	0.5789	0.3944	0.3536	0.0740	20.00
PT	0.6025	0.5123	0.1353	0.1358	20.00
PT	0.5301	0.1679	0.3293	0.1145	20.00
PT	0.5154	0.4654	0.2800	0.1554	20.00
PT	0.3325	0.0347	0.3078	0.0855	20.00

As fases dos fatores de estrutura da proteína foram calculadas pelo método de Substituição Isomorfa Múltipla descrito brevemente acima. A figura de mérito final foi de 0.512 incluindo todos os dados disponíveis até 2.5Å.

II.4 Interpretação do Mapa de Densidade Eletrônica.

O mapa final calculado com amplitudes medidas e fases obtidas por MIR mostra fronteiras claras entre a região da proteína e a região de solvente na cela unitária (Figura II.10). Com o objetivo de melhorar as fases experimentais, aplicou-se o procedimento de nivelamento do solvente (Wang, 1985), no qual a densidade eletrônica da região correspondente ao solvente é igualada a um valor fixo (densidade média prevista para o solvente, conhecidos os reagentes de cristalização) e novas fases são calculadas por anti-transformação de Fourier no mapa modificado.

O mapa resultante, calculado com fases até 2.5Å de resolução, apresentou excelente qualidade, com todos os elementos de estrutura secundária plenamente identificáveis na densidade eletrônica. Na Figura II.11 ve-se partes típicas do mapa de densidade eletrônica para uma região com estrutura de hélice-α (a) e folha ß paralela (b). Este mapa foi interpretado com um modelo atômico e a representação do enovelamento da cadeia proteica encontra-se na Figura II.12. A estrutura consiste essencialmente de uma folha ß paralela de 7 fitas, entrelaças por hélices-α empacotadas sobre as faces superior e inferior da folha ß, numa corformação do tipo $(\alpha/\beta)_{\text{paralela}}$ presente em outras famílias de proteínas como as desidrogenases.

O modelô atômico final esta sendo refinado com os dados completos de difração dos cristais da enzima nativa que se estendem a 2.1Å de resolução.

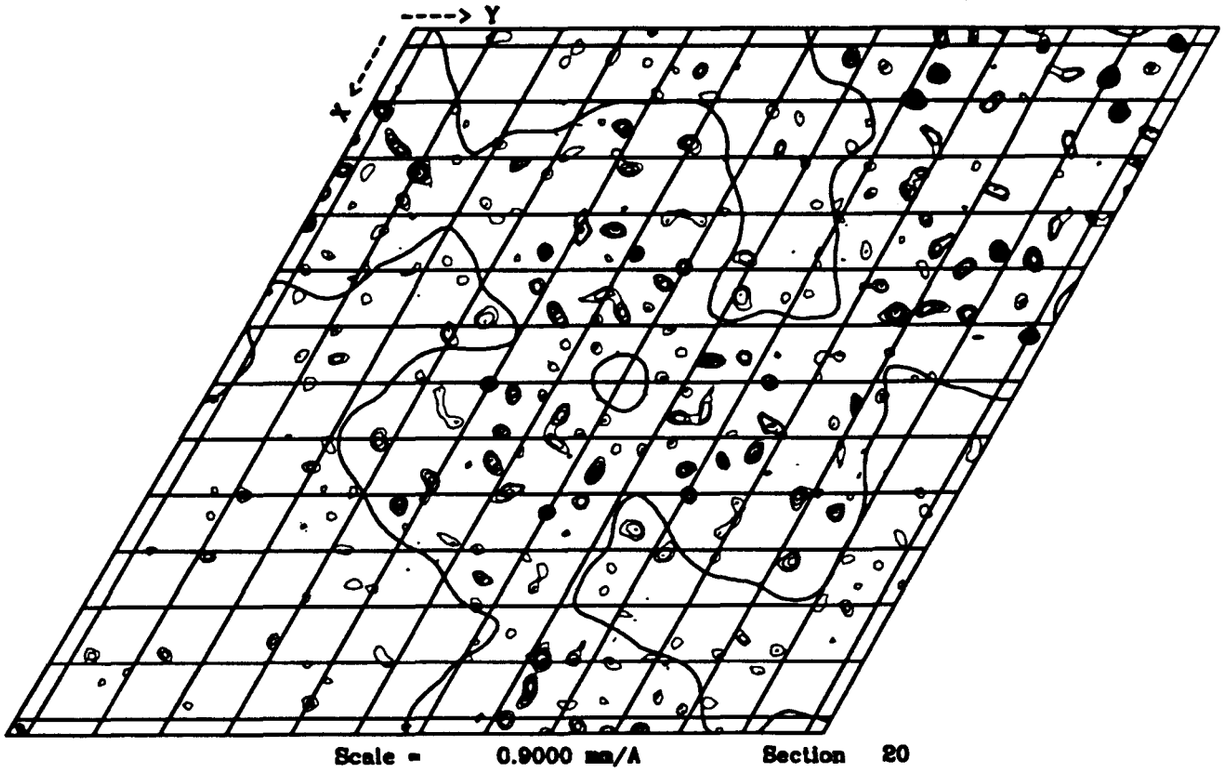

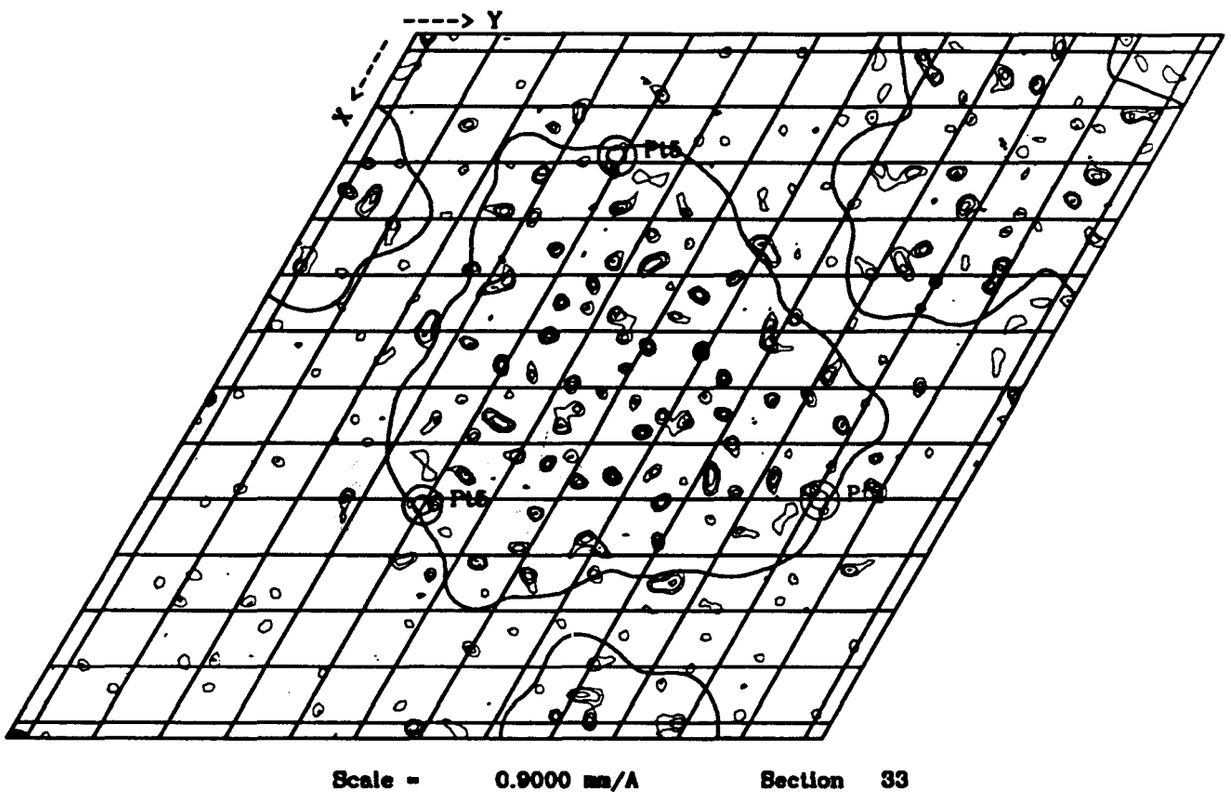

Figura II.10 Duas seçoes típicas do mapa de densidade eletrônica calculado com fases MIR a 3Å de resolução, indicando o envelope molecular utilizado no procedimento de nivelamento do solvente.

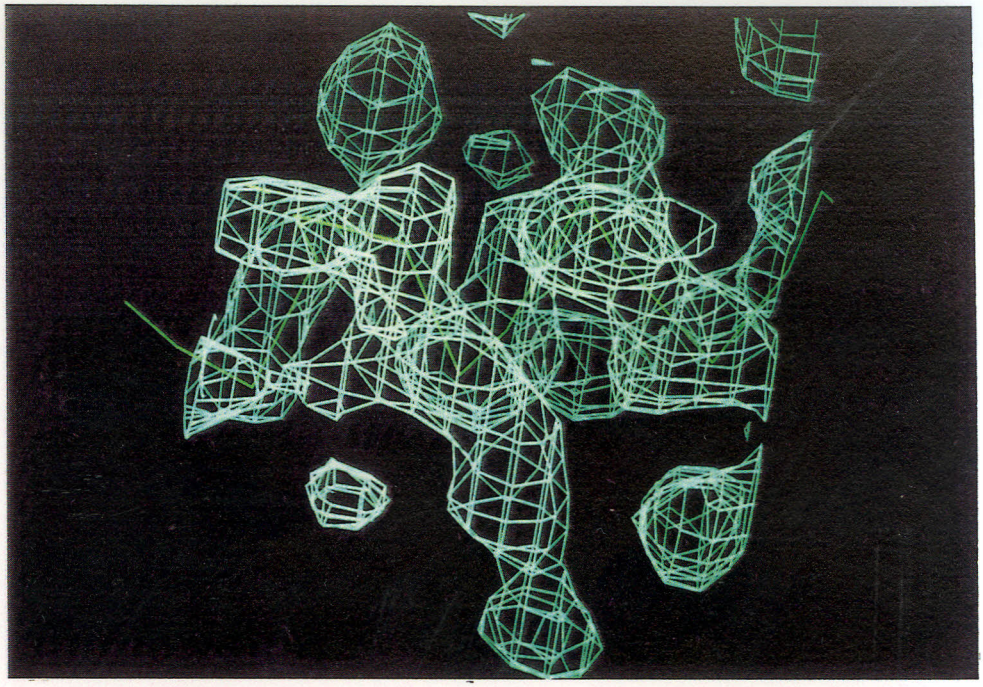

(a)

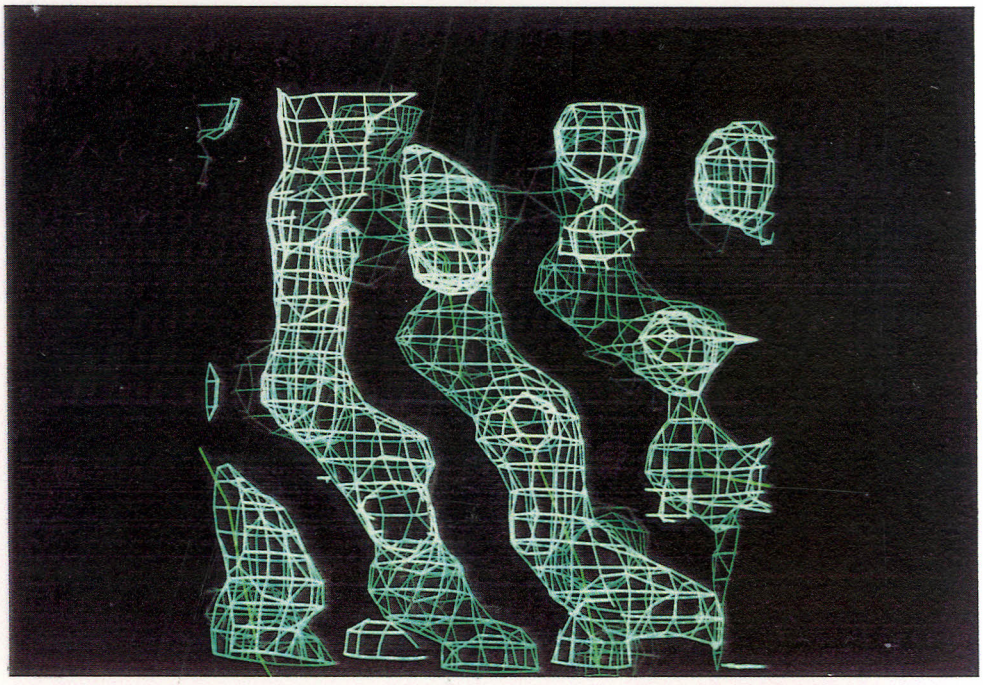

(b)

Figura II.11 Regiões do mapa de densidade eletrônica final correspondentes a elementos de estrutura secundária específicos (a) hélice-α e (b) folha-ß paralela.

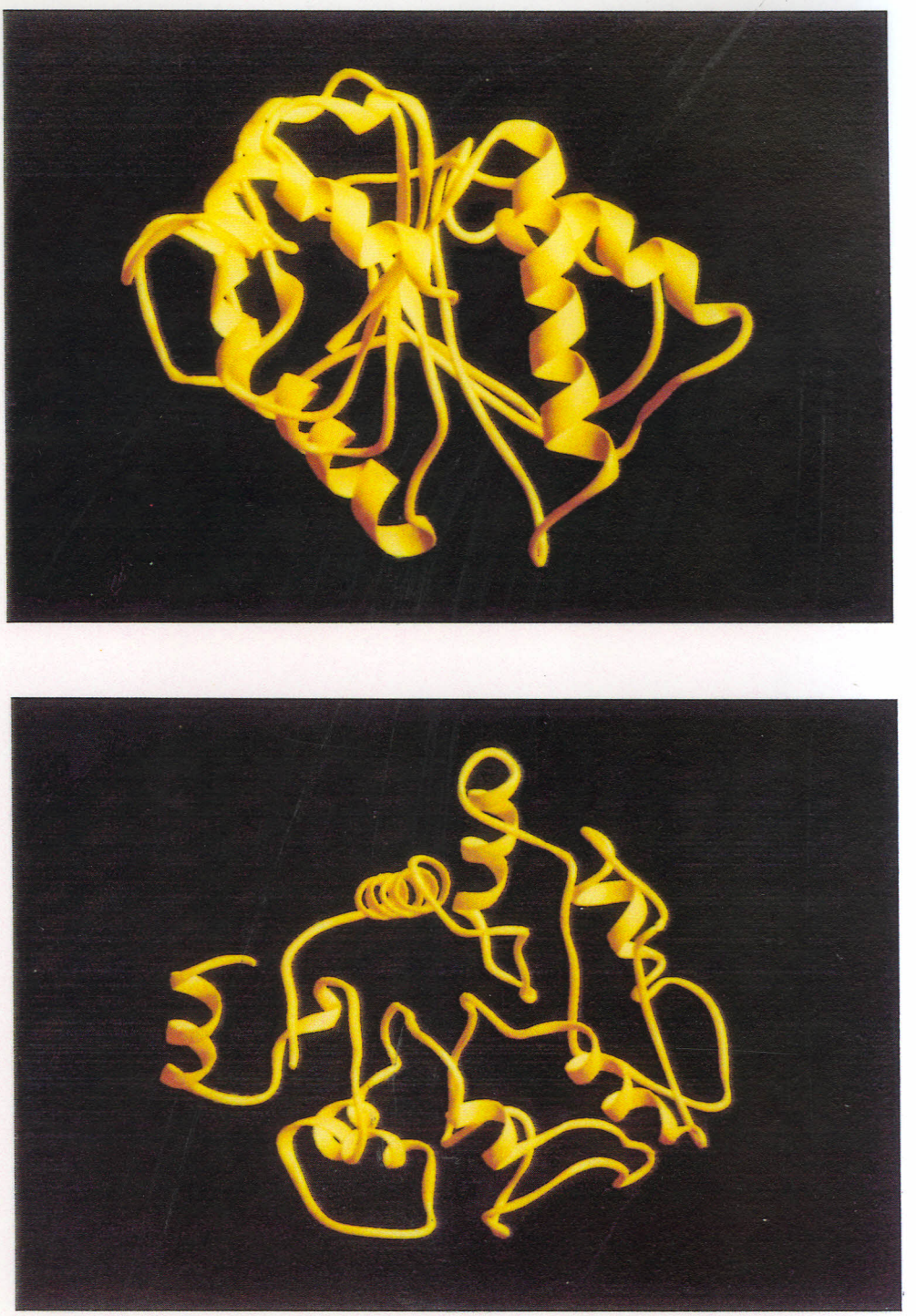

Figura II.12 Enovelamento da cadeia principal do monômero de Glucosamina-6-fosfato deaminase em duas orientações. (Programa *RIBBONS*)

REFERÊNCIAS

Altamirano, M.M., Mulliert, G. and Calcagno,M. (1987). *Arch.Biochem.Biophys.*, **258**, 95-100.

Altamirano, M.M., Plumbridge, J.A., Hérnandez-Arana,A. & Calcagno, M. (1991). *Biochem.Biophys.Acta*, **1076**, 266-272

Altamirano M.M., Plumbridge, J.A. and Calcagno, M. (1992). *Biochemistry*, **31**, 1153-1158.

Amemiya,Y., Kamiya,N., Satow,Y., Matsushita,T., Chikawa,J, Wakabayashi,K., Tanaka,H and Miyahara,J. (1987). in *Biophysics and Synchrotron Radiation*, eds A.Bianconi and A.A.Castellano, Springer-Verlag, Berlin, 61-72.

Bleasby, A. and Wootton, J. (1990). *Protein Eng.*, **3**, 153-159.

Blundell, T.L. & Johnson, L.N. (1976). *Protein Crystallography*, Academic Press, New York.

Calcagno,M., Campos,P.J., Mulliert,G. and Suastegui,J. (1984). *Biochem.Biophys.Acta.* **787**, 165-173.

Green,D.W., Ingram,V.M. & Perutz,M.F. (1954). *Proc. Roy. Soc.*, **A225**, 287.

Hodge, J.E. (1955). *Adv. Carbohydr. Chem.* **10**, 169-205.

Noltmann,E.A. (1972) in *The Enzymes*, 3rd Edn. (Boyer P.D. ed.), Vol.6, 314-318, Academic Press, New York.

Plumbridge, J.A. (1989). *Mol.Microbiol.*, **3**, 506-515.

Plumbridge, J.A. (1991). *Mol.Microbiol.*, **5**, 2053-2062.

Rogers, M.J, Ohgi, T. , Plumbridge, J.A. & Söll, D. (1988). *Gene*, **62**, 197-207.

Takahashi,K., Kohda,K., Miyahara,J., Kanemitsu,Y., Amitani,K. and Shionoya,S. *J.Lumin.*, **31-32**, p266, (1984).

Takahashi, K., Miyahara, J. and Shibahara, Y. (1985). *J. Electrochem. Soc.*, **132**, 1492.

Wang, B.C. (1985). In *Methods in Enzymology*, ed. by Wyckoff, h.W., Hirs, C.H.W. & Timasheff, S.N., vol **115**, 90-112.

White, R.J. (1968). *Biochem J.*, **106**, 847-858.

SERVIÇO DE [illegible] INFORMAÇÃO - IFQSC
FÍSICA

III. Proteína Sérica Humana Componente P de Amilóide

III.1 Introdução

A proteína sérica humana Componente P de Amilóide (SAP) é uma glicoproteína normal do plasma, presente em concentrações de cerca de 40 $mg.l^{-1}$, tendo sido inicialmente encontrada como um componente menor, não-fibrilar, de depósitos de amilóide (Pepys et al., 1982). Ela está presente em todas as diferentes formas de amiloidose, incluindo as placas intracorticais associadas à doença de Alzheimer. SAP pertence à família de proteínas conhecida por "pentraxinas", da qual, o outro membro presente no homem é a Proteína reativa C (CRP), uma das mais conhecidas proteínas de fase aguda (Pepys & Baltz, 1983). Estas macromoléculas apresentam um típico arranjo de subunidades ligadas não-covalentemente com simetria pentamérica cíclica, numa configuração de um disco plano. SAP e CRP humanas compartilham 51% de identidade de aminoácidos na sequência. Esta figura sobe para 66% se substituições conservativas são consideradas (Ohnishi et al., 1986). Proteínas com sequências homólogas e com a mesma estrutura quaternária pentamérica estão presentes no sôro de todos os vertebrados nos quais ela foi buscada (Lei et al., 1985). Nenhuma pessoa foi encontrada até hoje que não apresente SAP ou CRP em seu sôro, indicando que estas moléculas certamente desempenham importante papel biológico.

Em adição à conservação da estrutura, todas as pentraxinas compartilham a propriedade de ligação cálcio-dependente a substratos, ainda que a diferentes ligantes. No caso de SAP, esta propriedade é responsável pela sua ligação aos depósitos de amilóide, uma vez que todos estes depósitos fibrilares contém ligantes aos quais SAP apresenta afinidade cálcio-dependente (Pepys et al., 1979).

Recentemente foi demonstrado que SAP é a proteína sérica de maior afinidade de ligação específica a DNA e cromatina nuclear, também de uma maneira cálcio-dependente (Pepys & Butler, 1988). Portanto a função fisiológica *in vivo* de SAP pode estar relacionada à manipulação destes materiais quando eles forem expostos ou lançados em circulação por células mortas ou danificadas. Além disso, foi encontrada homologia marcante entre trechos das sequências altamente conservadas nas pentraxinas e certas regiões nas porções globulares das histonas H1 e H4 supostamente envolvidas na ligação com DNA.

Estas observações sugerem que SAP é muito importante, tanto fisiologicamente quanto fisio-patologicamente, e que a elucidação de sua estrutura tridimensional é de interesse não apenas na identificação das bases moleculares de suas interações, como também do ponto de vista clínico.

Cada subunidade de SAP humana é composta de 204 aminoácidos, com uma única ponte dissulfeto intra-cadeia, e carrega um único oligossacarídeo. Micrografias eletrônicas, estimativas de peso molecular por análise de sedimentação (Painter et al., 1982) e estudos de espalhamento de raios-X e neutrons à baixo ângulo (Perkins & Pepys, 1986) indicam que sob condições fisiológicas SAP se apresenta como decâmeros, com dois discos pentaméricos interagindo face-contra-face.

III.2 Trabalhos publicados no *Journal of Molecular Biology*, *Journal of Crystal Growth*, capítulo no livro *Acute Phase Proteins in the Acute Phase Response* e trabalho submetido à *Nature*.

Sob condições de baixo pH e alta força iônica, SAP foi cristalizada de forma adequada para a análise por difração de raios-X. A cristalização, caracterização inicial e determinação da espécie pentamérica cristalizada bem como a simetria não cristalografica estão descritas nas seguintes publicações:

WOOD, S.P., **OLIVA, G.**, O'HARA, B.P., WHITE, H.E., BLUNDELL, T.L., PERKINS, S.J., SARDHARWALLA, I. & PEPYS, M.B.
"A Pentameric Form of Human Serum Amyloid P Component. Crystallization, X-Ray Diffraction and Neutron Scattering Studies."
J.Mol.Biol, **202**, 169-173, 1988.

O'HARA, B.P., WOOD, S.P., **OLIVA, G.** & WHITE, H.E.
"Crystallizations of Human Serum Amyloid P Component (SAP)".
Journal of Crystal Growth, **90**, 209-212, 1988.

Os resultados iniciais da determinação da estrutura pela técnica de Substituição

Isomorfa Múltipla estão descritos no trabalho publicado como capítulo do livro intitulado *Acute Phase Proteins in the Acute Phase Response* :

WHITE,H.E., O'HARA,B.P., **OLIVA, G.**, BLUNDELL,T.L., PEPYS,M.B. & WOOD,S.P.
"The Three Dimensional Structure of SAP"
In, Acute Phase Proteins in the Acute Phase Response, ed. by M.B.Pepys, London, Springer-Verlag, pp.123-136., 1989

A completa determinação e refinamento da estrutura da proteína nativa, a identificação dos sítios de ligação dos ligantes MOßDG e Fosfoetanolamina em mapas de Fourier Diferença e a interpretação das características funcionais da proteína à luz dos resultados estruturais estão apresentados no manuscrito submetido recentemente para publicação na revista *Nature*. Figura III.1 mostra a estrutura do monômero e pentâmero de SAP.

EMSLEY, J., WHITE, H.E., O'HARA, B.P., **OLIVA, G.**, SRINIVASAN, N., TICKLE, I.J., BLUNDELL, T.L., PEPYS, M.B. and WOOD, S.W.
"The 3D structure of pentameric human serum amyloid P component defined at 2Å resolution reveals a lectin-like fold and calcium mediated ligand binding"
Submitted to *Nature*, August 1993.

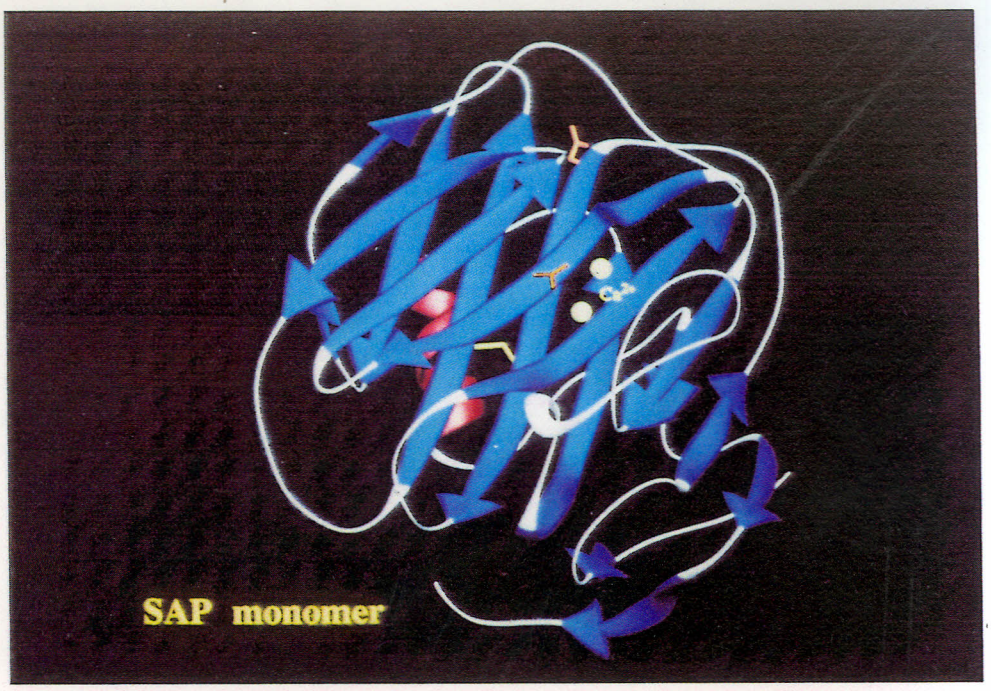

(a)

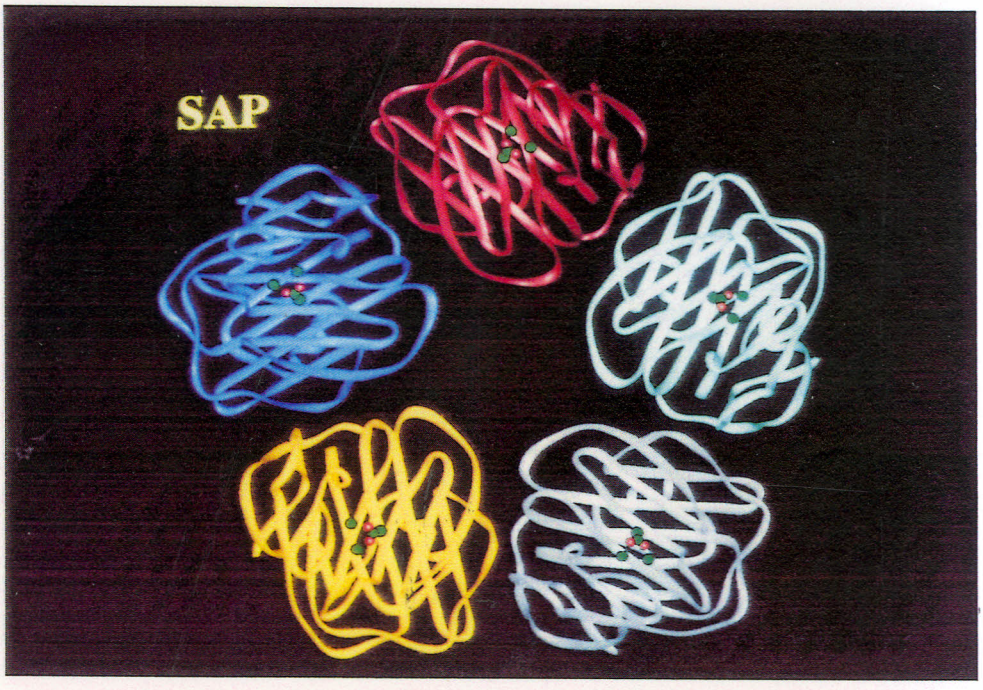

(b)

Figura III.1 Enovelamento da cadeia principal do monômero (a) e pentâmero (b) da proteína sérica humana Componente P de Amilóide (SAP). (Programa *RIBBONS*)

REFERÊNCIAS

Bricogne, G. (1976). *Acta Cryst.*, **A32**, 832

Lei, K.-J., Lin, T., Zon, G., Soravia, E., Liu T.-Y. and Goldman, N.D. (1985). *J.Biol.Chem.* **260**, 13377-13383.

Ohnishi, S., Maeda, S., Shimada, K. and Arao, T. (1986). *J.Biol.Chem.* **261**, 849-858.

O'Hara, B.P., Wood, S.P., Oliva, G. & White, H.E. (1988). *Journal of Crystal Growth*, **90**, 209-212.

Oliva,G., O'Hara,B.P., Wood,S., Pepys.M.B. and Blundell,T.L. (1986) *Protides Biol. Fluids*, 34, 371-374.

Painter, R.H., De Escállon, I., Massey, A., Pinteric, L. and Stern, S.B. (1982). *Ann.N.Y.Acad.Sci.* **389**, 199-215.

Pepys, M.B. and Baltz, M.L. (1983). *Adv.Immunol.* **34**, 141-212.

Pepys, M.B. and Butler, P.L.G. (1987). *Biochem. Biophys. Res.Comm.* **148**, 308.

Pepys, M.B., Baltz, M., de Beer, F.C., Dyck, R.F., Holford, S., Breathnach, S.M., Balck, M.M., Tribe, C.R.F., Evans, D.J. and Feinstein, A. (1982) *Ann.N.Y.Acad.Sci.* **389**, 286-297.

Pepys, M.B., Dyck, R.F., de Beer, F.C., Skinner, M. and Cohen, A.S. (1979). *Clin.Exp.Immunol.* **38**, 284-293.

Perkins, S.J. and Pepys, M.B. (1986). *Protides Biol.Fluids.* **34**, 323-326.

Wang, B.C. (1985). in *Methods in Enzimology*, ed. by Wyckoff, H.W., Hirs, C.H.W & Timasheff, S.N., vol. **115**, 90-112.

Wood, S.P., Oliva, G., O'Hara, B.P., White, H.E., Blundell, T.L., Perkins, S.J., Sardharwalla, I. & Pepys, M.B. (1988). *J.Mol.Biol.*, **202**, 169-173.

De acordo com as políticas editoriais, estes artigos não podem ser depositados em repositório de acesso aberto. Para acesso aos artigos completos entre em contato com o(a) autor(a) ou com o Serviço de Biblioteca e Informação IFSC - USP (bib@ifsc.usp.br).

WOOD, S. P.; OLIVA, G.; O'HARA, B. P.; WHITE, H. E.; BLUNDELL, T. L.; PERKINS, S. J.; SARDHARWALLA, I.; PEPYS, M. B. Pentameric form of human serum amyloid P component. **Journal of Molecular Biological**, New York, v.202, n.1 , p.169-73, July 1988.

O'HARA, B. P.; WOOD, S. P.; OLIVA, G.; WHITE, H. E.; PEPYS, M. B. Crystallization of human serum amyloid P component (SAP). **Journal of Crystal Growth**, Amsterdam, v.90, n.1-3, p.209-12, July 1988.

M. B. Pepys (Ed.)

Acute Phase Proteins in the Acute Phase Response

With 45 figures

Springer-Verlag
London Berlin Heidelberg New York
Paris Tokyo Hong Kong

Chapter 10

The Three Dimensional Structure of SAP

H. E. White, B. P. O'Hara, G. Oliva, T. L. Blundell, M. B. Pepys and S. P. Wood

Serum amyloid P (SAP) component and C-reactive protein (CRP) are members of a closely related family of pentameric or decameric proteins called pentraxins which are involved in amyloidosis and the acute phase response (Pepys and Baltz 1983). Although CRP was crystallised in 1947 (McCarty 1947), no detailed three dimensional structural information has been obtained by X-ray analysis. However, several recent reports of CRP (DeLucas et al. 1987) and SAP (Wood et al. 1988) crystals have demonstrated that this is now a realistic objective. In this paper we review progress made on the X-ray analysis in our laboratory, and describe for the first time preliminary, medium resolution electron density maps of a pentameric form of SAP.

As isolated from human serum in calcium free media, SAP has a molecular weight of 254 000 and comprises 10 subunits each of 204 amino acids. Each subunit contains a single intrachain disulphide bridge, and carries a single asparagine linked complex oligosaccharide which contributes about 8% of the total mass. CRP on the other hand has a molecular weight of 115 000 and comprises five subunits, each of 206 amino acids with no attached carbohydrate. The amino acid sequences are included in Fig. 10.11.

The pentagonal arrangement of subunits, in disks 85–110 Å diameter and 30–40 Å deep have been reported by various researchers (Osmand et al. 1977; Painter et al. 1976; Pepys et al. 1977; Baltz et al. 1982a) for both proteins. Human SAP appears as two disks interacting through their planar faces (Fig. 10.1).

Our attempts to crystallize these proteins began in 1985 and quickly led to a crystal form of human SAP suitable for high resolution structure analysis (Oliva et al. 1986). Large prismatic crystals could be grown in 4–5 weeks from protein solutions containing calcium ions, at pH 5.5 (Fig. 10.2). The preliminary crystallographic details for this form and a number of others grown subsequently (O'Hara et al. 1988) are summarized in Table 10.1.

X-ray diffraction data for the original crystal form were measured to 5.5 Å resolution and the non-crystallographic symmetry was examined using the fast

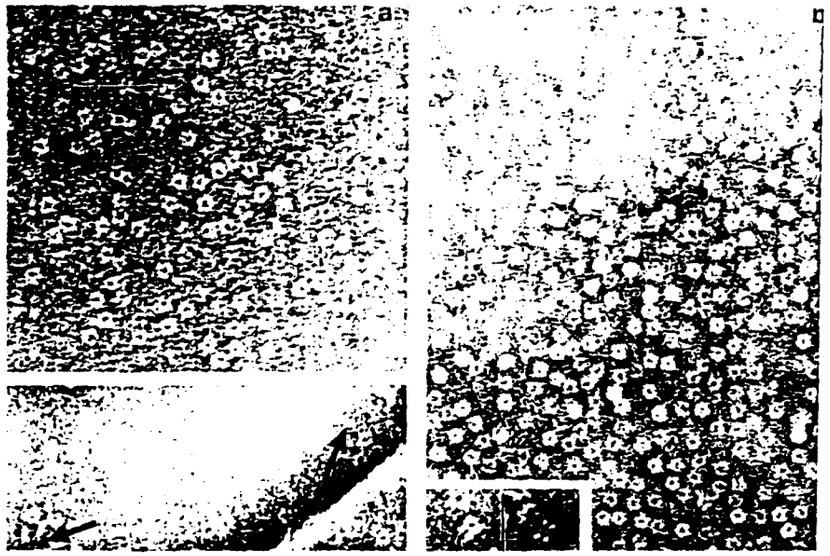

Fig. 10.1a,b. Electron micrographs of negatively stained preparations of **a** human C-reactive protein and **b** human serum amyloid P component. Most molecules are seen face-on but *arrows* in **a** and *insets* in **b** (at higher magnification) show views of the disk-like molecules side-on. Magnification, × 320000. Micrography performed by Dr E. A. Munn, Department of Biochemistry, ARC Institute of Animal Physiology, Babraham.

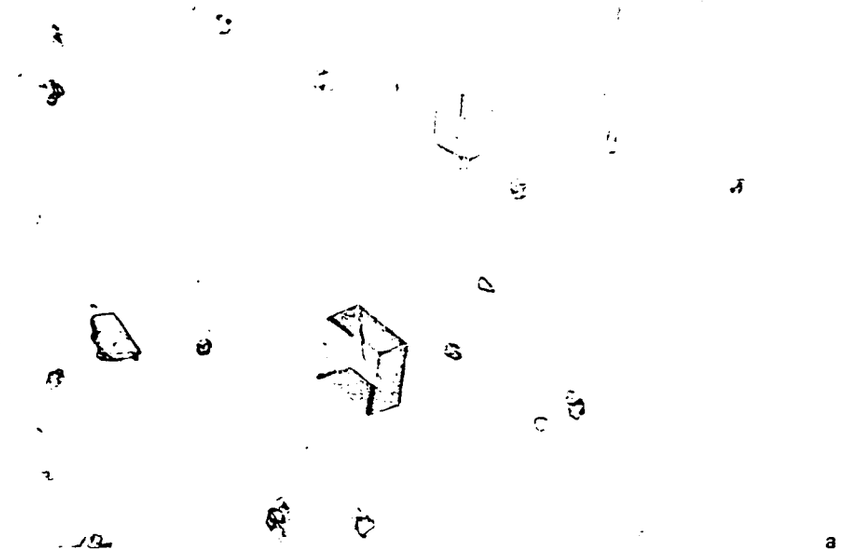

Fig. 10.2a. Prismatic crystals of SAP (dimension 0.5–1.0 mm) grown at pH 5.5 in the presence of calcium ions. (Figure continued on p. 125.)

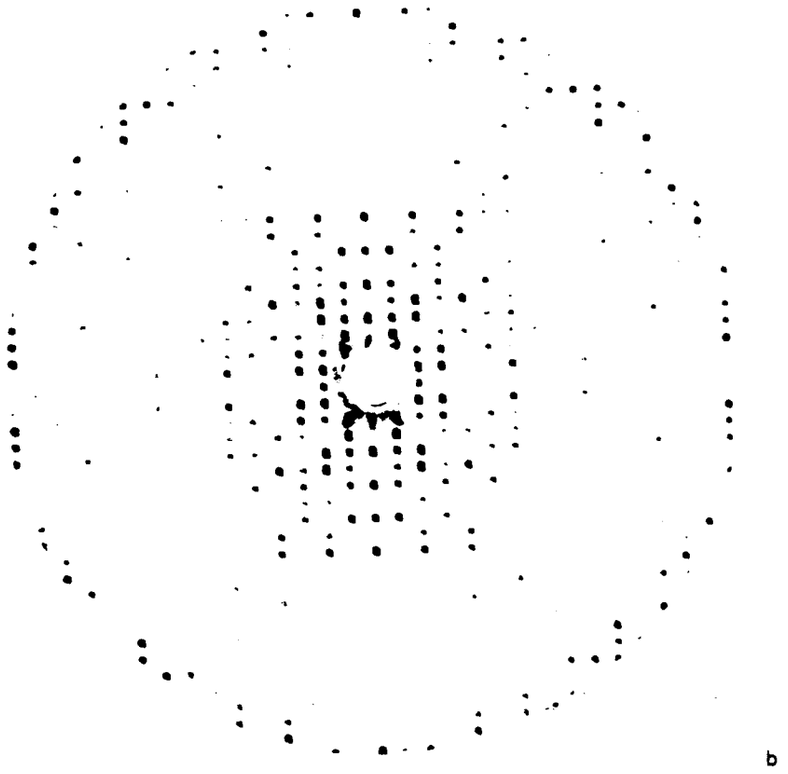

Fig. 10.2b. Zero layer (hk0) X-ray precession photograph (μ = 12°).

Table 10.1. Crystal forms of SAP

Shape	Conditions	Space group	Cell			
			a	b	c	β°
1. Prismatic	pH 5.5	$P2_1$	69.0	99.3	96.8	96.1
2. Prismatic	pH 5.5/Ca/MOβDG	$P2_1$	69.0	99.3	96.8	96.1
3. Rods/plates	pH 8/Ca	?				
4. Rods	pH 8/Ca/MOβDG	$P2_1$	121.6	108.9	117.2	94.5
5. Rods	pH 5.5/Sr		Very soft			
6. Prismatic	pH 5.5/Ba	$P2_1$	60.7	106.5	103.0	94.6
7. Prismatic	pH 5.5/La	$P2_1$	74.0	164.5	185.0	95.0

rotation function of Crowther (1972). The rotation function showed 52 symmetry as expected for a decamer in the asymmetric unit of the crystal. However, the volume of the crystal unit cell was not large enough to accommodate such a decamer together with the quantity of solvent usually found in protein crystals (Wood et al. 1988). The apparent 2-fold symmetry was subsequently found to be an attribute of the calculation at low resolution but the implication that SAP was present in a pentameric form was not consistent with the expected decameric organisation of the molecule. Low angle scattering of neutrons and X-rays by solutions of SAP and CRP (Perkins and Pepys 1986) showed that, at neutral pH, SAP exists as a monodisperse population of decamers independent of protein concentration, while CRP shows evidence of aggregation of pentamers to higher oligomers with increasing protein concentration (Fig. 10.3). However, further

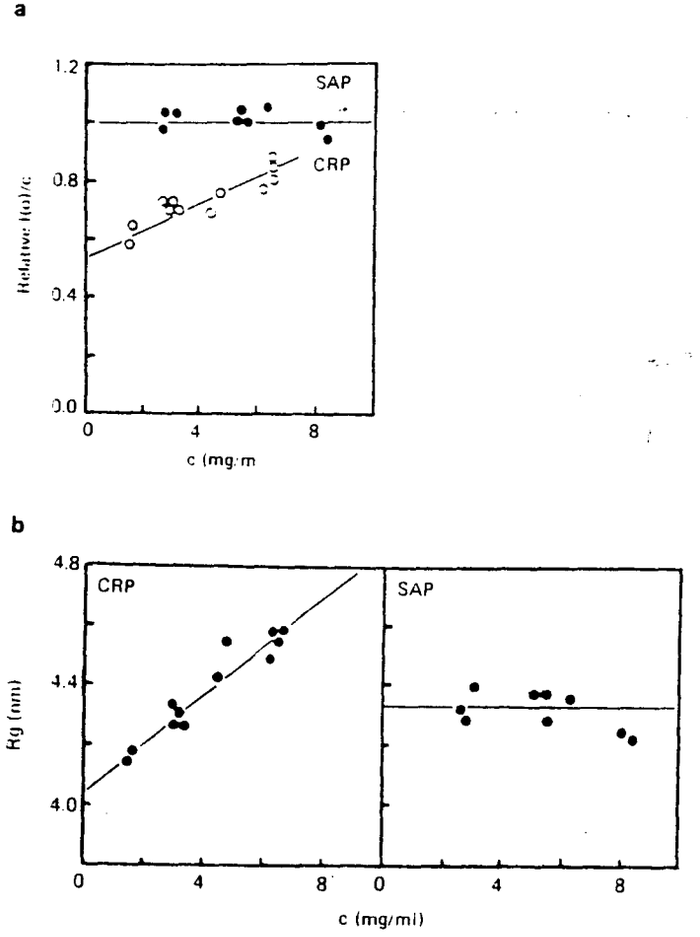

Fig. 10.3a,b. Plots of the **a** relative molecular weights (I(o)/c – the forward scattering X-ray intensity) and **b** radius of gyration (Rg) for SAP and CRP as a function of protein concentration, determined by low angle X-ray scattering of protein solutions, show the aggregation tendency for CRP and the larger more stable molecular form for SAP (Perkins and Pepys 1986).

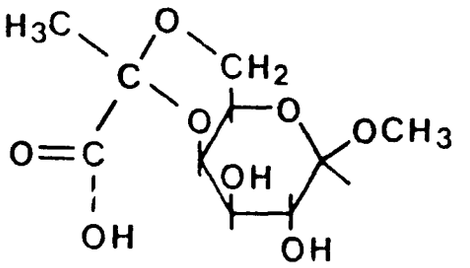

Fig. 10.4. The synthetic monosaccharide, methyl 4,6-O-(1-carboxyethylidene)-β-D-galactopyranoside (MOβDG) which has been used to control the rate of SAP crystal growth and modify the crystal form.

measurements carried out in the crystallization solvent buffer showed that the SAP had dissociated into pentamers. Gel filtration experiments confirmed the pentameric nature of SAP under these conditions and, furthermore, demonstrated that SAP could be readily converted between pentameric and decameric forms simply by suitable buffer exchange (Wood et al. 1988).

In Table 10.1 are listed several additional crystal forms of SAP which were grown subsequently and which raise further questions about the aggregation state of the molecule. At pH 5.5 we found that the galactose derivative (MOβDG) (Fig. 10.4) shown by Pepys and co-workers (Hind et al. 1984a), to be the constituent of agarose to which SAP binds in the presence of calcium ions, dramatically slows the rate of crystal growth but does not affect the final product. From precipitates of SAP which rapidly develop on adding calcium ions at pH 8 (Baltz et al. 1982b), distinctive plates and prisms grew together. When MOβDG was included at pH 8 the normal precipitation was not observed, but overnight at 4° C rod shaped crystals grew. The volume of the asymmetric unit of these crystals was large enough to accommodate a decamer of SAP (O'Hara et al. 1988). Slow cooling of this mixture, however, gave rise to the crystal form seen at pH 5.5. These experiments again indicate that the equilibrium between pentameric and decameric SAP populations can be readily perturbed to provide different crystalline forms. Further recent neutron scattering experiments at pH 5 in the presence of calcium ions and MOβDG indicate a pentameric population of SAP molecules (S. Perkins, unpublished observations). We have successfully substituted other metals such as strontium, barium and lanthanum for calcium in the crystallization of SAP but there is clearly disturbance to the crystal lattice with these other metals.

In Fig. 10.5 some of these observations are summarized together with some implications in cartoon form. The central point seems to be that in the presence of calcium ions the pentamer–decamer equilibrium is displaced towards pentamers which at near neutral pH can only be retained in solution by co-ordination of MOβDG. In its absence, calcium-mediated intermolecular interactions lead to precipitation (Baltz et al. 1982b; Hind et al. 1984b). At lower pH, calcium binding via sidechain carboxylates would be somewhat less favourable and calcium does not precipitate SAP at pH 5.5. However, MOβDG can still compete for the calcium-mediated intermolecular interaction and retard crystal growth. This proposed role for calcium involvement in the interactions between pentamers seems to be confirmed by the packing changes observed with other metals

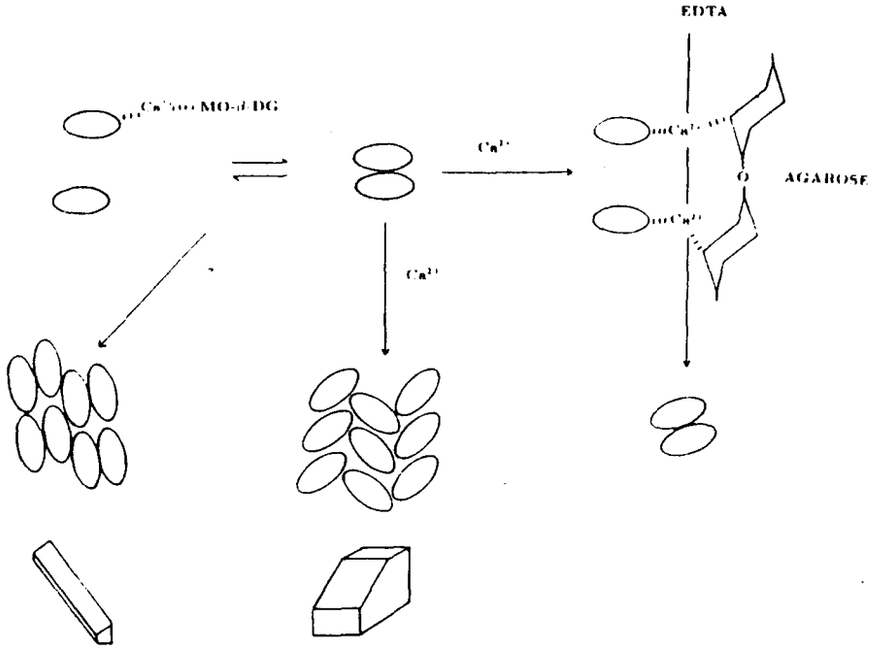

Fig. 10.5. Each oval signifies a pentameric disk of SAP. Two of these are shown interacting face-to-face in the centre of the figure and represent the molecular species (decameric) encountered in the absence of calcium ions. To the left and right pentameric forms are favoured in the presence of calcium and these may be the species involved in binding agarose or the related synthetic galactose derivative (MOβDG). EDTA sequesters calcium to release a decameric product (*right*) from affinity columns of agarose while suitable manipulation of the equilibrium (*left*) by change of protein concentration pH, temperature, precipitant or MOβDG addition during crystallization leads to the production of crystal lattices where pentamers (*centre*) or decamers (*left*) are packed.

such as barium. Calcium pentamers form prismatic crystals rather slowly while rapid growth at pH 8 traps what appears to be a decameric form. The ease with which the SAP aggregation state can change, in particular in response to calcium ions, raises the question of what form is involved in ligand binding. The cartoon in Fig. 10.5 implies that pentamers associate with agarose in the presence of calcium ions, and following elution of SAP with EDTA the protein reassociates to form decamers. In serum, SAP sediments as a decamer in spite of calcium ion concentrations capable of causing precipitation in the isolated protein (Baltz et al. 1982b). More quantitative data on the aggregation behaviour of SAP is required in order to determine the species that interacts with natural ligands.

A variety of different X-ray data sets have now been collected (summarized in Table 10.2). The native protein data measured by oscillation photography at the Daresbury synchrotron source extend to 2 Å resolution (Fig. 10.6). Many attempts have been made to produce suitable heavy atom derivatives of the SAP crystals. Most of the more commonly used reagents have not been successful. Of the derivative data sets collected so far, only those for thorium nitrate and tungsten-cluster soaked crystals has been of use in phase calculation. Two binding

Table 10.2. X-ray data sets collected for SAP

Crystal	Collection method	Resolution (Å)	Refls. measured	Refls. unique	R symmetry (%)
Native	Diffractometer	5.6	10341	4112	4.5
K_2PtCl_4	Diffractometer	6.0	7387	3372	5.0
Na_2WO_4	Diffractometer	6.0	6574	3294	5.1
Native	Fast	3.8	43175	11802	5.3
$Th(NO_3)_4$	Fast	4.0	34176	9521	6.7
$Na_3PO_4\ 12WO_3$	Fast	4.0	38419	12107	7.0
$Th(NO_3)_2$	Fast	2.8	96444	29551	5.0
Native	Synchrotron	2.0	345000	86000	7.7
K_2PtI_6	Fast	3.5	41778	15119	8.4
NAT/PE[a]	Diffractometer	5.0	6272	5659	5.0
NAT/Ba[b]	Fast	3.5	77468	17078	9.8

[a] PE: crystals soaked in phosphoethanolamine.
[b] Ba: co-crystallisation product with Ba^{2+} ions.

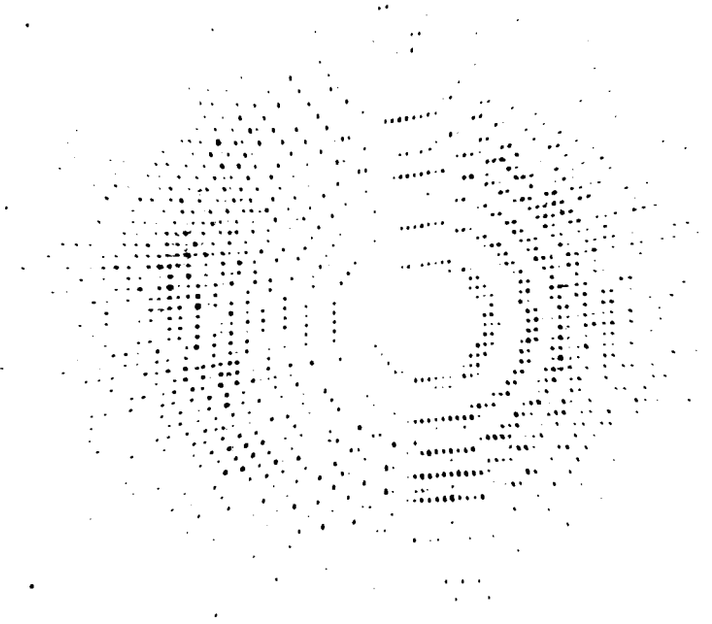

Fig. 10.6. An oscillation photograph (φ = 1.1°) of a human SAP crystal taken at the Daresbury synchrotron source (λ = 1.488 Å) showing the resolution of data collected so far (2 Å).

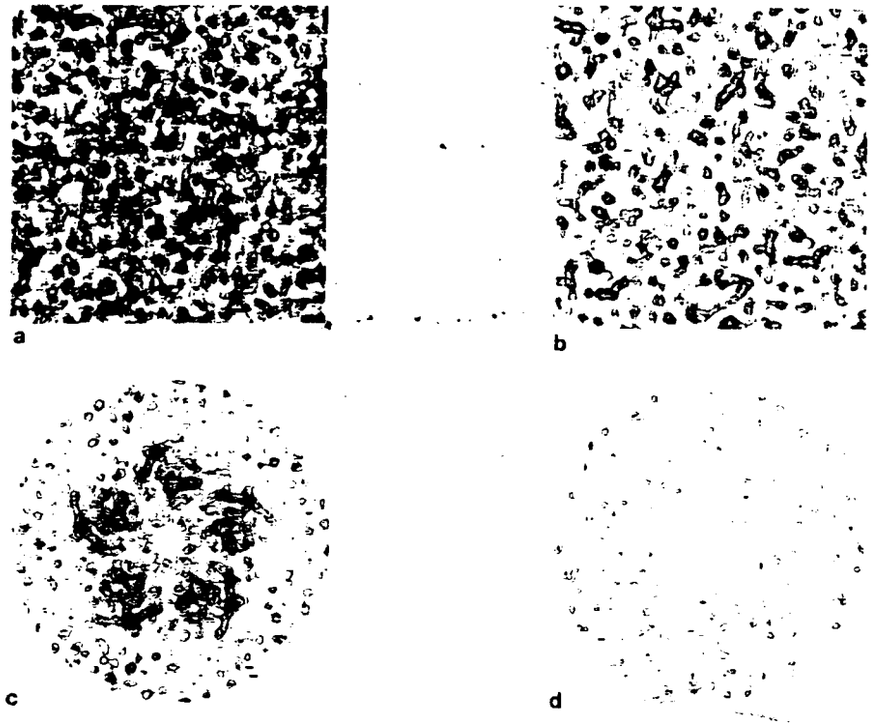

Fig. 10.7a Corresponds to a region of the 6 Å MIR map which traverses the molecular disk, and the averaged map in the position shows clear inner and outer boundaries **c**, **b** and **d** correspond to sections perpendicular to the 5-fold axis but above the molecular disk, and after averaging **d** show no strong electron density.

sites for thorium and three sites for tungsten were located. The tungsten cluster apparently degrades in the crystal mother liquor, to provide a slow release of tungstate ions, since sodium tungstate alone reacts rather vigorously and disorders the crystals to some extent, although binding at the same principal site. Both of the usable derivatives suffer from severe lack of isomorphism, limiting their phasing power to low resolution. The packing arrangement of protein molecules in the crystal has so far not permitted a 5-fold symmetric distribution of heavy atom binding sites.

More good heavy atom derivatives will probably be required to determine such a large structure but the potential power of the non-crystallographic 5-fold symmetry for phase extension tempted us to calculate an initial electron density map at 6 Å resolution. The map has distinctive regions related by the predicted 5-fold symmetry. Following an extended refinement of the location of the 5-fold axis, a single cycle of 5-fold electron density averaging was carried out using a large cylindrical envelope. The resultant map is shown in Figure 10.7, where the same sections of the original 6 Å MIR map and of the averaged map are represented. Figure 10.7a and c correspond to a region of the map which traverses the molecular disk, and indeed the averaged map shows clear inner and outer

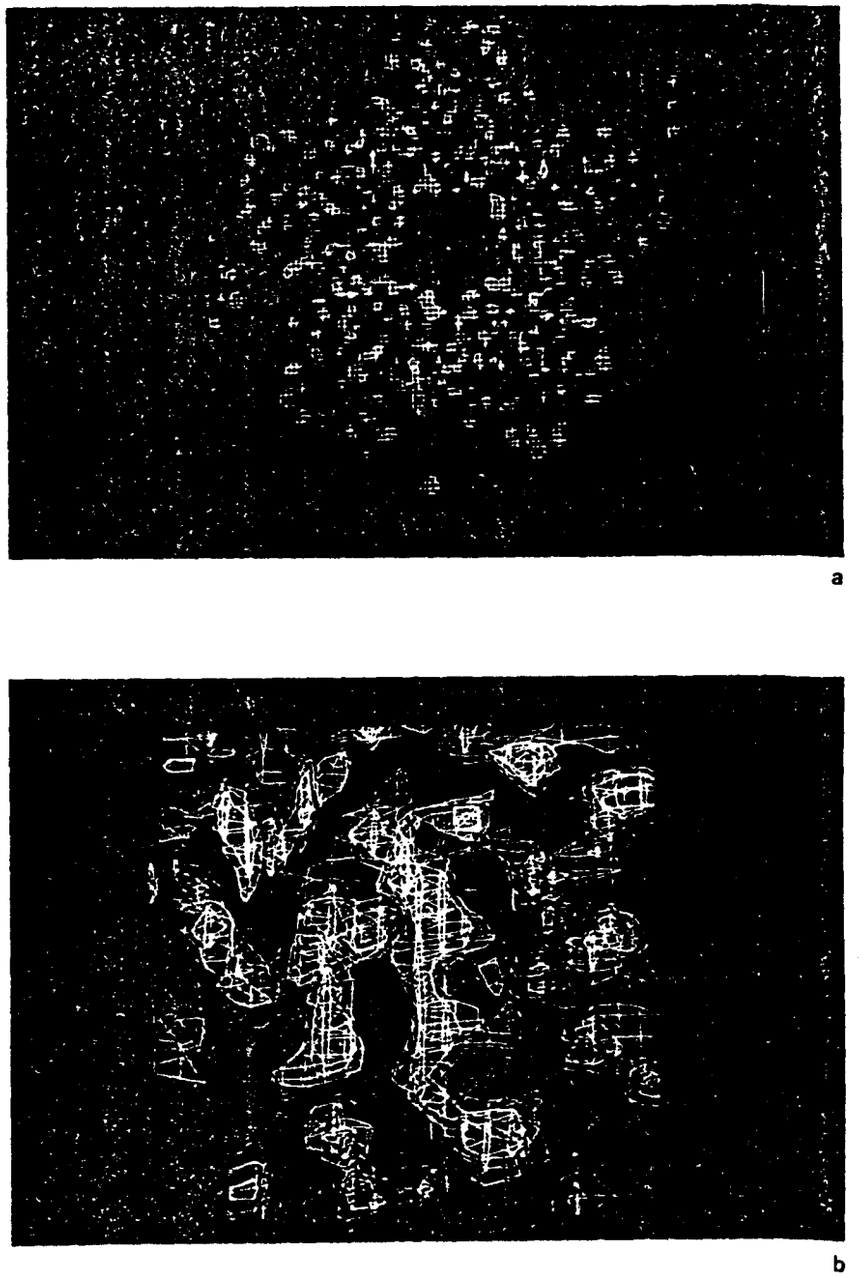

Fig. 10.8a. A shallow slice of electron density for the SAP molecule perpendicular to the 5-fold axis calculated at 3.5 Å resolution revealing a molecule about 100 Å across. Closer examination of a small region of one subunit (**b**) shows extended regions of density to which a polypeptide fragment could be built.

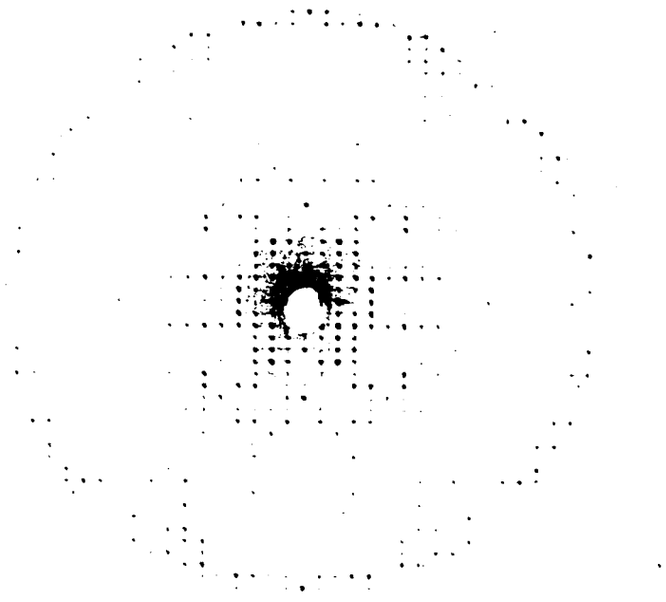

Fig. 10.9. X-ray precession photograph (μ = 10°) for an orthorhombic crystal of human CRP (Birkbeck).

molecular boundaries. Figure 10.7b and d correspond to sections perpendicular to the molecular 5-fold axis but above the molecular disk, and the averaged sections, as expected, do not show any strong electron density. As a convincing test, the phases from the averaged map were capable of locating the heavy atom positions and these are situated at the exposed periphery of the subunits. We proceeded to extend the resolution of the phase information using the 5-fold symmetry to constrain the phases by the method of Bricogne (1976). At intervals we checked that the heavy atoms were still detectable. Solvent flattening was also employed (Wang 1985). At 3.5 Å resolution the electron density map shows rather clear subunits with dimensions in accord with those seen by electron microscopy (Fig. 10.8). Some extended regions of interconnecting electron density are clearly visible. However, at this resolution it is not possible to follow reliably the complete polypeptide chain, and a detailed interpretation must await further improvement and extension of the phases.

Structural studies on CRP are somewhat less advanced but are proceeding steadily in three laboratories on different crystal forms, in research by Greenhough and co-workers (Keele/Alabama, DeLucas et al. 1987), Turnell, Bloomer and Pepys (LMB, Cambridge/RPMS, unpublished results) and Wood et al. (Birkbeck/RPMS, unpublished results; orthorhombic a = 102.5, b = 106.0, c = 118.4 Å; Fig. 10.9). Clearly, all these crystallographic analyses of CRP are closely

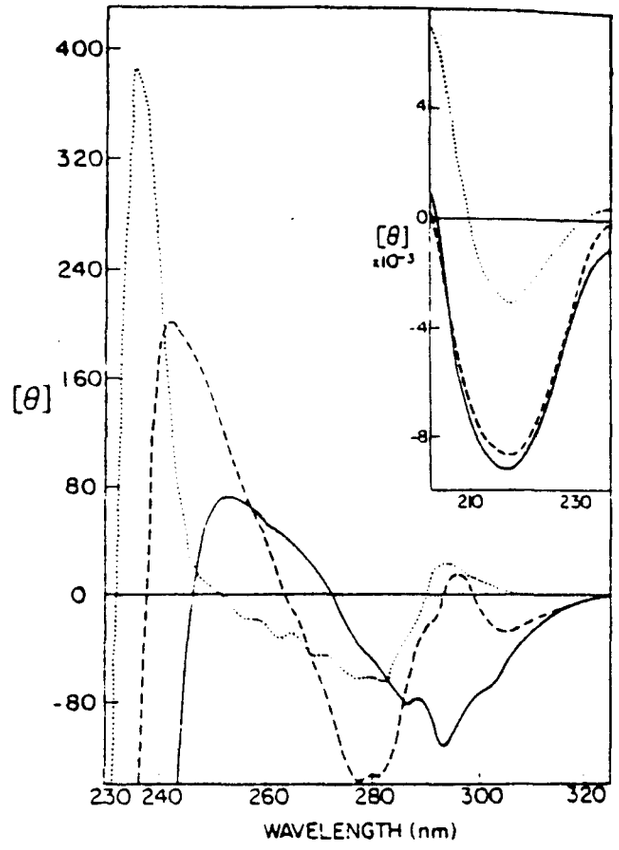

Fig. 10.10. CD spectra for SAP (·····) and CRP (____) in the near and far UV measured at pH 7.5 and 1 mg ml^{-1} protein concentration, showing close similarity to the peptide region but more distinct features in the aromatic region (Young and Williams 1978).

related and a successful structure determination for any one of them, or for SAP, should be catalytic for solving the various other crystal forms.

What sort of structural features do we expect to find in these molecules? Both circular dichroism and sequence based prediction methods have provided indications of the amount and types of secondary structure to be expected. Young and Williams (1978) showed that SAP and CRP were very similar in the far ultraviolet region of the CD spectrum and estimated that there was 34% helix and 45% sheet (Fig. 10.10). In the near UV region the spectra are more distinct. We have measured the near UV spectrum of SAP in conditions which favour pentamers or decamers at the same protein concentration. For some proteins the trapping of aromatic sidechains at subunit interfaces during association can give rise to very convenient changes in rotational strength which can provide rough measure of the degree of association (Wood et al. 1975). Apart from a small change in the tryptophan region no major differences were observed. Aromatic

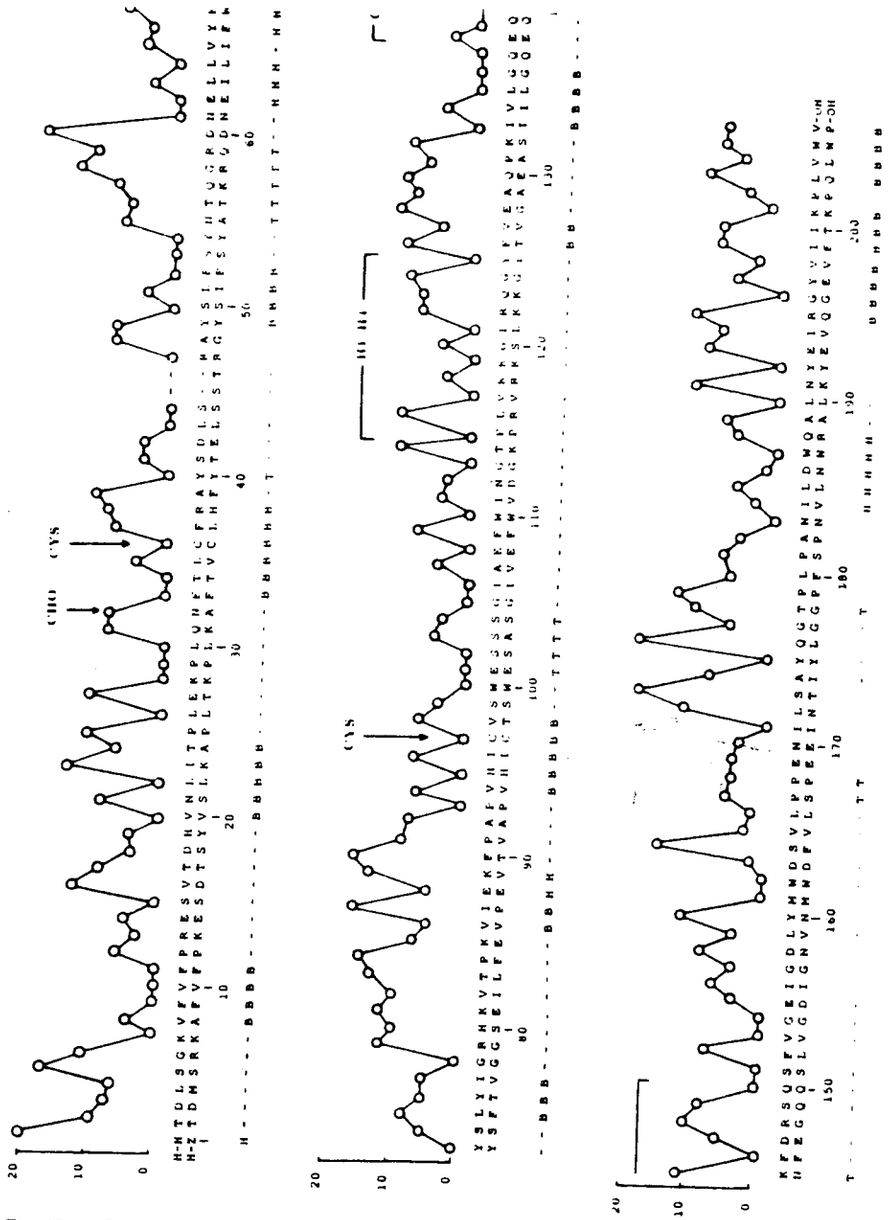

Fig. 10.11. Summary of some amino acid sequence based predictions of secondary structure in the pentraxins. Eight available sequences from Anderson et al. (1989) were aligned and the residue "likeness" at each position (see text) is plotted on a scale from 1 to 20 against sequence number and the common secondary structure predicted from seven different prediction algorithms (*H*: helix, *B*: sheet, *T*: turn). The complete sequences for human SAP (top) and CRP (bottom) are included. A region homologous to histones H1 and H4, and possibly responsible for DNA binding, and a putative calcium binding region (Turnell et al. 1988) are shown.

residues may therefore not be buried at the pentamer–pentamer interface (B. O'Hara, unpublished results).

Secondary structure prediction methods generally confirm the estimate from circular dichroism of the amount of helix and sheet. Figure 10.11 shows a combined prediction summary. The ordinate of the graph is a residue "likeness" index scored at each sequence position from a comparison of seven aligned pentraxin sequences, using a relatedness Venn diagram based on features of size, polarity, aromacity, etc., for each amino acid, as proposed by Taylor (1986a,b). Beneath the abscissa (residue number) the consensus secondary structure prediction for human SAP, derived from seven different prediction algorithms (available within the Leeds University sequence data base), is plotted. This figure provides an overview of the conservation of residue type in the pentraxin family, likely position (buried or exposed) and possible secondary structure. The sequences shown for human SAP (upper) and CRP are much more alike than some other members of the set analysed. Some regions of predicted sheet are clearly quite well conserved, particularly if they are hydrophobic and possibly buried. Some regions are consistently predicted to be helical (e.g. 60–70). Also included in the prediction summary are regions proposed by Turnell et al. (1988) to be homologous with histones H1 and H4 and to be a putative helical DNA binding region adjacent to a calcium binding region (Nguyen et al. 1986; Turnell 1989).

The physiological and pathophysiological role of SAP is of increasing interest in view of the recent discovery that it is the major specific calcium-dependent DNA and chromatin binding protein of the serum (Pepys and Butler 1987), and the development of labelled SAP as a specific targeting agent for clinical diagnosis of amyloidosis (Hawkins et al. 1988). It is evident that these properties and uses of SAP are determined by its specific ligand binding properties and it is hoped that elucidation of the protein structure to high resolution will both explain these interactions and open the way for manipulation of protein function.

References

Anderson JK, Taylor JA, Baltz ML et al. (1989) Primary structure of murine serum amyloid P component (submitted)

Baltz ML, de Beer FC, Feinstein A et al. (1982a) Phylogenetic aspects of C-reactive protein and related proteins. Ann NY Acad Sci 389:49–75

Baltz ML, de Beer FC, Feinstein A, Pepys MB (1982b) Calcium-dependent aggregation of human serum amyloid P component. Biochim Biophys Acta 701:229–236

Bricogne G (1976) Methods and programs for direct-space exploitation of geometric redundancies. Acta Cryst A32:832–847

Crowther RA (1972) In: Rossman MG (ed) The molecular replacement method. Gordon and Breach, pp 173–175

DeLucas LJ, Greenhough TJ, Rule SA (1987) Preliminary X-ray study of crystals of human C-reactive protein. J Mol Biol 196:741–742

Hawkins PN, Myers MJ, Lavender JP, Pepys MB (1988) Diagnostic radionuclide imaging of amyloid: biological targeting by circulating human serum amyloid P component. Lancet i:1413–1418

Hind CRK, Collins PM, Renn D et al. (1984a) Binding specificity of serum amyloid P-component for the pyruvate acetal of galactose. J Exp Med 159:1058–1069

Hind CRK, Collins PM, Pepys MB (1984b) Calcium-dependent aggregation of human serum amyloid P component. Inhibition of the cyclic 4,6-pyruvate acetal of galactose. Biochim Biophys Acta 802:148–150
McCarty MJ (1947) The occurrence during acute infections of a protein not normally present in the blood IV. Crystallization of the C-reactive protein. J Exp Med 85:491–498
McCarty MJ (1982) Historical perspective on C-reactive protein. Ann NY Acad Sci 389:1–9
Ngkuyen NY, Suzuki A, Boykins RA, Liu T-Y (1986) The amino acid sequence of *Limulus* C-reactive protein. Evidence of polymorphism. J Biol Chem 261:10456–10465
O'Hara BP, Wood SP, Oliva G et al. (1988) Crystallizations of human serum amyloid P component (SAP). J Crystal Growth 90:209–212
Oliva G, O'Hara BP, Wood SP et al. (1986) Preliminary crystallographic studies of human serum amyloid P component (SAP). In: Peeters H (ed) Protides of the biological fluids, vol 34. Pergamon Press, Oxford, pp 371–374
Osmand AP, Freidenson B, Gewurz H (1977) The characteristics of C-reactive protein and the complement subcomponent C1t as homologous proteins displaying cyclic pentameric symmetry (pentraxins). Proc Natl Acad Sci USA 74:739–743
Painter RH, Pintenc L, Hoffman T, Kells DIC, Katz A (1976) Ultrastructure and chemistry of C1t subcomponent of C1: Similarities to amyloid P-component. J Immunol 116:1745
Painter RH, de Escallion I, Massey A et al. (1982) The structure and binding characteristics of serum amyloid protein (9.5S α1-glycoprotein). Ann NY Acad Sci 389:199–215
Pepys MB, Baltz ML (1983) Acute phase proteins with special reference to C-reactive protein and related proteins and serum amyloid A protein. Adv Immunol 34:141–212
Pepys MB, Butler PJG (1987) Serum amyloid P component is the major calcium-dependent specific DNA binding protein of the serum. Biochem Biophys Res Commun 148:308–313
Pepys MB, Dash AC, Munn EA, Feinstein A, Skinner M, Cohen AS, Gewurz H, Osmand AP, Painter RH (1977) Isolation of amyloid P-component (protein AP) from normal serum as a calcium-dependent binding protein. Lancet i:1029–1031
Perkins SJ, Pepys MB (1986) X-ray and neutron scattering studies on CRP and SAP. In: Peeters H (ed) Protides of the biological fluids colloquium XXXIV. Pergamon Press, Oxford, pp 323–326
Taylor WR (1986a) The classification of amino acid conservation. J Theor Biol 119:205–218
Taylor WR (1986b) Identification of protein sequence homology by consensus template alignment. J Mol Biol 188:233–258
Turnell WG (1989) Searches for calcium-binding motifs in protein sequences. In: Reid E, Cook GMW, Luzio JP (eds) Biochemical approaches to cellular calcium. Royal Soc Chem, London (Methodological surveys in biochemistry and analysis, vol 19) (in press)
Turnell WG, Satchwell SC, Travers AA (1988) Hypothesis: a decapeptide motif for binding to the minor groove of DNA—a proposal. FEBS Lett 232:263–268
Wang BC (1985) Resolution of phase ambiguity in macromolecular crystallography. Meth Enzymol 115:90–112
Wood SP, Blundell TL, Wollmer A et al. (1975) The relation of conformation and association of insulin to receptor binding: X-ray and circular dichroism studies on bovine and hystriomorph insulins. Eur J Biochem 55:531–542
Wood SP, Oliva G, O'Hara BP et al. (1988) A pentameric form of human serum amyloid P component. Crystallization, X-ray diffraction and neutron scattering studies. J Mol Biol 202:169–173
Young NM, Williams RE (1978) Comparison of the secondary structures and binding of C-reactive protein and the phosphorylcholine-binding murine myeloma proteins. J Immunol 121:1893–1898

Chapter 11

Structure, Metabolism and Function of Acute Phase High Density Lipoprotein

F. C. de Beer, A. F. Strachan and E. G. Shephard

Introduction

The acute phase response is a multi-system adaptation induced by autologous cell death or by products of exogenous invasion (Kushner 1982). These influence macrophages to secrete various monokines that, among other functions, affect hepatic gene expression for many proteins (Ramadori et al. 1985). This response consists of a variety of biochemical, cellular, hormonal and metabolic changes with characteristic increases in many plasma proteins. Serum amyloid A protein (apo-SAA) is particularly notable in that it is normally present in trace amounts in human serum, but the concentration increases up to 100-fold within 48 hours of initiation of the acute phase. (Eriksen and Benditt 1984; McAdam et al. 1978; de Beer et al. 1982). Segrest et al. (1976) first noted that a 45-residue fragment of the apo-SAA cleavage product, amyloid A protein (AA), formed stable complexes with phospholipid. This finding preceded the discovery, by Benditt and Eriksen (1977), that apo-SAA is transported in human plasma mainly with high density lipoproteins (HDL) and is thus classified as an apolipoprotein. Although HDL (expressed as HDL cholesterol) is a significant negative acute phase reactant, it can play a role in inflammation. HDL has been reported to function as a vehicle to transfer damaged cellular constituents to the liver and to bind bacterial lipopolysaccharides (Ulevitch et al. 1981) and neutrophil elastase (Jacob et al. 1981). The function of apo-SAA rich HDL in response to injury is, however, unknown. The phylogenetic conservation of the association of apo-SAA with HDL suggests that it plays an important role.

In rare instances during chronic inflammation cleavage of apo-SAA (Mr 11 500; 104 amino acids) at the 76–77 serine–leucine bond yields amyloid A protein (residues 1–76 of apo-SAA) (Parmelee et al. 1982). During an ill-

Submitted to Nature 6/8/93

The 3D structure of pentameric human serum amyloid P component defined at 2Å resolution reveals a lectin-like fold and calcium-mediated ligand binding

Jonas Emsley*, Helen E. White*, Bernard P. O'Hara†, Glaucius Oliva‡, Narayanaswamy Srinivasan, Ian J. Tickle, Tom L. Blundell, Mark B. Pepys§ & Steve P. Woodll

Laboratory of Molecular Biology, Department of Crystallography, Birkbeck College, London WC1E 7HX, UK

§Immunological Medicine Unit, Royal Postgraduate Medical School, Hammersmith Hospital, London W12 0NN, UK

*Joint first authors

llTo whom correspondence should be addressed.

Current addresses: †Department of Biochemistry and Molecular Biology, University College, London; ‡Instituto de Fisica e Quimica de Sao Carlos, Departamento de Fisica e Ciencia dos Materials, Universitade de Sao Paulo, Sao Carlos, Brazil

The three-dimensional structure of pentameric human SAP at high resolution, the first reported for a pentraxin, reveals that the tertiary fold is remarkably similar to that of the legume C-type lectins. Carboxylate and phosphate compounds bind directly to two calcium ions; interactions with a carboxyethylidene ring are mediated by Asn59 and Gln148 ligands of the calciums. These X-ray studies indicate the probable modes of binding of the biologically important ligands, DNA and amyloid fibrils.

HUMAN serum amyloid P component (SAP) is a decameric plasma glycoprotein composed of identical subunits non-covalently associated in two pentameric rings interacting face-to-face. SAP binds to all forms of amyloid fibril[1] and is universally present in amyloid deposits, including the cerebral amyloid of Alzheimer's disease[2]. Although SAP is not required for amyloid fibrillogenesis *in vitro*, it may protect the fibrils from degradation *in vivo*[3]. SAP is also the major DNA and chromatin binding protein of plasma[4,5] and other autologous ligands for SAP include fibronectin, C4-binding protein[6] and glycosaminoglycans[7]; SAP is also a normal tissue matrix constituent associated with elastic fibres[8] and the glomerular basement membrane[9]. Finally, SAP is a calcium-dependent lectin, the best characterised ligand of which is the 4,6-cyclic pyruvate acetal of β-D-galactose (MOβDG)[10].

Human SAP shows no polymorphism or heterogeneity of its protein or its glycan[11] and no individual deficient in SAP has yet been described, suggesting that the molecule has important functions. Furthermore, SAP and C-reactive protein (CRP), the classical acute phase protein with which it shares over 50% sequence identity, belong to the pentraxin family of plasma proteins which have been stably conserved throughout vertebrate evolution[12,13]. The structure and structure-function relationships of SAP are thus of considerable fundamental interest, in addition to their clinical importance which arises from the invaluable new information provided by use of radio-labelled SAP as a specific quantitative *in vivo* tracer for amyloid deposits[14].

Recently we reported the crystallisation of SAP in conditions that induce a reversible dissociation of the decamer into a pentameric form[15]. We now report the X-ray analysis of the crystals at 2Å resolution, defining the complete three-dimensional structure of the pentamer. This human plasma protein has a tertiary fold which resembles that of the legume C-type lectins, concanavalin A and pea lectin. There are two calcium sites and these are shown to be involved in binding of carbohydrate and the synthetic ligand phosphoethanolamine. However, the calcium sites in SAP and the calcium and manganese sites of concanavalin A differ in their relationship to the common topology. The SAP pentamer shows nearly perfect five-fold symmetry and sequence comparisons suggest that very similar interactions are retained in CRP pentamers.

Three-dimensional structure

Serum amyloid P component was isolated at greater than 99% purity from pooled human ascites and pleural effusion fluids[16]. The crystals obtained at pH 5.5 in a medium containing calcium and acetate ions as described earlier[15] were of space group $P2_1$ and cell dimensions a = 68.9Å, b = 99.3Å, c = 96.7Å and $\beta = 95.9°$. The initial model of pentameric SAP was based on X-ray analysis at 2.8Å resolution using the multiple isomorphous replacement (MIR) technique followed by solvent flattening[17] and five-fold molecular averaging[18]. The refinement statistics are shown in Table 1, the legend of which gives further details of the X-ray analysis. The final model was refined at 2.0Å resolution to an agreement (R) value of 0.18 to give a clear electron density for all residues of the five subunits (see Fig. 1*a*).

The SAP pentamer consists of five subunits of 204 amino acid residues, each with a closely similar three-dimensional structure constructed from anti-parallel β-strands (A-O) arranged in two sheets as shown in Fig. 2*a*. The tertiary fold can be envisaged as a jellyroll of strands ABCDKLNO, elaborated by the addition of three further anti-parallel strands (EFG and HIJ) forming a β-meander at the same end of each of the sheets to give the topology: +11-9+7-1-1-1-3+1+1+5-9-1+12-13. In this arrangement strands A and M

are both hydrogen bonded to strand L as shown in Fig. 3. The disulphide between Cys36 and Cys95 links the two adjacent strands (L and C) of one β-sheet. A long α-helix between strands L and M is folded on top of this β-sheet. There is also an N-linked oligosaccharide at Asn32 on this sheet; only one saccharide residue is visible in the electron density.

The hydrophobic core between the two sheets is comprised mainly of tryptophans, tyrosines, phenylalanines and leucines. The core is closed off by two β-arches between the two sheets; strands joining B to C and J to K are hydrogen bonded and anti-parallel, an arrangement characteristic of proteins derived from a jellyroll motif. One end of the core, formed by 11 residues at the N-terminus and those in the N and O strands at the C-terminus (Figs. 2, 3*)*, has hydrophobic residues accessible to solvent. The other end of the core is involved in interactions with a neighbouring protomer (see below) and so is inaccessible to solvent.

Tertiary fold comparisons

The similarities of the amino acid sequences of SAP, human CRP, CRP of the arachnid *Limulus polyphemus* (the horseshoe crab), and hamster SAP suggest that they may have similar three-dimensional structures. Comparative modelling[19] shows that these pentraxins can have equivalent anti-parallel structures with insertions and deletions in the loops between the β-strands and α-helices (Srinivasan, N., White, H.E. & Blundell, T.L. *unpublished results)*. Fig. 4 shows that most solvent-inaccessible aromatic side-chains are conserved to give compact hydrophobic cores in all members of the family.

The jellyroll topology of the pentraxins is reminiscent of that of the picornavirus coat proteins, which also have pentameric structures. However, pentraxins resemble most closely legume lectins such as concanavalin A[20] and pea lectin[21] (Fig. 2*a*). In each case the arrangement of strands is identical but the N- and C- termini are in different positions (Fig. 3). In pea lectin the N-terminus is at strand M and the C-terminus at strand L (labelling of the topologically equivalent strands follows those in SAP as shown in Fig. 3).

The strands A and M are both hydrogen-bonded to strand L in a similar manner to those in SAP. In the three-dimensional structure of concanavalin A the N-terminus is at strand E and the C-terminus at the end of strand D due to a post-translational cleavage which follows ligation of the true termini between strands L and M[22]. Pea lectin is additionally cleaved at the loop connecting strands I and J.

Alignment of sequences (Fig. 4) on the basis of topologically equivalent features of the three-dimensional structures[23] shows that helices occupy different positions in the pentraxins and legume lectins and that the amino acid sequences of the two families have identities of only ~11%. The two main helices in SAP occur before and after strand L, whereas the helices in the legume lectins occur at the C-terminus of strand J. There is a long insertion between the end of the helix after strand D and the beginning of strand E in the lectins relative to the pentraxins. Strands G, H and I, together with the type IV β-hairpin between H and I, are identical in both SAP and pea lectin. The so-called pentraxin octapeptide signature sequence, H X C X S/T W X S, is in this region, but this is not conserved in the legume lectins.

Structure of the pentamer and decamer

The structure of the pentamer is shown in Fig. 2*b*. The five subunits are arranged in a ring with a hole that is 20Å in diameter and 35Å deep at the centre. The two layers of β-strands in each subunit are in planes normal to the five-fold axis. Strands G, I, J of one protomer interact with strand N and loops between strands A and B, C and D, G and H, K and L of an adjacent protomer (Fig. 2*b*). When SAP is overlaid on the pea lectin, strand J does not give as good a fit as other strands. In SAP this strand has moved to provide inter-protomer contacts, with all residues between Pro113 and Leu119 being involved. The subunit interactions consist of hydrogen bonds between main chain peptide groups, three salt bridges and some hydrophobic contacts, in contrast to other pentameric systems where there are often inter-subunit β-sheets. The surface area of the protomer that is buried on formation of the pentamer is 410.5Å^2, comprising 15.4% of the total surface of

the protomer. The residues involved in these extensive interactions and which account for the considerable stability of the SAP pentamer are shown in Fig. 4.

In contrast the SAP decamer is readily dissociated by reducing the pH to 5.5. The simplest explanation for this is that the decamer is stabilised by ionic interactions involving carboxylate and/or imidazole groups. Electron microscopy has clearly shown that the SAP pentamers are packed face-to-face[24] and it seems probable that the faces in contact are those carrying the α-helix since we show (see below) that the calcium-dependent ligand-binding sites are on the other face and such binding is exhibited by the decamer. Furthermore adjacent sites are accessible to chymotryptic cleavage in the decamer in the absence of calcium ions. It is not clear which groups are involved in the decamer stabilisation although Glu167, positioned on the helix, is a likely candidate. A compact decamer can be modelled if the pentamer five-fold axes are in line but the subunits are out of step, allowing the helices from one layer to pack between those of the opposite layer. Structure analysis of a crystal form produced at neutral pH with ten protomers in the asymmetric unit is in progress.

The models of CRP and hamster SAP demonstrate that the pentamers can have very similar inter-subunit interactions. *Limulus* CRP is hexameric[25] and we have also been able to construct this arrangement of protomers by operating with a six-fold axis placed slightly further from the subunit than the five-fold axis of SAP.

Calcium binding site

In serum amyloid P component we have identified two large spheres of density which are too heavy to be oxygen atoms and are in positions that imply the presence of calcium ions, between 4.0Å and 4.3Å apart in the five subunits and bridged by a common side-chains. Calcium (1) is coordinated to the side chains of Asp58, Asn59, Glu136, Asp138 and the main-chain carbonyl of Gln137 (Fig. 5*a*). Unlike many calcium-binding sites in proteins, such as parvalbumin, the coordinating residues come from different parts of the sequence. This is achieved by a distortion at the start of strand E carrying residues Asp58 and Asn59

56
SERVIÇO DE ... INFORMAÇÃO ... FÍSICA

and the region containing Glu136 and Asp138 looping over towards calcium (1) (Fig. 5*a*). The calcium ligation is likely to be an important local structural determinant. The seventh coordination site is occupied by a ligand that has the appearance of an acetate ion from the crystallisation buffer in protomers 1, 2, 4 and 5, but in protomer 3 this position is filled by the side-chain of Glu167 of an adjacent molecule in the crystal lattice. Glu136, Asp138 and the acetate/lattice contact form a bridge to a second, more loosely bound calcium ion (2). The coordination of calcium (2) is completed by Gln148 and two water molecules. In a cross-phase difference Fourier of cerium sulphate soaked crystals, we find that calcium (2) is displaced by a cerium ion. Calcium (2) is also removed when the crystals are soaked in calcium free buffers. These observations are consistent with the more solvent accessible position and fewer protein ligands of calcium (2).

Residues which provide ligands to the calcium ions are conserved in all SAPs but although Asp58 is found in hamster SAP, human CRP and *Limulus* CRP it varies in other CRPs. Nevertheless, the general organisation of the site is probably retained. The disposition of these groups on surface loops where sequence differences accumulate could explain the considerable change in calcium affinity between CRP and SAP. In CRP there is evidence that both calciums bind with the same affinity at neutral pH[26] whereas in SAP our results show that site calcium (2) has fewer protein ligands and can be preferentially unloaded. The tighter calcium binding and equivalence of the sites in CRP could also be due to the substitution of Asp145 in SAP by glutamate in CRP. The longer side-chain in CRP would permit a full complement of protein ligands to calcium site (2).

The existence of two metal ions bridged by protein ligands is reminiscent of concanavalin A. However, although the metal binding sites in the legume lectins are on the same face of the protein, they are at a different position between strands E and F compared to D and E on SAP. There are no ligands of the two calciums that are topologically equivalent to those for the calcium and the manganese of the lectins. Thus, although there is evidence for divergent evolution of the protein folds of the plant lectins and the pentraxins, this is not supported by a conservation of similar metal binding sites.

Ligand binding

SAP binds to methyl 4,6-O-(1-carboxyethylidene)-β-D-galactopyranoside (MOβDG) which is not recognised by CRP. Fig. 1*b* shows the electron density for MOβDG complexed with SAP. The sugar derivative binds directly through the acidic group to the two calcium ions in a similar way to the acetate which it replaces. The other interactions include two hydrogen bonds formed between the 4,6 oxygen atoms of the ring and the amide nitrogen atoms of Gln148 and Asn59 respectively, each of which bind to the calcium ions through their amide oxygens (Fig. 5*b*). Thus the role of calcium is not to bind the galactopyranoside ring directly but rather to mediate its binding by orienting side-chain amides in a way that resembles saccharide binding in lectins. There is only one hydrogen bond to the galactopyranoside ring (Fig. 5*b*). Thus it is the methyl 4,6-O-(1-carboxyethylidene) ring that forms the main interactions with the protein, explaining why neither the non-cyclic acetal of MOβDG nor the simple monosaccharides bind[3,10,27]. The R-isomer bridge methyl group points into a hydrophobic pocket formed by Leu62, Tyr64 and Tyr74. The differences in the hydrophobic pocket and the ligand distribution at the calciums in CRP may explain the poor binding to MOβDG. It is probable that this site is involved in binding to amyloid fibrils, and its specificity is further discussed in the accompanying paper[27].

The highest affinity interaction of human CRP is its calcium-dependent binding to phosphocholine (PC). Studies carried out on human CRP[28,29] have implicated amino acid residues 50-60 in the ability to bind PC while more recent mutagenesis experiments[30] have identified Lys55 and Arg56 as key residues. The native SAP structure shows that Asp58 and Asn59 from this loop are involved in coordinating one of the two calcium ions. Human SAP, in contrast, does not bind to PC although in common with CRP it does bind to phosphoethanolamine (PE). The electron density maps for SAP co-crystallised with PE (Fig. 1*c*) show a major site in all subunits, which coincides with that which binds acetate ions and MOβDG and indicates a direct interaction between the phosphate group and both calcium ions. In contrast to MOβDG this interaction with PE displaces Glu167 from its

intermolecular interaction with the calciums of protomer 3, explaining the observed disturbance of crystal packing. Binding of MOβDG or PE in the common site probably stabilises the whole calcium binding region including Asn59 which binds MOβDG and calcium and Asp58 which binds calcium. Both PE and PC probably bind at the calcium in CRP.

SAP rapidly aggregates in neutral solutions in the presence of calcium ions presumably due to intermolecular interactions involving the surface of the decamer with the exposed calcium binding site. This is consistent with the observation that this interaction can be inhibited by MOβDG[31] and by PE[27]. Similarly they compete for the calcium site with Glu167 which is an important lattice contact in the pentamer crystals.

In the presence of calcium SAP also binds polyanions such as heparan sulphate, dermatan sulphate[7] and DNA[4]. It has been suggested that the DNA interaction involves a decapeptide around Arg120, with some resemblance to certain histone sequences, and for which a helical structure was proposed[32]. However, in human SAP this region is not helical and other SAPs do not have arginine at this position. Nevertheless it does have affinity for multivalent anions, as demonstrated by the binding of phosphotungstate at this site in the heavy atom isomorphous derivative (see Table 1). There are several basic patches in SAP, for example Arg120, Arg77, His78, Lys79 and Arg57, which are on the same surface as the calcium and PE binding sites. It seems more likely that the phosphate backbone of DNA and the sulphated polysaccharides bind both at the calciums and at the basic sites, possibly on more than one subunit simultaneously. These extensive interactions probably account for the ability of SAP to displace from DNA the H1-type histones in chromatin[5]. The sequence differences in the basic regions and in the calcium binding region could explain the variable affinity for DNA shown by different pentraxins. Human CRP, for instance, only binds DNA at low, non-physiological ionic strength. Low concentrations of both PE and MOβDG enhance the binding of SAP to DNA and both compete with the interaction at high concentration[27]. Similar effects are observed for SAP binding to immobilised PE[27]. As we can find no evidence for a second binding site for PE

or MOβDG in the present experimental conditions, these effects must be mediated through inter-subunit interactions.

Ligands for SAP, such as PE in phosphatidylethanolamine and MOβDG-like sugars[33], are common in microorganisms. In this respect SAP resembles CRP[13] and the mammalian C-type lectin, mannose-binding protein[34], which both recognise widely distributed microbial epitopes and are involved in host defence against infection. SAP could act either directly or via complement, since aggregated or complexed SAP[5,35] like mannose-binding protein[34] and CRP[13], can activate the classical complement pathway.

Proteinase-resistance of pentraxins and the treatment of amyloidosis

SAP and CRP are both remarkably resistant to proteolytic degradation in the presence of calcium. In contrast, in the absence of calcium both are cleaved by some enzymes, particularly α-chymotrypsin and pronase[26,36]. Although this cleavage does not cause fragmentation of either the whole molecule or of the individual subunits under non-denaturing conditions, it does cause loss of calcium-binding activity by the pentraxins and abolishes their capacity for calcium-dependent ligand binding. It is, therefore, of interest that the major site of cleavage of SAP is between residues 144 and 145 whilst in CRP it is between residues 146-147 (pronase) or 145-146 (Nagarse protease). This is part of a loop that is held in place by calcium ligation, and which, in the calcium-free form, may be only loosely associated with the body of the protein and, therefore, susceptible to proteolysis. Most loops of SAP are held close to the body of the pentamer and this makes them less easily accessible to the active sites of proteolytic enzymes.

Resistance to proteinase digestion is likely to be an important aspect of the normal function of SAP, and may also contribute to the persistence of amyloid deposits. The SAP normally associated with the glomerular basement membrane and the surface of elastic fibre microfibrils[8,9] may protect these extracellular matrix constituents from inappropriate degradation. On the other hand, amyloid fibrils are abnormal extracellular structures which should be recognised and degraded, but which nevertheless persist *in vivo*. In this

pathological situation the binding of SAP to amyloid fibrils may be responsible. Protection could result simply from coating by SAP, which is completely unaltered with respect to its normal circulating form[11], and which would, therefore, not be expected to trigger macrophage activation or phagocytosis. However, the proteinase resistance of SAP itself may be a significant factor. Availability of the complete high resolution structure of SAP and its ligand-binding site now offer the opportunity for direct modelling of competitive inhibitors of SAP binding and for engineering binding site homologues, either of which could be used as drugs to displace SAP from amyloid deposits *in vivo*. This would open up new avenues for treatment of amyloidosis, enabling the body to mobilise and degrade the fibrils which may otherwise be inappropriately protected by SAP.

1. Pepys, M.B., Dyck, R.F., de Beer, F.C., Skinner, M. & Cohen, A.S. *Clin. exp. Immunol.* **38,** 284-293 (1979).

2. Coria, F., *et al. Lab. Invest.* **58,** 454-458 (1988).

3. Hind, C.R.K., Collins, P.M., Caspi, D., Baltz, M.L. & Pepys, M.B. *Lancet* ii, 376-378 (1984).

4. Pepys, M.B. & Butler, P.J.G. *Biochem. Biophys. Res. Comm.* 148, 308-313 (1987).

5. Butler, P.J.G., Tennent, G.A. & Pepys, M.B. *J. exp. Med.* **172,** 13-18 (1990).

6. de Beer, F.C., Baltz, M.L., Holford, S., Feinstein, A. & Pepys, M.B. *J. exp. Med.* **154,** 1134-1149 (1981).

7. Hamazaki, H. *J. biol. Chem.* **262,** 1456-1460 (1987).

8. Breathnach, S.M., *et al. Nature* **293,** 652-654 (1981).

9. Dyck, R.F., *et al. J. exp. Med.* **152,** 1162-1174 (1980).

10. Hind, C.R.K., *et al. J. exp. Med.* **159,** 1058-1069 (1984).

11. Pepys, M.B., *et al. Proc. 41st ASMS Conference on Mass Spectrometry and Allied Topics,* San Francisco, California, May 30-June 4, 1993 (in press).

12. Pepys, M.B., *et al. Nature* **273,** 168-170 (1978).

13. Pepys, M.B. & Baltz, M.L. *Adv. Immun.* **34,** 141-212 (1983).

14. Hawkins, P.N., Lavender, P.J. & Pepys, M.B. *New Engl. J. Med.* 323, 508-513 (1990).

15. Wood, S.P., *et al. J. molec. Biol.* **202,** 169-173 (1988).

16. Hawkins, P.N., Tennent, G.A., Woo, P. & Pepys, M.B. *Clin. exp. Immunol.* **84,** 308-316 (1991).

17. Wang, B.C. *Meth. Enzymol.* **115,** 90-112 (1985).

18. Bricogne, G *Acta Cryst.* **A32,** 832-847 (1976).

19. Sali, A., Overington, J.P., Johnson, M.S. & Blundell, T.L. *Trends Biochem. Sci.* **15,** 235-240 (1990).

20. Hardman, K.D. & Ainsworth, C.F. *Biochemistry* 11, 4910-4919 (1972).

21. Einspahr, H., Parks, E.H., Suguna, K., Subramanian, E. & Suddath, F.L. *J. biol. Chem.* **261,** 16518-16527 (1986).

22. Carrington, D.M., Auffret, A. & Hanke, D.E. *Nature* **313,** 64-67 (1985).

23. Sali, A. & Blundell, T.L. *J. mol. Biol.* **212,** 403-442 (1990).

24. Pepys, M.B., *et al. Lancet* **i,** 1029-1031 (1977).

25. Tennent, G.A., *et al. Eur. J. Biochem.* **214,** 91-97 (1993).

26. Kinoshita, C.M., *et al. Biochemistry* **28,** 9840-9848 (1989).

27. Emsley, J. *et al. Nature* (submitted for publication).

28. Swanson, S.J. & Mortenson, R.F. *Molec. Immun.* **27,** 679-687 (1992).

29. Liu, T.-Y. *et al. J. Protein Chem.* **6,** 263-272 (1987).

30. Agrawal, A., Xu, Y., Ansardi, D., Macon, K.J. & Volanakis, J.E. *J. biol. Chem.* **267,** 25352-25358 (1992).

31. Hind, C.R.K., Collins. P.M. & Pepys, M.B. *Biochim. Biophys. Acta* 802, 148-150 (1984).

32. Turnell, W.G., Satchwell, S.C. & Travers, A.A. *FEBS Lett.* **232,** 263-268 (1988).

33. Hind, C.R.K., Collins, P.M., Baltz, M.L. & Pepys, M.B. *Biochem. J.* 225, 107-111 (1985).

34. Hartshorn, K.L.,*et al. J. clin. Invest.* **91,** 1414-1420 (1993).

35. Ying, S.C., Gewurz, A.T., Jiang, H. & Gewurz, H. *J. Immunol.* **150:** 169-176 (1993).

36. Kinoshita, C.M., *et al. Protein Sci.* **1,** 700-709 (1992).

37. Jones, T.A. *J. appl. Cryst.* **11,** 272-282 (1978).

38. Brunger, A.T., Karplus, M. & Petsko, G.A. *Acta Cryst.* **A45,** 50-61 (1989).

39. Haneef, I., Moss, D.S., Stanford, M.J. & Borkakoti, N. *Acta Cryst.* A41, 426-433 (1985).

40. Ramachandran, G.N., Ramakrishnan, C. & Sasisekharan, V. *J. molec. Biol.* **1,** 95-99 (1963).

41. Evans, S.V. *J. molec. Graphics* **11,** 134-138 (1993).

42. Hutchinson, E.G. & Thornton, J.M. *Proteins* **8,** 203-212 (1990).

43. Kabsch, W. & Sander, C. *Biopolymers* **22,** 2577-2637 (1983).

44. Overington, J.P., Johnson, M.S., Sali, A. & Blundell, T.L. *Proc. roy. Soc. London ser. B* **241,** 146-152 (1990).

ACKNOWLEDGEMENTS. This work was supported by project and programme grants from the MRC. We thank Prof D.M. Blow FRS for use of film scanning facilities at Imperial College, Dr R. Pickersgill, AFRC Institute of Food Research, Reading for data collection on the uranyl derivative, Dr R. Laskowski for running LOCROT, D. Carvin and Dr. G Louie for helpful discussions, and Ms J. Ruth Gallimore and Ms Glenys A. Tennent for technical assistance.

Legend for TABLE 1

Heavy atom derivatives used for multiple isomorphous replacement and data collection statistics are shown in Table 1. Native data were collected from one crystal on a Hilger-Watts 290 4-circle diffractometer with Rsym = 4.5% for 4112 independent reflections to 5.6Å. High resolution native data were also collected on film at the Synchrotron Radiation Source at Daresbury Laboratory (l= 1.468Å) using three crystals (Rsym = 7.7% for 78951 unique reflections to 2.02Å). The final merged data set comprised low resolution data from the diffractometer and high resolution data from the synchrotron. The major heavy atom sites were determined from inspection of difference Patterson functions and cross-phase difference Fouriers. A multiple isomorphous replacement (MIR) map was calculated, solvent flattened and averaged. Phases from both maps were used in cross-phase difference Fouriers to determine those minor sites related by the 5-fold axis to the major sites. All sites were initially refined with VECREF (I.J. Tickle) to eliminate spurious sites and then with PHARE. A final MIR map was calculated to 2.8Å and the phasing analysis gave a figure of merit of 0.61. This map was solvent flattened[17], phases calculated and recombined with the MIR phases to give a combined figure of merit of 0.85. The solvent flattened map was then averaged using PSAVER (I.J Tickle) and the envelope determined in the solvent flattening. The polypeptide of the β-sheet and helix were well defined. Derivative data were also scaled to native data collected from three crystals on a FAST area detector mounted on a CuKα microfocus tube (800W) (Rsym = 10.0% for 30996 independent reflections to 2.8Å). Heavy atom sites were determined independently from those in Table 1 and were refined using MLPHARE. The resulting electron density map was solvent flattened and averaged using the programs supplied with O release 5.7. The map was similar to that used for the refinement. Problems in obtaining an interpretable map arose because not all substituted sites related by the non-crystallographic

symmetry were present on early cross-phase difference Fouriers due to poor phasing from the derivatives available at the time. Two of the three derivatives with the highest phasing power were the last to be collected. These extra derivatives allowed minor sites related to the major sites by the 5-fold axis to be determined in the early derivatives as well as multiple occupancy in some sites previously thought to be singly occupied. For example the dominant thorium nitrate derivative formed a complex with eleven thorium sites comprising two octahedra, each with edges of approximately 4Å and sharing an apex.

The direction of the 5-fold axis was determined from a self-rotation function[15], and the approximate position of the molecule on this axis was found by positioning a pentagonal prism in a low resolution MIR map. A six-dimensional search (3 rotations and 3 translations) for a best correlation in the map for a given rotational operation was performed using LOCROT (I.J. Tickle). The parameters were then refined with the density correlation programs of Bricogne[18].

One averaged subunit of the electron density map obtained from the solvent flattening was displayed in FRODO[37] on an Evans and Sutherland PS390. The sequence could be assigned from the position of the disulphide bridge and the putative calcium binding site for all residues in the sheets and helix. The resolution was extended with simulated annealing using non-crystallographic restraints in XPLOR[38] and rebuilding into electron density maps (coefficients 2Fo-Fc,Fo-Fc) calculated from phases that had been combined with the MIR phases until all residues had been inserted. The resolution was then extended to 2Å and 10 calcium ions, 4 acetate ions and 879 water molecules were added. Least squares refinement in RESTRAIN[39] gave a crystallographic R-factor of 0.179 for all 78910 reflections in the resolution range 8-2Å. The r.m.s. deviations from stereochemical ideality are 0.017Å for bond distances and 3.45° for bond angles. The average isotropic B values are 22.9Å^2 for protein and 37.7Å^2 for solvent molecules. There were no residues in the

disallowed region of a Ramachandran plot[40]. The CCP4 suite of programs (SERC Daresbury) has been used for all crystallographic calculations, except the structural refinement.

Merging R factor $\sum_{hkl} \sum_{i=1}^{n} |I(hkl)_i - I(hkl)| / \sum_{hkl} \sum_{i=1}^{n} I(hkl)_i$

Isomorphous R factor $\sum_{hkl} |F_{deriv}(hkl) - F_{nat}(hkl)| / \sum_{hkl} |F_{nat}(hkl)|$

Phasing power $[\sum_{hkl} F^{2}_{heavy}(hkl)| / \sum_{hkl} e^{2}(hkl)]^{1/2}$

FIG. 1 Final refined electron density of SAP. *a*, Refined electron density map (2Fo-Fc) calculated at 2Å resolution and contoured at 1 r.m.s. This illustrates the SAP helix packing against the b-pleated sheets in the region of the disulphide bridge Cys36-Cys95. The top left hand of the diagram illustrates a region where the side chain Glu167 contacts the calcium binding site of a symmetry-related molecule. The region of the calcium ions is contoured at 5 r.m.s. showing that the glutamate bridges the two ions in a manner similar to the acetate ion. *b*, MOβDG complexed with SAP contoured at 1 r.m.s. electron density level at 2.9Å resolution. Crystals of SAP prepared by the batch method[15] in the presence of MOβDG were isomorphous with crystals of native SAP and had cell dimensions a=69.06Å, b=99.3Å, c=96.75Å and b=95.84°. Data were collected on a MAR imaging plate system mounted on a Siemens XP-18 rotating anode and a final R_{Merge} of 5.3% was obtained. Data were 95.8% complete to 2.9Å resolution. A final crystallographic R factor of 0.197 for all reflections in the range 10-2.9Å was obtained after refinement in XPLOR without non-crystallographic restraints. The success of this experiment depended on soaking in an excess of the sugar in order displace the acetate ion which otherwise occupies the same position at the calcium-binding site. The MOβDG is well defined only in protomer 3, shown here, where it is involved in a crystal contact. *c*, Phosphoethanolamine (PE) complexed with SAP contoured at 1 r.m.s. electron density level at 2.9Å resolution. Crystals of SAP prepared by the batch method[15] in the presence of 9 mM PE were not isomorphous with crystals of native SAP and had cell dimensions a=67.05Å, b=103.43Å, c=102.43Å and b=95.73°, in space group $P2_1$. Data were collected on a MAR imaging plate system mounted on a Siemens XP-18 rotating anode and a final R_{Merge} of 6.4% was obtained. Data were 95.5% complete to 2.9Å resolution. In the initial refinement the SAP pentamer was treated as single rigid body and R factor of 0.332 was obtained for the 3513 reflections between 30-6Å. The five subunits were then treated as individual rigid bodies and refinement produced an R factor

of 0.264 for the 11628 reflections between 18-4Å.. The final crystallographic R factor of 0.199 for all reflections in the range 10-2.9Å was obtained after refinement in XPLOR; non-crystallographic symmetry restraints were not applied.

FIG. 2 Ribbon drawings generated with Setor[41] with b-strands shown as blue arrows, helices as ribbons and loops as cords. *a*, The topology of SAP compared with the legume C-type lectin concanavalin A (conA). The strands are labelled from the N- terminus of SAP, ABCDEFGHIJKLMNO, with structurally equivalent strands in conA labelled similarly. The positions of the N- and C-termini in conA are altered with respect to the nascent protein by ligation of the original N- and C- termini and proteolytic cleavage between strands D and E. The two structures can be superimposed by a least squares fit using the Cα positions of the two sets of anti-parallel sheets to produce an r.m.s. deviation of 2.4Å. This is due to a greater angle between these sheets in SAP than conA. *b*, Structure of the pentamer of SAP viewed along the non-crystallographic five-fold axis of symmetry. The pairwise r.m.s. deviations for all main chain atoms range from 0.19Å between protomers 1 and 5 to 0.24Å between protomers 3 and 4.

FIG. 3 Hydrogen bonding diagrams generated by HERA[42] for SAP (above) and pea lectin (Brookhaven code 2LTN) (below). The secondary structural elements were assigned according to the criteria defined by Kabsch and Sander[43].

FIG. 4 Alignment of the sequences of the pentraxins (one protomer sapm and one pentamer sapp) of SAP, human C-reactive protein (hcrp), hamster SAP (female hamster protein) (1fhp) and *Limulus* CRP (1lim) with the sequences of legume lectins, concanavalin A (3cna) and pea lectin (2ltn and 1lte). These alignments are based on comparing the three-dimensional structure of SAP with

those of the C-type legume lectins[23]. Key to JoY alignments[44]: Solvent inaccessible, UPPER CASE X; solvent accessible, lower case x; positive ϕ, *italic x*; *cis*-peptide, breve x; hydrogen bond to other sidechain, tilde x̃; hydrogen bond to mainchain amide, **bold x**; hydrogen bond to mainchain carbonyl, underline x; disulphide bond, cedilla x̧; metal binding sites in SAP and conA, *; residues of SAP involved in inter-protomer contacts ¶.

FIG. 5 The calcium and ligand binding sites in SAP. Diagrams generated using Setor[41] Important interactions between calcium ions, ligands and the protein are shown by dotted lines. *a*, Topology around the calcium binding site showing the residues involved in calcium coordination and those in the hydrophobic pocket, (Leu62, Tyr64, Tyr74) and the cleavage site (Phe144, Asp145) in SAP. Calcium (1) has heptagonal coordination, whilst Calcium (2) has hexagonal coordination. *b*, MOβDG binding site. The main interaction involves coordination between the calcium ions and the carboxylate of the carboxyethylidene ring. The amide nitrogens of Asn59 and Gln 148 form hydrogen bonds to the 4,6 oxygens of the carboxyethylidene ring. The only interaction between the protein and the galactopyranoside ring is a hydrogen bond between the 3 oxygen and the amide nitrogen of Gln148.

TABLE 1 Structure determination of SAP

DERIVATIVE	K_2PTI_6	$Na_3PO_4.12WO_3$	$Th(NO_3)_4$	$Th(NO_3)_4$	$Ce(SO_4)_2$	K_2AuCl_4	UO_2SO_4	$AgNO_3$	Na_2WO_4
CONCENTRATION (mM)	5.0	5.0	4.5	4.5	17.0	2.5	25.0	5.0	11.0
SOAKING TIME (h) at 20°C	24.0	60.0	28.0	28.0	48.0	1.0	24.0	24.0	19.0 (4°C)
COLLECTION DEVICE	F	F	F	F	F	F	X	I	D
RESOLUTION (Å)	3.5	3.5	4.1	2.8	3.0	3.5	3.2	3.4	6.0
MERGING R FACTOR	0.084	0.069	0.062	0.049	0.101	0.110	0.045	0.118	0.075
ISOMORPHOUS R FACTOR	0.317	0.237	0.203	0.278	0.222	0.310	0.251	0.165	0.225
% COMPLETE	88.3	80.3	91.7	85.8	76.7	71.1	81.0	93.4	97.1
NUMBER OF SITES	28	21	17	14	27	22	22	26	-
PHASING POWER	1.00	1.15	1.43	2.02 (4.1-2.8Å)	1.02	1.55	1.29	1.04	-

D, Enraf-Nonius CAD-4 diffractometer mounted on a 1500W sealed tube; F, Enraf-Nonius FAST area-detector mounted on a Cukα microfocus tube (800W); X, Siemens Xentronics area-detector mounted on a Siemens XP18 generator; I, MAR research imaging plate mounted on a Siemens XP18 generator.

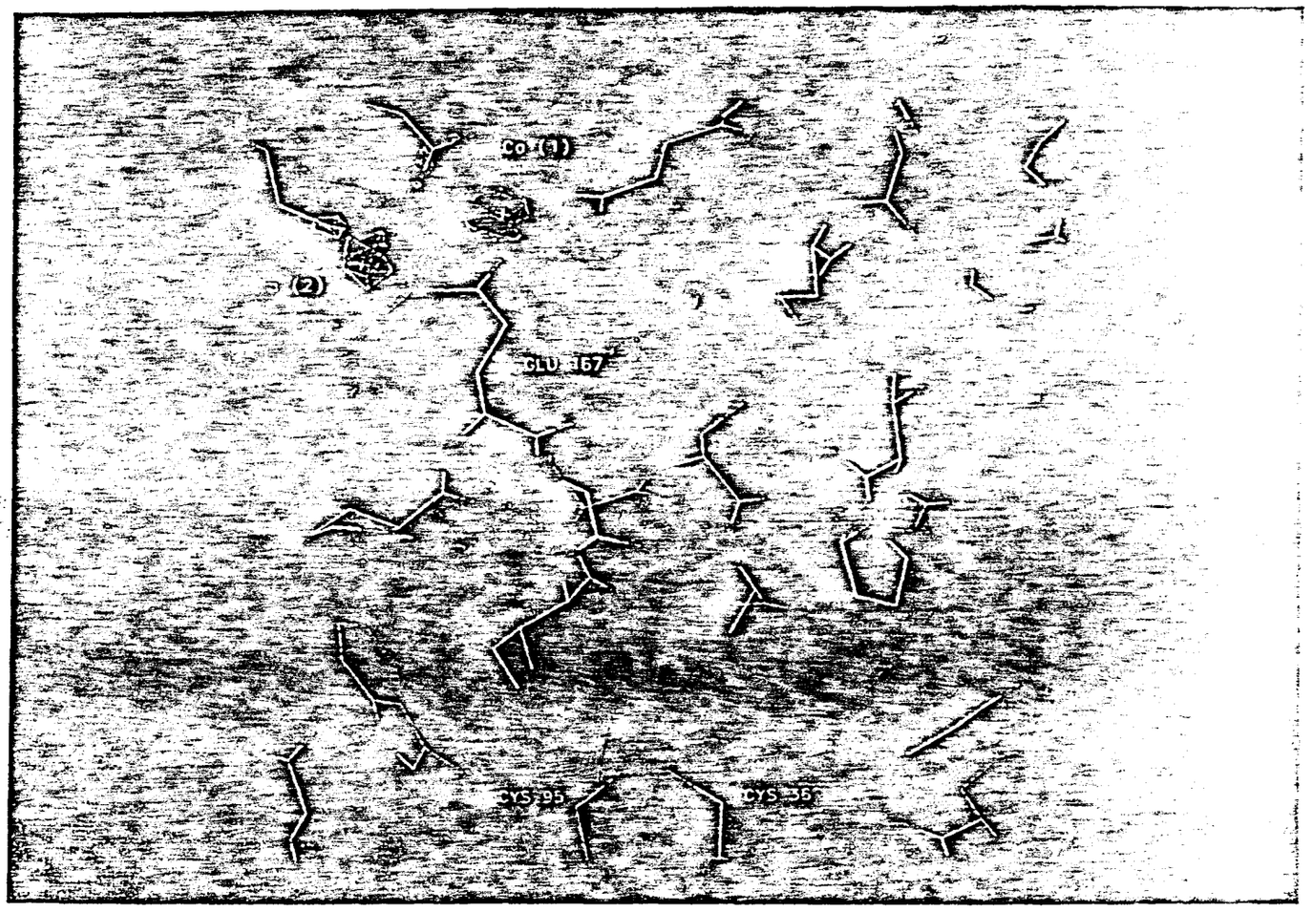

Fig. 1a

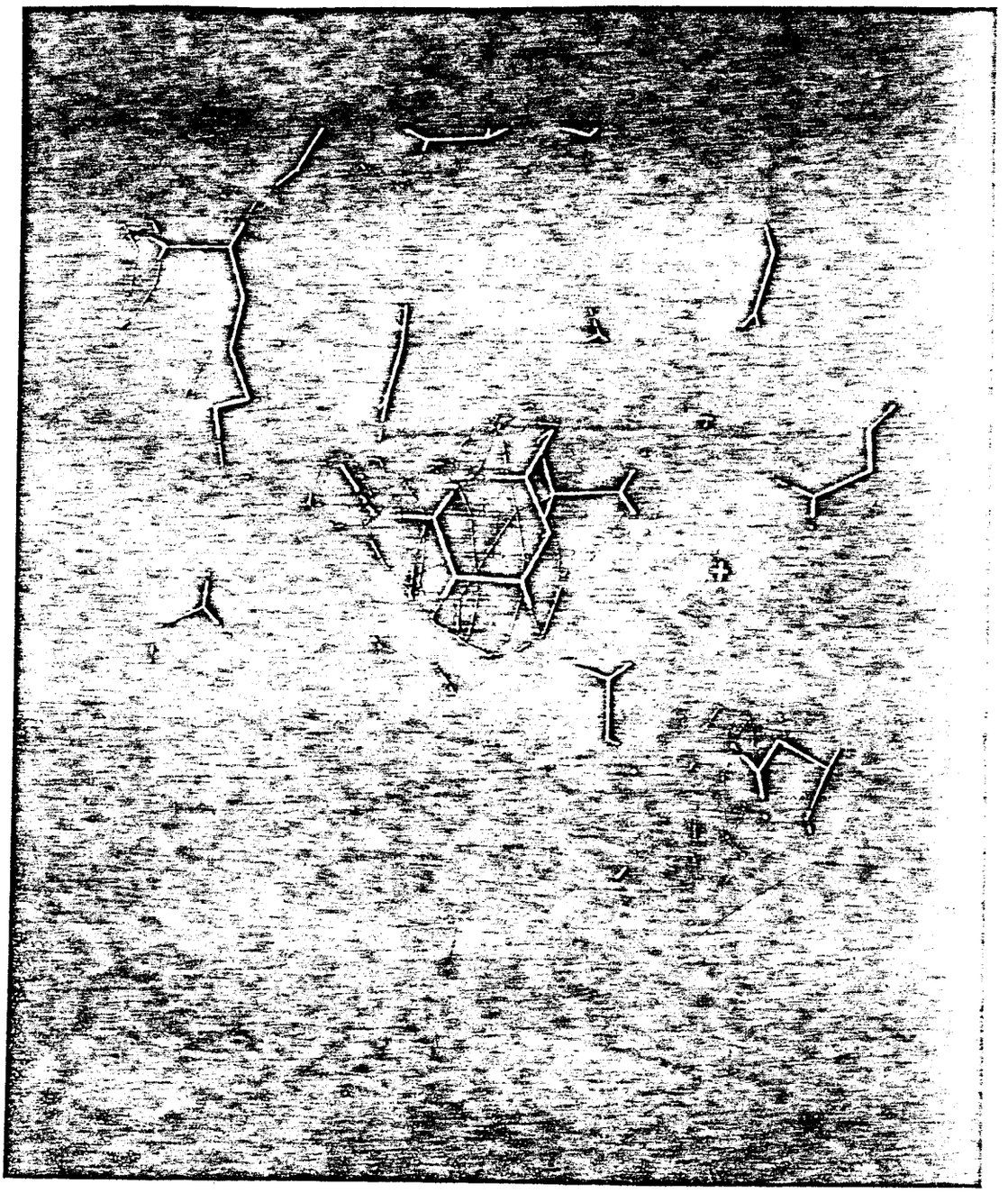

Fig. 1b

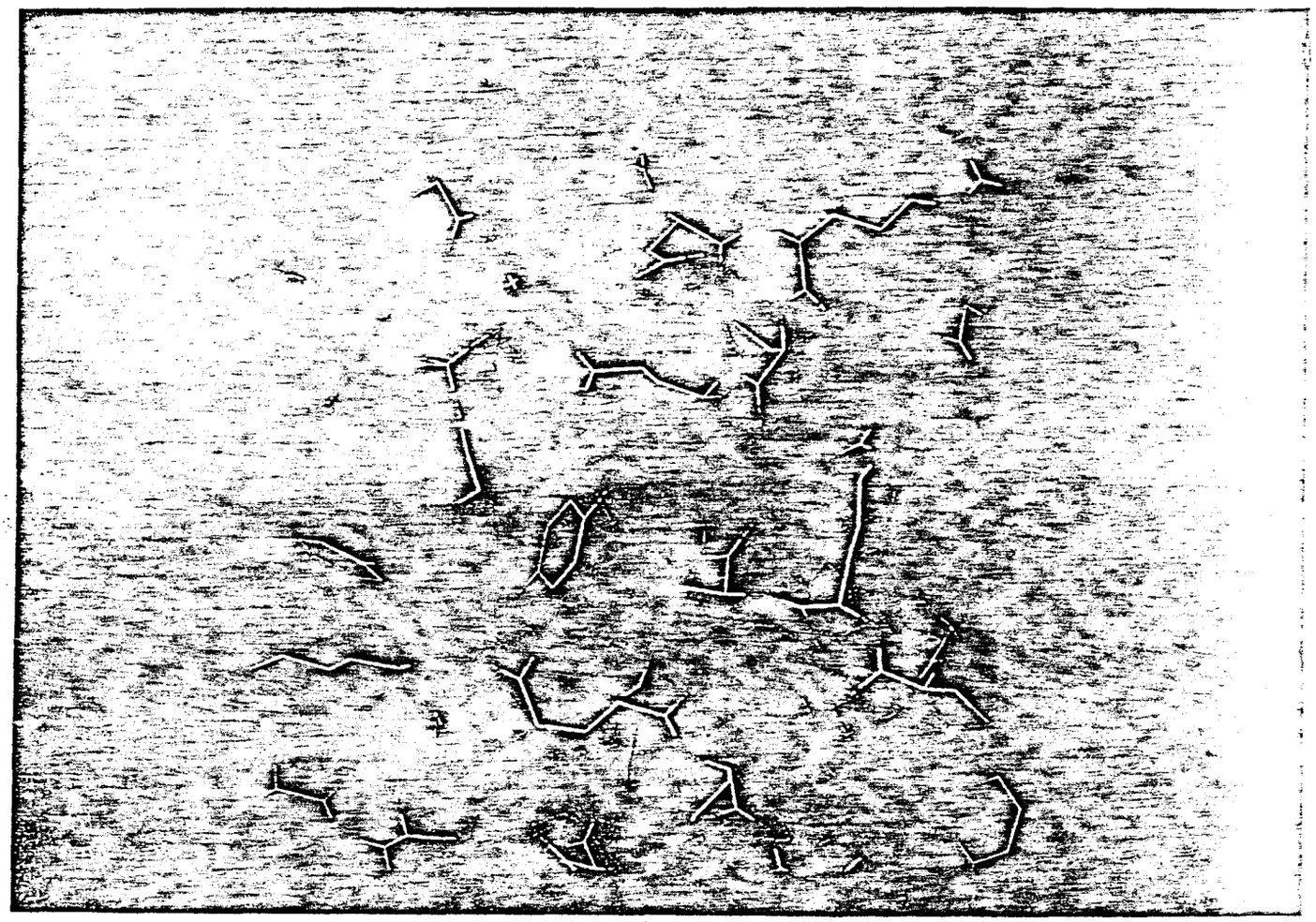

Fig. 1c

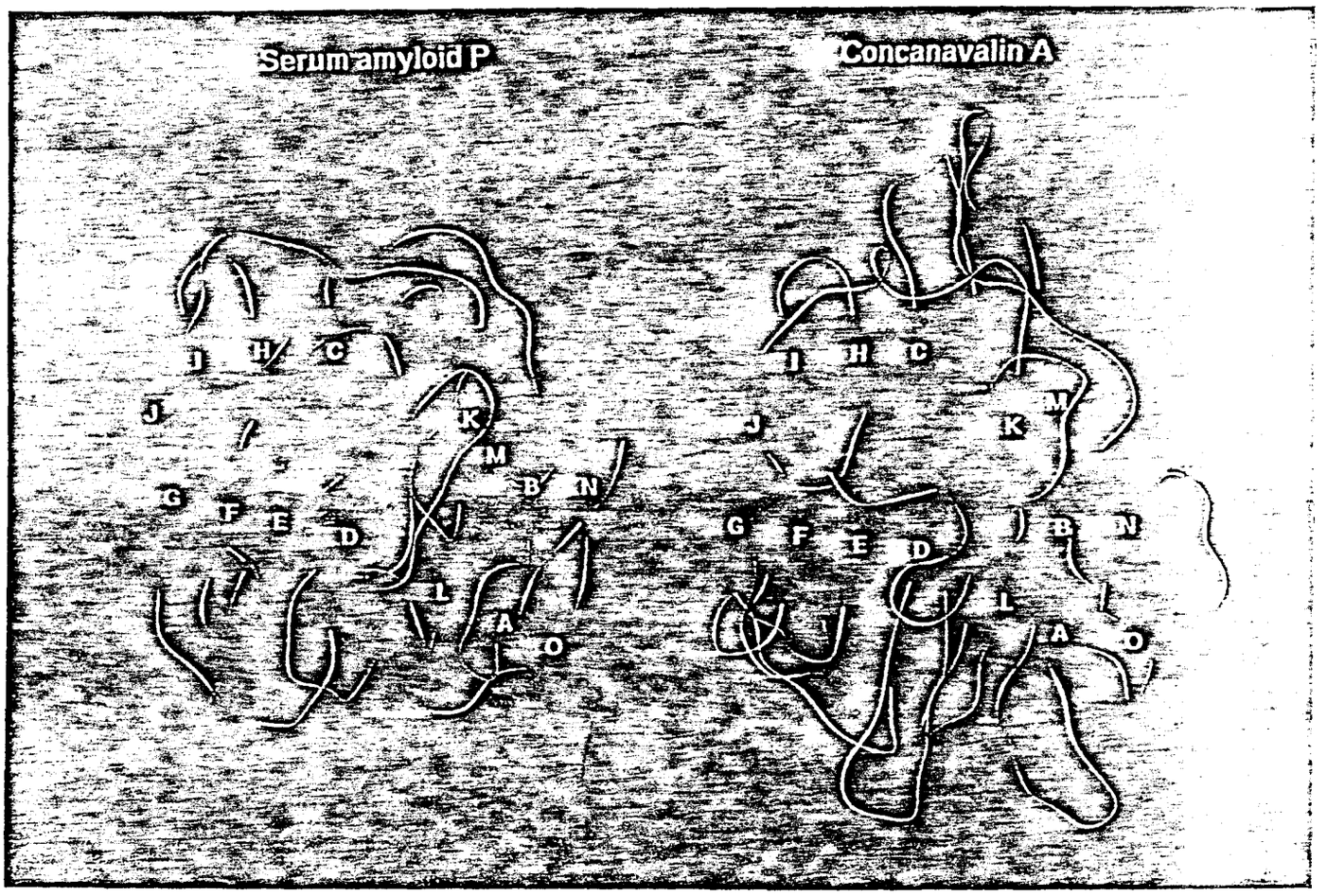

Fig. 2a

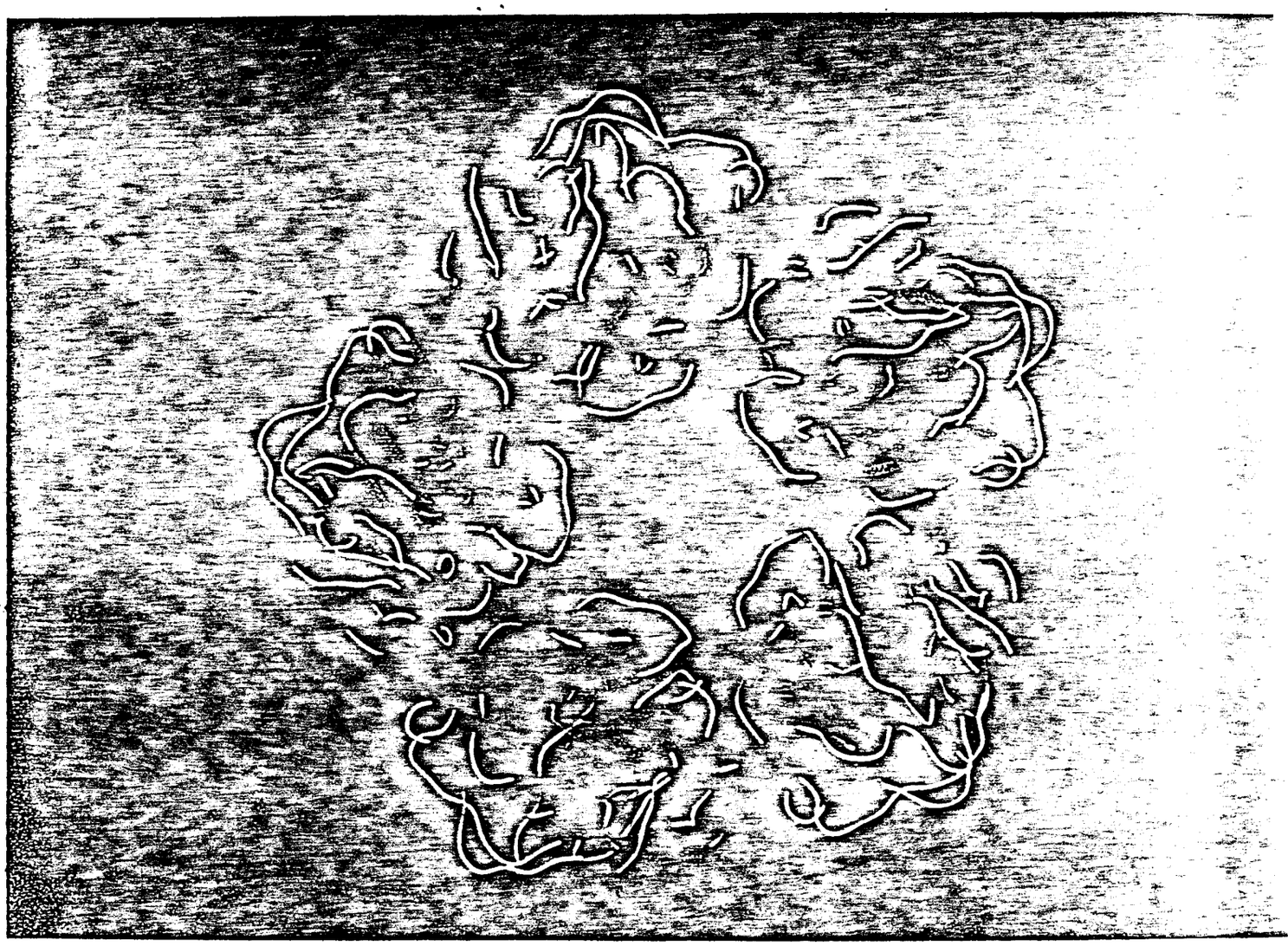

Fig. 2b

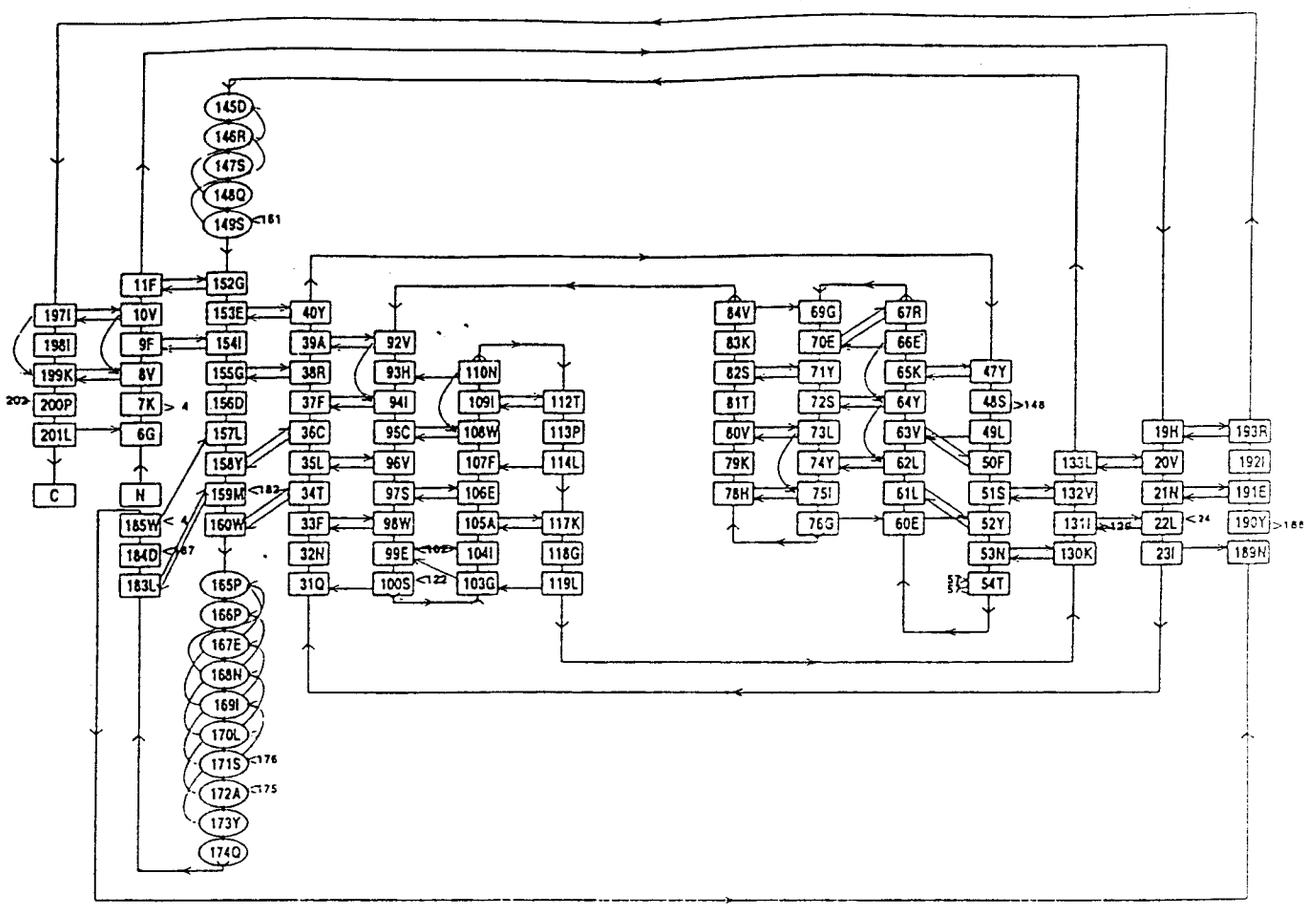

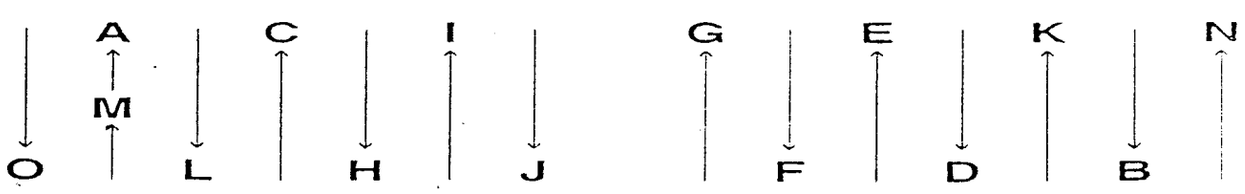
A
C
I
G
E
K
N
M
O
L
H
J
F
D
B

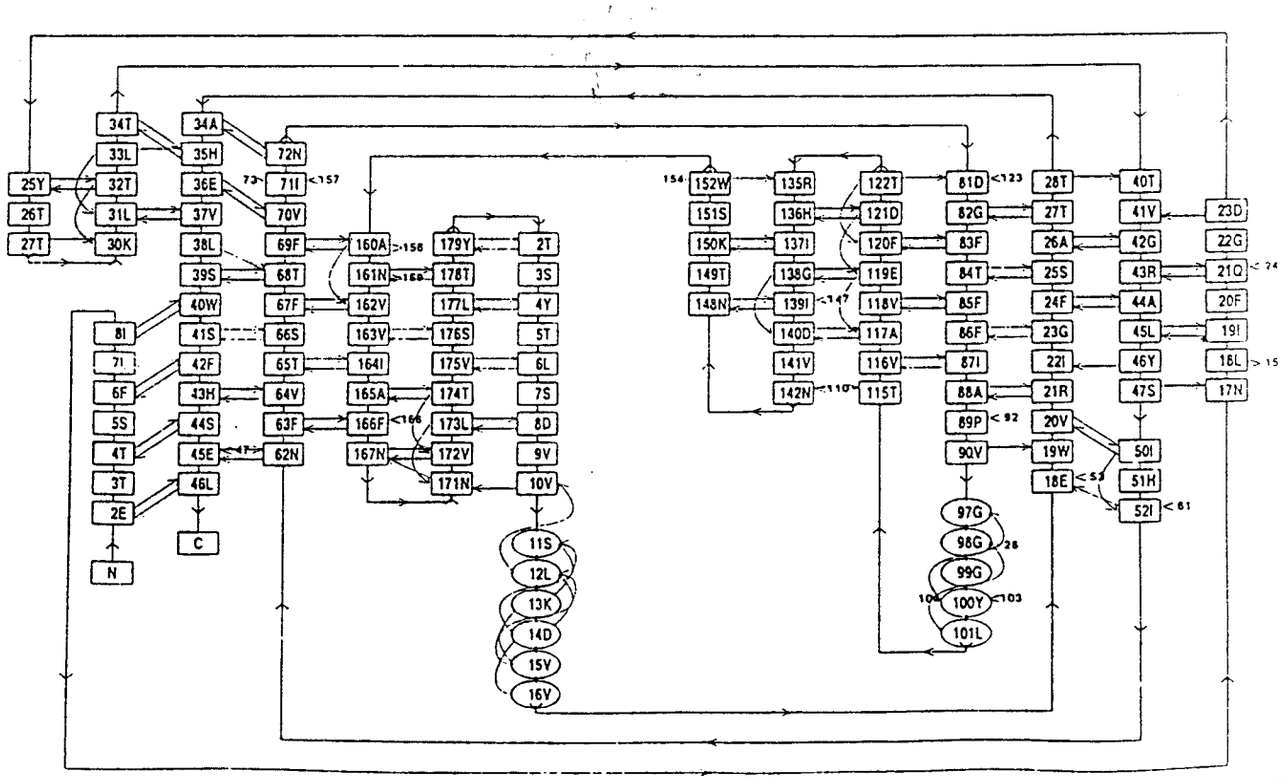

sapm
sapp
3cna
2ltn
1lte
hcrp
1fhp
1lim
STRAND A
STRAND B
STRAND C
STRAND D
STRAND E
STRAND F
STRAND G
STRAND H
STRAND I
STRAND J
STRAND K
STRAND L
STRAND M
STRAND N
STRAND O

Fig. 4

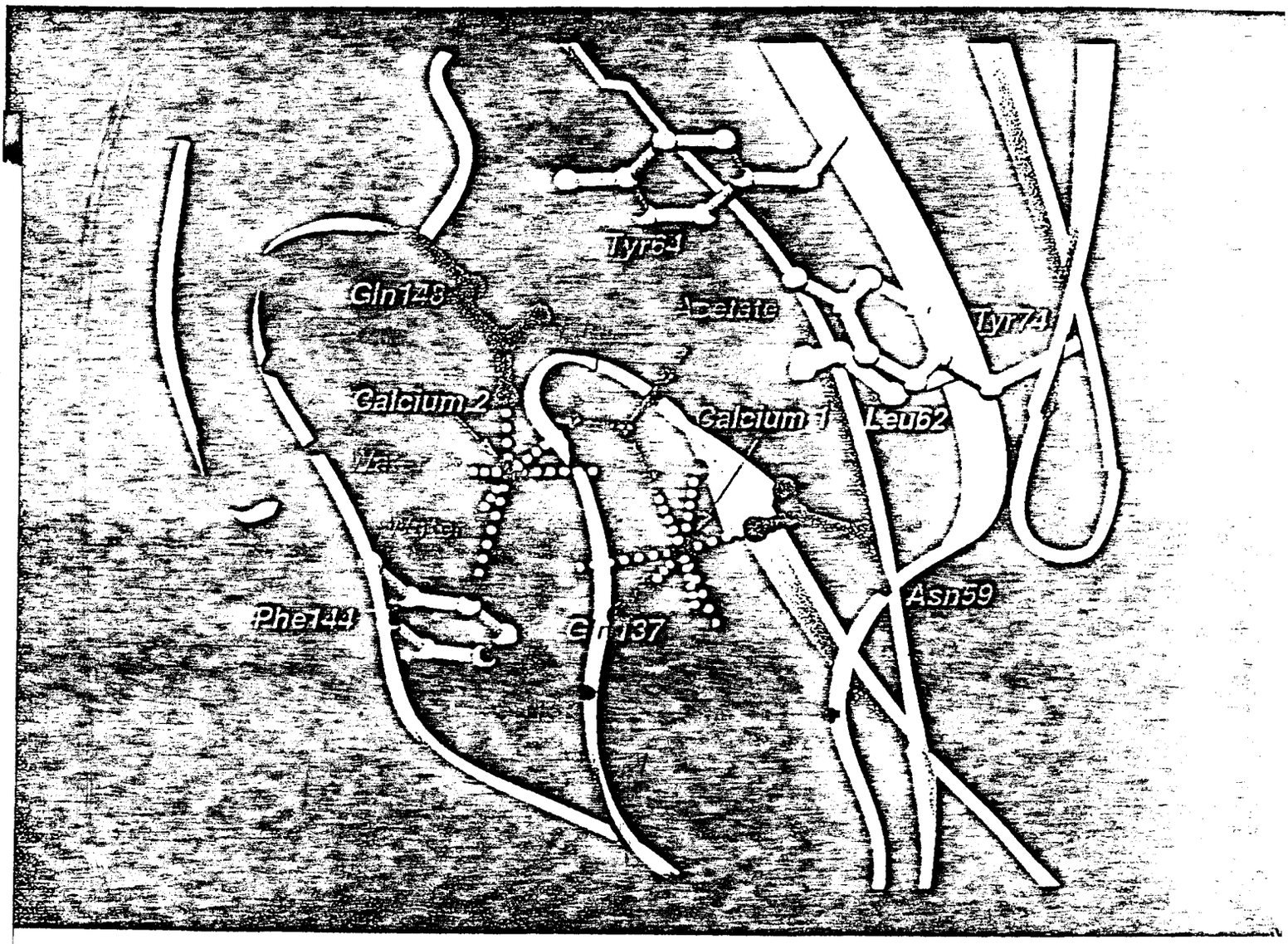

Fig. 5a

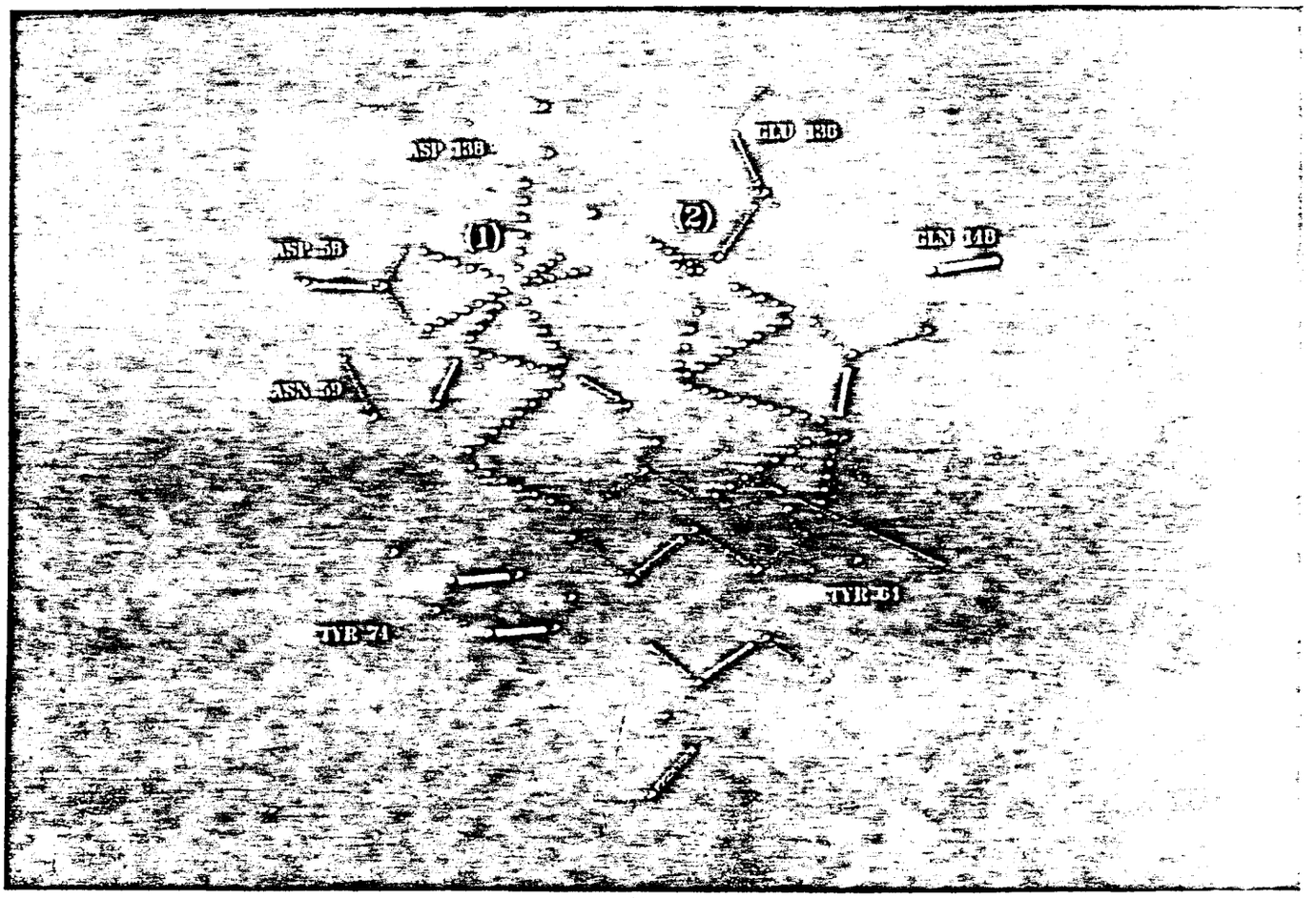

Fig. 5b

IV. Métodos em Cristalografia de Proteínas

IV.1 Introdução

Com a crescente disponibilidade de estruturas de proteínas determinadas à alta resolução, observa-se um significativo aumento de interesse na utilização da técnica de Substituição Molecular como ferramenta na determinação de estruturas de novas proteínas quando há proteínas homólogas com estrutura 3D conhecida. Este método compreende uma variedade de técnicas que buscam identificar os parâmetros que definem a orientação e o posicionamento de uma molécula ou fragmento conhecido, na cela unitária do cristal cuja estrutura busca-se determinar. O problema pode ser apresentado de forma geral em termos da determinação da matriz de rotação [C] e o vetor de translação **t** que transformam um dado objeto $\mathbf{P}_1$ de forma a superpô-lo a um outro objeto similar ou idêntico $\mathbf{P}_2$. Se $\mathbf{x}_1$ e $\mathbf{x}_2$ são pontos equivalentes de $\mathbf{P}_1$ e $\mathbf{P}_2$, respectivamente, então busca-se encontrar [C] e **t** tais que:

$$\mathbf{x}_2 = [\mathbf{C}]\cdot\mathbf{x}_1 + \mathbf{t}$$

Em geral, a determinação da matriz de rotação [C] e do vetor de translação **t** envolve uma busca por seis parâmetros (três ângulos e três translações) para encontrar a melhor superposição entre os objetos $\mathbf{P}_1$ e $\mathbf{P}_2$. Rossmann e Blow (1962) notaram que se os objetos de busca e alvo são funções de Patterson, então a busca hexa-dimensional poderia ser reduzida à uma sequência de duas buscas tridimensionais, em cada uma das quais se determina a orientação relativa e então a translação. O método consiste em três estágios em sequência: encontrar uma orientação (aproximada) para o modelo, localizar sua posição (aproximada) e otimizar os parâmetros obtidos e finalmente avaliar a qualidade de uma solução potencial. O primeiro e segundo estágios são conduzidos com técnicas de busca no espaço de Patterson: varia-se as posições do modelo até que a função de Patterson calculada apresente alta correlação com a função de Patterson observada para a estrutura desconhecida. A orientação é usualmente determinada usando a função rotação. Para uma dada orientação, a translação do modelo é então determinada usando a função translação. Como o sucesso desta segunda etapa depende drasticamente da precisão do resultado da primeira, em geral chega-se a vários conjuntos de soluções possíveis. É necessário, portanto, uma medida de correção para auxiliar na identificação da melhor solução.

No trabalho apresentado a seguir é descrito um método alternativo para o refinamento de corpo-rígido por mínimos quadrados quando um modelo de densidade eletrônica é utilizado em Substituição Molecular. Embora originalmente desenhado simplesmente para otimizar os parâmetros de rotação e translação obtidos pelas técnicas de busca em mapas de Patterson, este método provou ser extremamente eficiente (isto é, rápido e preciso) na avaliação da correção de uma solução obtida por Substituição Molecular.

Combinado com implementações muito eficientes das funçoes de rotação e translação (Navaza, 1987, 1990), este método tornou factível a exploração de um número muito grande de potenciais soluções do problema de posicionamento em Substituição Molecular, permitindo a solução de diversas estruturas de novas proteínas nas quais os procedimentos mais antigos de Substituição Molecular haviam falhado. Como resultado, o sistema de programas que implementou estes conceitos (AMoRe-Automated Molecular Replacement) tornou-se o estado da arte atual em termos mundiais no que diz respeito à técnica de Substituição Molecular.

IV.2 Trabalho publicado no *Journal of Applied Crystallography*

CASTELLANO, E.E., **OLIVA, G.** and NAVAZA,J.
"Fast Rigid Body Refinement for Molecular Replacement Techniques"
J.Appl.Cryst. (1992), **25**, 281-284.

REFERÊNCIAS

Rossmann, M.G. & Blow, D.M. (1962). *Acta Cryst.*, **15**, 24.

Navaza, J. (1987). *Acta Cryst.*, **A43**, 645-653.

Navaza, J. (1987). *Acta Cryst.*, **A43**, 619-620.

De acordo com as políticas editoriais, este artigo não pode ser depositado em repositório de acesso aberto. Para acesso ao artigo completo entre em contato com o(a) autor(a) ou com o Serviço de Biblioteca e Informação IFSC - USP (bib@ifsc.usp.br)

CASTELLANO, E. E.; OLIVA, G.; NAVAZA, J. Fast rigid-body refinement for molecular-replacement techniques. **Journal of Applied Crystallography**, Chester,v. 25, p.281-284, 1992.

V. Proteínas de Armazenamento em Sementes: Coixinas

V.1 Introdução

Embora as técnicas experimentais e computacionais utilizadas para a determinação de estruturas moleculares por difração de raios-X tenham alcançado enorme progresso na última década, a determinação de estruturas por essa técnica ainda demanda o investimento de longo tempo e substancial esforço. Por essa razão é de enorme interesse a possibilidade de previsão de estruturas moleculares de proteínas. Executar essa tarefa a partir de primeiros princípios é entretanto um objetivo que está longe de ser alcançado. Entretanto, uma hipótese de trabalho extremamente tentadora e atraente é admitir que a estrutura secundária e terciária de uma proteína seja dependente de sua estrutura primária. Assim, seria possível a previsão da estrutura de uma proteína sempre que sua estrutura primária seja conhecida. Este processo torna-se ainda mais promissor quando a proteína em estudo apresente razoável homologia com proteínas (ou fragmentos substanciais das mesmas) cujas estruturas moleculares já sejam conhecidas por difração de raios-X. Um fator favorável para a determinação da estrutura terciária seria, na maioria dos casos, a presença de pontes di-sulfeto que restringem as possibilidades de enovelamento.

Finalmente, obtido um primeiro modelo relativamente grosseiro para a estrutura molecular, as interações entre resíduos e a presença de ligações hidrogênio que estabilizam as estruturas em hélice e as folhas e voltas-ß, poderão ser levadas em conta por técnicas de mecânica e/ou dinâmica molecular que conduzirão a estrutura molecular proposta a um mínimo de energia. A estrutura molecular assim encontrada deverá ser então analisada em relação às interações e funções conhecidas da molécula em estudo visando estabelecer relações entre estrutura e função. Outro objetivo do processo acima descrito é a proposição de alterações de aminoácidos na molécula em estudo visando obter uma nova molécula com uma nova função desejada ou a eliminação de algum efeito nocivo. Finalmente poder-se-á também introduzir substratos em sítios ativos de enzimas e prever alterações estruturais subsequentes e avaliar a estabilidade da ligação proteína-substrato.

O Laboratório de Cristalografia do IFQSC tem uma tradição de trabalhos de pesquisa em cooperação com outros grupos de pesquisa tanto nacionais como internacionais. Nos

últimos anos um grande esfoço está sendo desenvolvido com o objetivo de aprofundar e ampliar os trabalhos na área de macromoléculas de interesse biológico. Por essa razão, uma forte interação está sendo estabelecida com grupos de pesquisa em Bioquímica e Biologia Molecular nacionais. Frequentemente em tais grupos são feitas determinações de estruturas primária de proteínas e o Laboratório tem sido procurado para fornecer informações sobre possíveis estruturas secundárias e terciárias de tais proteínas, enquanto não se dispõe de quantidade suficiente de proteína purificada para se dar início ao trabalho de determinação da estrutura molecular por métodos de difração de raios-X por monocristais. Essa situação tem se tornado ainda mais frequente à medida que novos sistemas de sequenciamento de proteínas e ácidos nucleicos são instalados no país.

Neste contexto se insere o trabalho de modelagem molecular de proteínas da semente de plantas do gênero Coix a seguir descrito.

Costuma-se classificar as proteínas de sementes em dois grupos: as proteínas "de reserva", que constituem a maior parte do material protéico da semente, e as chamadas "house-keeping", essenciais para o normal funcionamento do metabolismo celular. Durante a embriogênese, as células do endosperma das sementes produzem uma grande quantidade de proteínas cuja função é o armazenamento de aminoácidos necessários para o período de germinação.

Tradicionalmente, as proteínas tem sido classificadas em quatro grupos, de acordo com o critério de solubilidade:

Albuminas	- solúveis em água ou soluções salinas diluídas
Globulinas	- solúveis em soluçoes salinas concentradas
Prolaminas	- solúveis em álcool
Glutelinas	- solúveis em soluçoes ácidas ou básicas

No milho, o conteúdo proteico total corresponde a 10% do peso seco da semente, sendo que 60% destas proteínas sao proteínas de reserva. Em milho, as proteínas de reserva são representadas pelas **prolaminas**, e caracterizam-se pela solubilidade em álcool, recebendo o nome específico de **zeínas**. O grupo do Prof. Paulo Arruda do Laboratório de Biologia Molecular de Plantas do Centro de Biologia Molecular e Engenharia Genética (CBMEG) da UNICAMP tem realizado estudos das proteínas de reserva de Adlay, uma variedade de *Coix lacryma-jobi L.* O gênero Coix pertence à sub-tribo Coicinae, tribo Andropogoneae, que

inclui cereais importantes como o milho e sorgo. As **coixinas**, prolaminas de Coix, apresentam composição de aminoácidos característica da tribo Andropogoneae: alta proporção dos aminoácidos glutamina, leucina e prolina e baixa proporção dos aminoácidos essenciais lisina e triptofano. A extração diferencial das coixinas por solubilidade em isopropanol permitiu sua classificação em duas classes principais:α e γ-coixinas (Ottoboni et. al., 1990). Com a preparação dos clones genômicos de α e γ-coixinas, foi possível estabelecer as sequências completas dos clones de cDNA e daí inferir a sequência de aminoácidos da proteína. De posse destas sequências, nós analisamos a homologia entre as prolaminas de milho, sorgo e coix da qual pudemos inferir relações filogenéticas e evolutivas desta família de proteínas, assim como propor modelos estruturais para as coixinas e sugerir potenciais regiões favoráveis para introdução de mutações sítio-dirigidas que não interfiram com a estabilidade do enovelamento da proteína e sua incorporação e armazenamento no corpúsculo protéico.

Estes resultados estão apresentados no trabalho publicado na revista *Proteins: Structure Function and Evolution* que se segue.

V.2 Trabalho publicado em *Proteins: Structure Function and Evolution*

GARRATT,R., **OLIVA, G.**, CARACELLI,I., LEITE,A. and ARRUDA,P.
"Studies of the zein-like α-prolamins based on an analysis of amino acid sequences: implications for their evolution and three-dimensional structure"
Proteins : Structure, Function and Genetics, **15**, 88-99, 1993.

REFERÊNCIAS

Ottoboni, L.M.M., Leite, A., Targon, M.L.N., Crozier, A. & Arruda, P. (1990). *J.Agric.Food Chem.*, **38**, 631-635.

De acordo com as políticas editoriais, este artigo não pode ser depositado em repositório de acesso aberto. Para acesso ao artigo completo entre em contato com o(a) autor(a) ou com o Serviço de Biblioteca e Informação IFSC - USP (bib@ifsc.usp.br)

GARRATT, R. C.; OLIVA, G.; CARACELLI, I.; LEITE, A.; ARRUDA, P. Studies of the zein-like α–prolamins based on an analysis of amino acid sequences: implications for their evolution and three-dimensional structure. **Proteins**: structure, function, and genetics, New York, v.15, p.88-99, 1993.

VI. Estruturas de Moléculas Pequenas.

VI.1 Introdução

Do conhecimento da estrutura de uma substância advêm inúmeras informações úteis aos mais variados ramos da ciência: em Física e Ciência dos Materiais é fundamental a relação entre propriedades físicas e a estrutura interna dos sólidos; em Química as características estéricas de novos compostos ou complexos e sua relação com as propriedades funcionais, só podem, em muitos casos, serem conhecidas através da determinação de sua estrutura; em Bioquímica e Biologia Molecular a atividade funcional de uma macromolécula está intimamente relacionada com sua estrutura tridimensional; em Medicina e Farmacologia a ação de drogas envolve interações entre arranjos atômicos tridimensionais, sendo que a maneira como a união droga-receptor acontece é determinada pela estrutura de ambos os componentes.

O Laboratório de Cristalografia do DFCM/IFQSC tem se dedicado a investigações estruturais por difração de raios-X aplicadas a estes diversos campos. Desde a sua implantação, na década de 70, a linha principal de pesquisas tem sido o estudo de estruturas de moléculas consideradas pequenas pelos cristalógrafos (até cerca de 200 átomos sem contar hidrogênios). Com o apoio das instituições de fomento à pesquisa, através de sucessivos contratos, este laboratório tornou-se o único no Brasil com a infraestrutura e recursos humanos para a determinação de estruturas moleculares por difração de Raios-X em monocristais.

Como resultado deste investimento, estabeleceu-se um Laboratório de Cristalografia que ao longo dos anos realizou pesquisas contínuas, tendo publicado, somente nos últimos 12 anos, mais de 200 artigos originais de pesquisa em revistas internacionais, formou 18 mestres e 8 doutores e estabeleceu pesquisa em colaboração com muitos centros nacionais e internacionais.

Características relevantes das atividades aí desenvolvidas são o caráter amplo e interdisciplinar das mesmas. As pesquisas em andamento representam colaboração com vários grupos de pesquisa nacionais e internacionais, onde são sintetizadas ou extraídas as substâncias cujas estruturas cristalinas são determinadas no Laboratório de Cristalografia de São Carlos. As substâncias estudadas são complexos de metais com ligantes orgânicos,

produtos naturais, substâncias orgânicas sintéticas, produtos com propriedades farmacológicas e outros. O conhecimento da estrutura e empacotamento molecular no cristal possibilita a interpretação, a nível atômico, das propriedades físicas, químicas e biológicas do composto em estudo.

Por outro lado, as atividades de pesquisa em Química de Síntese no Brasil tem crescido significativamente, e nos padrões atuais para publicações em revistas internacionais relatando sínteses químicas, requer-se quase sempre a estrutura detalhada determinada por difração de raios-X. Como resultado temos tido no Laboratório de Cristalografia do DFCM um afluxo muito grande de novos cristais para serem caracterizados: como um parametro para medir este crescimento, no ano de 1992, foram medidas e determinadas cerca de 100 estruturas de moléculas pequenas.

No entanto, atualmente, considerável esforço dos pesquisadores deste laboratório tem sido dirigido para a área de cristalografia de proteínas, uma técnica com importantes aplicações em áreas de pesquisa consideradas estratégicas como Biotecnologia aplicada à Saúde Humana, Agropecuária e Biologia Molecular. Mesmo assim temos procurado não desativar a área de cristaloquímica, pela importância no contexto da química nacional que nosso laboratório tem alcançado. Além disso, todos os projetos de pesquisa desenvolvidos em nossos laboratórios envolvem a formação de alunos de graduação e pós-graduação para a área de cristalografia e neste sentido, é de fundamental importância introduzir os estudantes às técnicas cristalográficas através do estudo de sistemas mais simples e previsíveis, como são as estruturas cristalinas de moléculas pequenas.

VI.2 Complexos de Rutênio com Potenciais Propriedades Anti-tumorais.

Trabalhos publicados em *Inorganica Chimica Acta* (2 trabalhos publicados, 1 submetido), *Journal of Coordination Chemistry* (2 trabalhos aceitos), *Polyhedron* (submetido).

Nos últimos anos a catálise tem sido objeto de estudo intenso devido a sua importância acadêmica e tecnológica. Do ponto de vista acadêmico existem diversas áreas de interesse, podendo-se citar o estudo da interação entre o catalisador e o substrato na catálise heterogênea, a determinação do mecanismo de reação na catálise homogênea e o estudo das reações enzimáticas. Já do ponto de vista tecnológico, a utilização de catalisadores homogêneos ou heterogêneos possibilitou a síntese de novas substâncias e a produção de substâncias já conhecidas, porém a um custo menor, como por exemplo polímeros e fibras, detergentes, gordura hidrogenada e borracha (Haensel & Burwell, 1971). Os catalisadores heterogêneos têm sido mais utilizados devido a maior facilidade de serem separados do meio reacional, embora exista uma expectativa de aumento na aplicação de catalizadores homogêneos devido a maior seletividade destes durante as reações químicas (Parshall, 1980).

Dentre os catalisadores homogêneos destacam-se os complexos de metais de transição, como aqueles de Ródio, Irídio, Ferro e Rutênio (Wilkinson *et al.*, 1982; Stille & Becker, 1980; Jordan, 1988; James & Wang, 1980; Augustine & Van Peppen, 1970). Os catalisadores baseados em Rutênio têm sido intensamente estudados nos últimos anos devido ao seu potencial em diversos tipos de reações, como por exemplo, $RuCl_2(PPh_3)_3$ e $HRuCl(PPh_3)_3$ utilizados na hidrogenação de olefinas (Fahey, 1973; James *et al.*, 1975; Knifton, 1976), $Ru(CO)_3(PPh_3)_3$ utilizado em hidroformilação de olefinas e acetilenos (Evans *et al.*, 1965), e $RuCl_2(PPh_3)_3$ em isomerização de olefinas (Lyons, 1971).

Mais recentemente os complexos de Rutênio têm sido testados no tratamento de tumores malígnos (Keppler *et al.*, 1987a,b). A atividade antitumoral foi estudada em Leucemia P388, Carcinosarcoma de Walker 256 e Sarcoma 180. Os testes foram feitos usando o composto cis-diaminodicloroplatino(II) como controle positivo. Os resultados apresentados indicam que animais portadores de Leucemia P388, quando tratados com complexos de Rutênio, apresentam um aumento no período de vida, além de uma sensível

diminuição de efeitos colaterais. Resultados positivos também foram obtidos para Carcinosarcoma de Walker 256 e Sarcoma 180.

Um aspecto importante no estudo de complexos com o objetivo de usá-los como catalisadores e potenciais drogas antitumorais é a determinação de sua estrutura tridimensional uma vez que desta dependem as interações entre substrato e catalisador num caso, e entre droga e receptor no outro. O objetivo dos trabalhos que se seguem consiste na síntese de complexos de Rutênio, caracterização por métodos espectroscópicos e eletroquímicos, determinação das estruturas dos complexos por métodos cristalográficos e estudos das propriedades catalíticas dos mesmos. Neste sentido, temos desenvolvido projeto em colaboração com o Prof. Alzir A. Batista do Departamento de Quimica da UFSCar, o qual tem trabalhado na área de síntese, caracterização e reatividade de complexos de rutênio. Os compostos de Rutênio obtidos são do tipo $RuCl_2$ 1,4-bis(difenilfosfina)butano-(N-heterociclicos)$_2$; $RuCl_2(CO)_2L_2$, onde L=N-heterociclicos ou fosfinas; $HRuCl_3(CO)(PPh_3)_2$; $RuCl_5(CO)(PPh_3)_3$ (binuclear de valência mista); $LH^+[RuCl_4(CO)(L)]$, $LH^+[RuCl_4L_2]$ onde L=N-heterociclico. A primeira série acima citada apresenta compostos com potenciais catalíticos e reações de hidrogenação e/ou isomerização de substratos orgânicos insaturados (Batista *et al.*, 1990), enquanto a segunda série contem compostos muito semelhantes àqueles com atividades antitumorais ja confirmadas (Keppler *et al.*, 1987a,b). Neste último caso, ressaltamos que além de novos compostos sintetizados, foi desenvolvido pelo Prof. Alzir um método simples de síntese desta classe de complexos (Batista *et al.*, 1992).

A respeito da importância das pesquisas em pauta pode-se resumidamente mencionar que complexos de metais de transição tem sido amplamente utilizados em processos catalíticos, nos quais a seletividade assume fundamental importância. Um exemplo já clássico nesta área refere-se à produção industrial do L-Dopa, o qual é usado no tratamento da doença de Parkinson, obtido através da síntese seletiva via um catalisador de ródio (Elschenbroich *et al.*, 1989). Complexos de Rutênio do tipo $[RuCl_2(CO)_2(PPh_3)_2]$ tem sido, por exemplo, usados como efetivos catalisadores em reações seletivas de hidrocarbonetos insaturados, como é o caso da hidrogenação do 1,5,9-ciclododecatrieno(ciclopoliofeina), para ciclododeceno(ciclomonoolefina) (Fahey, 1978). Em vista do interesse nesta classe de compostos de Rutênio parte do presente trabalho trata de novo método de síntese específica de alguns isômeros de complexos de fórmula geral $[RuCl_2(CO)_2(PPh_3)_2]$ ou $[RuCl_2(CO)_2(AsPh_3)_2]$. O domínio da metodologia de síntese de catalisadores efetivos, na forma pura, poderá óbviamente conduzir à um melhor rendimento dos processos catalíticos desejados, ou mesmo obter compostos puros que possam servir de reagentes de partida para

síntese de novos compostos com composições mais complexas, os quais tem suas obtenções por vias diretas dificultadas ou mesmo impossibilitadas. Neste aspecto, a síntese do isômero ttt-$[RuCl_2(CO)_2(PPh_3)_2]$ permitiu seu uso como reagente de partida para o obtenção do binuclear $[Ru_2Cl_5(CO)(PPh_3)_3]$. A partir deste processo, desenvolveu-se uma rota simples de obtenção de uma ampla série de compostos binucleares de valência mista, de fórmula geral $[(L_1)_2(CO)Ru^{II}Cl_3Ru^{III}(Cl_2)(L_2)]$, a qual encontra-se em prática, na síntese de complexos contendo trifenilarsina, trifenilfosfina, p-trifeniltoluidina e N-heterocíclicos, como ligantes L_1 e L_2, no laboratório do Prof. Alzir, no Departamento de Química da UFSCar. Esta família de compostos poderá servir como sonda na avaliação da influência dos ligantes L_1 e L_2 nos processos de transferência de carga entre os dois centros metálicos. Neste aspecto, como nos demais que tratamos nos trabalhos a seguir, a determinação dos parâmetros estruturais dos compostos, obtidos pela técnica de raios-X foi de fundamental importância, principalmente quando se tem em vista o fato de que, nos compostos binucleares, por exemplo, a efetividade ou não dos processos de transferência de elétrons em complexos de valência mista depende também da distância entre os centros metálicos e até mesmo da posição angular entre os metais envolvidos nestes compostos, informações estas que são somente obtidas pela técnica de difração de raios-X.

No trabalho com os compostos com potencial atividade antitumoral, as propriedades quimioterápicas destes complexos de Rutênio podem, em parte, ser atribuídas às suas características físicas, ou seja, às suas estruturas, de onde se infere novamente a importância do conhecimento de dados cristalográficos de uma determinada substância, para se avaliar sua atividade funcional (Farrell, 1989). Esta é também uma nova linha de pesquisas em andamento nos laboratórios do Prof. Alzir, na UFSCar, ainda em fase de síntese de compostos de Rutênio com potencialidades farmacológicas. Neste caso o Prof. Alzir pretende se associar ao Prof. Dr. Renato Najjar, do Instituto de Química da USP/SP, o qual tem experência nesta área, com o objetivo de verificar, de fato, a atividade antitumoral dos compostos sintetizados em seu laboratório.

Os trabalhos por nós publicados, aceitos e submetidos nesta linha de pesquisa são apresentados a seguir.

BATISTA, A.A., OLMO,L.R.V, **OLIVA,G.**, CASTELLANO,E.E. and NASCIMENTO, O.R. "Synthesis, characterization and molecular structure of the 1-methylimidazoliumcarbonyl-1-methylimidazoletetrachlororuthenate(III)" *Inorganica Chimica Acta*, **202** (1992), pp. 37-41

BATISTA, A.A., CORDEIRO, L.A.C. and **OLIVA, G.**

"Electrochemical Formation and X-Ray Structure of the Five-Coordinated Ruthemium(II) $[RuCl(dppp)_2](PF_6)$ Complex"

Inorganica Chimica Acta, **203** (1993) pp. 185-191

FONTES, M.R.M, **OLIVA,G.**, CORDEIRO,L.A.C and BATISTA,A.A.

"The Crystal and Molecular Structure of Bis[1,3-bis(diphenylphosphino)propane] dichlororuthenium(II)"

Journal of Coordination Chemistry, 1992, *accepted, in press.*

BATISTA,A.A, PORCU,O.M., NASCIMENTO,O.R., BARBOSA, V.M. and **OLIVA,G.**

"Trichloro-Bridged Diruthenium (II,III) Complex: Preparation, Properties and X-ray Structure of tri(-μ-chloro)-dichlorocarbonyltris(triphenylphosphine) diruthenium(II,III)"

Journal of Coordination Chem., 1992, *accepted, in press.*

BATISTA, A.A., ZUKERMAN-SCHPECTOR, J., PORCU, O.M., QUEIROZ, S.L., ARAÚJO, M.P., **OLIVA, G.** and SOUZA, D.H.F.

"Molecular structures, electrochemical and spectroscopical properties of dichlorodicarbonylbis(triphenylphosphine)ruthenium(II) and dichlorodicarbonylbis(triphenylarsine)ruthenium(II)"

Polyhedron, submmited (1993).

BATISTA,A.A., OLMO,L.R.V., FONTES,M.R.M. and **OLIVA, G.**

"The X-ray crystal structure of the dichlorocarbonylbis(methylimidazole) methanolruthenium(II) and some properties of the dichlorodicarbonylbis(methylimidazole) ruthenium(II) complex.

Inorganica Chimica Acta, submmited (1993)

Os trabalhos submetidos acima mencionados são, na sua forma de manuscritos, muito extensos. Buscando uma razoável concisão para este texto de sistematização, incluo apenas a página de rosto e sumário destes trabalhos. Cópias completas dos mesmos estão incluídas na documentação completa do Memorial que acompanha este texto

REFERÊNCIAS

Augustine, R.L. and Van Peppen, J.F. (1970). *Chem.Comm.*, 495-496.

Batista, A.A., Olmo, L.R.V., Oliva, G., Castellano, E.E. and Nascimento, O.R. (1990) in *VII International Symposium on Homogeneous Catalysis*, Lyon, France.

Batista, A.A., Olmo, L.R.V., Oliva, G., Castellano, E.E. and Nascimento, O.R. (1992) *Inorganica Chimica Acta*, **202**, 37-41.

Elschenbroich, C. and Salzer, V.C.H. (1989) *Organometallics - A Concise Introduction*, Verlagsgesellschaft, Weinheim, Germany, p.429.

Evans, D., Osborn, J.A., Jardine, F.H. and Wilkinson, G. (1965). *Nature*, 1203-1204.

Fahey, D.R. (1973). *J.Org.Chem.*, **38**, 3343-3348.

Fahey, D.R. (1978). *J.Org.Chem.*, **88**, 801.

Farrell, N. (1989). *Transition Metal Complexes on Drugs and Chemotherapeutic Agents*, Kluver Academic Publishers, London, Chapter 6.

Haensel, V. and Burwell, Jr.R.L. (1971). *Scientific American*,46-58.

James, B.R. and Wang, D.K.W. (1980) *Can. J. Chem.*, **58**, 245-250.

James, B.R., Wang, D.K.W. and Voight, R.F.(1975). *J.C.S.Chem.Comm.*, 574-575.

Jordan, R.F. (1988) *J. Chem. Ed.*, **65**, 4, 285-289.

Keppler, B.K., Wehe, D., Endres, H. and Rupp, W. (1987a). *Inorg.Chem.*, **26**, 844-846.

Keppler, B.K., Rupp, W., Juhl, U.M., Endres, H., Niebl, R. and Balzer, W. (1987b). *Inorg.Chem.*, **26**, 4366-4370.

Knifton, J.F. (1976). *J.Org.Chem.* **41**,7,1200-1206.

Lyons, J.E. (1971). *Chem.Comm.*, 562-563.

Parshall,G.W. (1980). *Homogeneous Catalysis-The applications and chemistry of catalysis by soluble transition metal complexes.*1st ed., New York, John Wiley.

Stille, J.K. and Becker, Y. (1980) *J.Org. Chem.*, **45**, 2139-2145.

Wilkinson, G., Stone, A., Gordon, F. and Abel, E.W. (1982) *Comprehensive Organometallic Chemistry - The Synthesis, Reactions and Structures of Organometallic Compounds.* 1st ed., New York, Pergamon Press, vol.**4**, 931-965.

De acordo com as políticas editoriais, estes artigos não podem ser depositados em repositório de acesso aberto. Para acesso aos artigos completos entre em contato com o(a) autor(a) ou com o Serviço de Biblioteca e Informação IFSC - USP (bib@ifsc.usp.br).

BATISTA, A. A.; OLMO, L. R. V.; OLIVA, G.; CASTELLANO, E. E.; NASCIMENTO, O. R. Synthesis, characterization and molecular structure of the 1-methylimidazolium carbonyl-1-methylimidazoletetrachloro-ruthenate (III). **Inorganica Chimica Acta**,Amsterdam , v. 202, n. 1, p.37-41, Dec. 1992.

BATISTA, A. A.; CORDEIRO, L. A. C.; OLIVA, G. Electrochemical formation and X-ray structure of the five-coordinated ruthenium (II) $[RuCl(dppp)_2](PF_6)$ complex. **Inorganica Chimica Acta**, Lausanne, v.203, p.185-91, 1993.

FONTES, M. F. M.; OLIVA, G.; CORDEIRO, L. A. C.; BATISTA, A. A. The crystal and molecular structure of bis[1,3-bis(diphenylphosphino)propane] dichlororuthenium (II). **Journal of Coordination Chemistry**, New York, v.30, p.125-9, 1993.

BATISTA, A. A.; PORCU, O. M.; NASCIMENTO, O. R.; BARBOSA, V. M.; OLIVA, G. A trichloro-bridged diruthenium (II,III) complex: preparation, properties and X-ray structure of tri(-μ–chloro) dichlorocarbonyltris (triphenylphosphine)diruthenium (II,III). **Journal of Coordination Chemistry**, New York, v.30, p.345-55, 1993.

MOLECULAR STRUCTURES, ELECTROCHEMICAL AND SPECTROSCOPICAL PROPERTIES OF DICHLORODICARBONYLBIS(TRIPHENYLPHOSPHINE)RUTHENIUM(II) AND DICHLORODICARBONYLBIS(TRIPHENYLARSINE)RUTHENIUM(II)

Batista, A.A.[a,§], Zukerman-Schpector, J.[a],Porcu, O.M.[a], Queiroz,S.L.[a], Araujo,M.P.[a], Oliva,G.[b], Souza,D.H.F.[c]

a - Universidade Federal de São Carlos, Departamento de Quimica, Rodovia Washington Luiz Km 235,13.560-São Carlos, SP, Brazil.

b - Universidade de São Paulo, Departamento de Fisica e Ciencia dos Materiais, Av. Carlos Botelho 1465,13.560-São Carlos, SP, Brazil.

c - Universidade Estadual Paulista, Departamento de Ciências, Ilha Solteira, SP, Brazil.

§ - Author to whom correspondence should be addressed.

ABSTRACT

The cct isomers $[RuCl_2(CO)_2(PPh_3)_2]$ (I) and $[RuCl_2(CO)_2(AsPh_3)_2]$ (II) were synthesized from $[RuCl_3(PPh_3)_2DMA]DMA$ and $[RuCl_3(AsPh_3)_2DMA]DMA$, respectively. The complexes were characterized by elemental analysis, IR and UV/Vis spectroscopy and their molecular structures were determined by X-ray crystallography. Both complexes crystallize in space group $P2_1/n$. The structures were solved by the heavy-atom Patterson method and refined by least-squares analysis; (I) a = 10.364(3), b = 25.913(5), c = 12.634(2)Å, ß = 100.29(4)°, R = 0.033 and R_w = 0.034 for 4438 unique reflections; (II) a = 10.519(1), b = 25.753(1), c = 12.7684(6)Å, ß = 101.116(7)°, R = O.030, R_w = 0.03 for 4304 unique reflections. Cyclic voltammetry data show that the triphenylphosphine stabilizes better the Ru(II) complex than the tryphenylarsine ligand.

INTRODUCTION

In view of the increasing necessity to obtain products of high degree of purity there has been a great deal of interest in catalysts that are capable of performing selective homogeneous processes like reactions of hydrogenation of unsaturated substrates. Transition metal complexes have figured prominently in these reactions as excellent catalysts, in particular, complexes of ruthenium in low oxidation state containing tertiary phosphine in their structures. Thus in 1965 Wilkinson's group have shown that the $[RuCl_2(PPh_3)_4]$ and $[RuCl_2(PPh_3)_3]$ are extremely efficient for the reduction of alkenes and alkynes at 25°C and 1 atm[1]. The accumulated data on the use of ruthenium-phosphine systems for hydrogenation reactions is now substantial and it is well

The Crystal Structure of the dichlorocarbonylbis(methylimidazole) methanolruthenium(II) and some properties of the dichlorodicarbonylbis(methylimidazole)ruthenium(II) complex

Alzir A. Batista and Lis R. V. Olmo[1]; Marcos R.M. Fontes and Glaucius Oliva[2]

[1]Departamento de Química, Universidade Federal de São Carlos, CP.676, 13560, São Carlos/SP, Brazil

[2]Instituto de Física e Química de São Carlos, Universidade de São Paulo, CP.369, 13560, São Carlos/SP, Brazil

Abstract

The $RuCl_2(CO)_2(MeIm)_2$ (MeIm = N-methylimidazole) complex has been synthesized and the ttt, tcc and ctc isomers were characterized by infrared and UV/Vis spectroscopy and their redox properties were studied by cyclic voltammetry. The ttt isomer catalyzes the hydrogenation/isomerization reactions of allyl alcohol in presence of hydrogen at 70 °C and 1 atm. This can be attributed to the lower redox potential of this isomer compared with the other two. Recrystallization of the ttt isomer produces the $RuCl_2(CO)(MeIm)_2(MeOH)$ complex. Its structure was determined by X-ray crystallography. The crystals are triclinic, $P\bar{1}$ a=8.609(3), b=8.060(3), c=10.581(4)Å, α=77.78(3), β=88.43(3), γ=66.88(3)°, V=740.4(5)Å^3, Mr=396.24, Z=2, D_x=1.777 g.cm^{-1}, λ(MoKα)=0.71073Å, μ=12.80 cm^{-1}, F(000)=386, T=296K, R_{int}=0.004, final R=0.025 and Rw=0.027 for 2489 independent observed reflections [I>3σ(I)].

VI.3 Outras estruturas. Trabalhos publicados em *Inorganica Chimica Acta* (1 publicado, 2 submetidos) e *Acta Crystallographica* (7 trabalhos publicados).

Durante os primeiros anos que se seguiram ao meu retorno ao DFCM após meu doutoramento na University of London, Inglaterra, enquanto estávamos instalando a infraestrutura do Laboratório de Cristalografia de Proteínas e buscando o estabelecimento de linhas próprias de pesquisa no campo, mantivemos atividade constante na área de cristaloquímica, estudando diversos problemas estruturais de moléculas pequenas. Desta atividade resultaram diversos trabalhos publicados, envolvendo estruturas de compostos orgânicos e complexos de metais de transição. Apresentamos estes trabalhos a seguir.

ZUKERMAN-SCHPECTOR, J., CASTELLANO, E.E. & **OLIVA, G.**

"The Crystal and Molecular Structure of Bromo bis(1-phenyl-3,5-dimethylpyrazole)copper(I), $CuBr(pdmp)_2$"

Inorganica Chimica Acta, (1990), **175**, 1-2.

CASTELLANO, E.E, **OLIVA, G.** & ZUKERMAN-SCHPECTOR, J.

"Structure of Dibromobis(triphenylarsine oxide)nickel(II), $NiBr_2(Ph_3AsO)_2$"

Acta Crystallographica (1991), **C47**, 654-655.

ZUKERMAN-SCHPECTOR, J., CASTELLANO, E.E., **OLIVA, G.**, BROCKSOM, T.J. & CATANI, V.

"Structure of Methyl [1r, 2r, 9r]-12-Isopropyl-9-methyl-10,13-dioxo-phenylthio-tricyclo[7.4.0.$0^{2,6}$]trideca-6,11-diene-1-carboxylate."

Acta Crystallographica (1991) **C47**, 358-360.

ZUKERMAN-SCHPECTOR,J., CASTELLANO,E.E., SIMONE, C.A., **OLIVA,G.** and MAURO,E.

"Structure of Di-μ-cyanato-bis[cyanato(N,N-diethylethylenediamine) copper(II), $[Cu(NCO)_2(diEten)]_2$"

Acta Crystallographica (1991) **C47**, 957-959.

ZUKERMAN-SCHPECTOR,J., CASTELLANO,E.E., **OLIVA,G.**, COMASSETO,J.V. and STEFANI,H.A.

"Structure of Dichloro [(Z)-2-chloro-2-p-tolylvinyl](p-methoxyphenyl)tellurium(IV)"
Acta Crystallographica (1991) **C47**, 960-962.

ZUKERMAN-SCHPECTOR,J., De SIMONE,C.A., CASTELLANO,E.E., **OLIVA,G.**, FERREIRA, J.T.B. and CATANI,V.

"Structure of 6,7-dimethoxy-2,2-dimEthyl-2H-chromene. A natural precocene. $C_{13}H_{16}O$"
Acta Crystallographica (1991) **C47**, 1111-1113.

FONTES, M.R.M., **OLIVA, G.**, ZUKERMAN-SCHPECTOR, J., QUEIROZ,S.L. and BATISTA,A.A.

"Structure of 1,4-bis(diphenylphosphinoyl)butane.
Acta Crystallographica (1991) **C47**, 2699-2700.

DELBONI, L.F. and **OLIVA,G.**

"Structure of 6(S)-cyanomethyl-3(S)-ethyl-2-oxo-1,2,3,4,6,7,12a,12b(S)-octahydroindolo [2,3-a]quinolizines, $C_{19}H_{21}N_3O$.
Acta Crystallographica (1992) **C48**, 953-955.

SIGNORINI, O., DOCKAL, E.R., CASTELLANO, G. and **OLIVA, G.**

"Synthesis, Characterization and Crystal Structure of the $UO_6N_2C_{20}H_{22}.2H_2O$ Complex"
Inorganica Chimica Acta, (1992), *submitted*

ZAMIAN, J.R., DOCKAL, E.R., CASTELLANO, G. and **OLIVA, G.**

"Synthesis, Characterization and Molecular Structure of the $VO_5N_2C_{20}H_{22}.H_2O$ Complex"
Inorganica Chimica Acta, (1992), *submitted*

Os trabalhos submetidos acima mencionados são, na sua forma de manuscritos, muito extensos. Buscando uma razoável concisão para este texto de sistematização, incluo apenas a página de rosto e sumário destes trabalhos. Cópias completas dos mesmos estão incluídas na documentação completa do Memorial que acompanha este texto

De acordo com as políticas editoriais, este artigo não pode ser depositado em repositório de acesso aberto. Para acesso ao artigo completo entre em contato com o(a) autor(a) ou com o Serviço de Biblioteca e Informação IFSC - USP (bib@ifsc.usp.br)

ZUKERMAN-SCHPECTOR, J.; CASTELLANO, E. E.; OLIVA, G. The crystal and molecular structure of bromo bis(1-phenyl-3,5-dimethylpyrazole)-copper(I), $CuBr(pdmp)_2$. **Inorganica Chimica Acta**, Amsterdam, v. 175, p.1-2, 1990.

complexes while Fig. 2 illustrates the molecular packing and the chiral nature of the two complexes. All computer programs from the *TEXSAN* crystal-structure-analysis package (Molecular Structure Corporation, 1985).

Related literature. The title compound is the first reported osmium compound containing the 1,4,7-triazacyclononane macrocycle. Compounds of this ligand with ruthenium have been reported by Wieghardt, Herrmann, Koppen, Jibril & Huttner (1984).

This research was supported in part by the Research Corporation.

References

BEURSKENS, P. T. (1984). *DIRDIF*. Tech. Rep. 1984/1. Crystallography Laboratory, Toernooiveld, 6525 Ed. Nijmegen, The Netherlands

Molecular Structure Corporation (1985). *TEXSAN. TEXRAY Structure Analysis Package*. MSC, 3200A Research Forest Drive, The Woodlands, TX77381, USA.

WIEGHARDT, K., HERRMANN, W., KOPPEN, M., JIBRIL, I. & HUTTNER, G. (1984). *Z. Naturforsch. Teil B*, **39**, 1335–1343.

Acta Cryst. (1991). C47, 654–655

Structure of Dibromobis(triphenylarsine oxide)nickel(II), $NiBr_2(Ph_3AsO)_2$

BY E. E. CASTELLANO, G. OLIVA AND J. ZUKERMAN-SCHPECTOR

Instituto de Fisica e Quimica de São Carlos, Universidade de São Paulo, Caixa Postal 369, 13560 *São Carlos SP, Brazil*

(*Received* 4 *June* 1990, *accepted* 17 *August* 1990)

Abstract. $C_{36}H_{30}As_2Br_2NiO_2$, $M_r = 863{\cdot}01$, orthorhombic, $Pca2_1$, $a = 18{\cdot}826\ (5)$, $b = 10{\cdot}594\ (6)$, $c = 17{\cdot}402\ (6)$ Å, $V = 3470\ (4)$ Å^3, $Z = 4$, $D_x = 1{\cdot}652$ g cm^{-3}, $\lambda(Mo\ K\alpha) = 0{\cdot}71073$ Å, $\mu = 47{\cdot}60$ cm^{-1}, $F(000) = 1704$, $T = 298$ K, $R = 0{\cdot}059$ for 724 observed reflections. The Ni^{II} atom is coordinated to two Br ions [Br—Ni = 2·39 (1), 2·364 (8) Å] and to the O atoms of the (Ph_3AsO) groups [Ni—O = 1·94 (3), 2·00 (3) Å] in a distorted tetrahedral configuration [Br—Ni—Br = 123·1 (5)°].

Experimental. Synthesis of the title compound was performed as previously reported (Oliva, Castellano, Zukerman-Schpector & Massabni, 1984). The data collection and refinement parameters for the title compound are summarized in Table 1.

The structure was solved by Patterson and difference Fourier synthesis techniques. In the final cycles of blocked-matrix refinement only the heavy atoms As, Br and Ni were refined anisotropically; the phenyl rings were treated as rigid groups with individual isotropic temperature factors for the C atoms and a fixed isotropic temperature factor ($B = 4{\cdot}7$ Å^2) for the H atoms. Scattering factors for non-H atoms were taken from Cromer & Mann (1968) with corrections for anomalous dispersion from Cromer & Liberman (1970) and for H atoms from Stewart, Davidson & Simpson (1965). Programs used were *SHELX76* (Sheldrick, 1976) and *ORTEP* (Johnson, 1965).

Final atomic coordinates are listed in Table 2,* selected interatomic distances and angles are given in Table 3. Fig. 1 is a stereoscopic projection of the complex.

Related literature. In a previous paper (Oliva, Castellano, Zukerman-Schpector & Massabni, 1984), the synthesis and the crystal structures of the two complexes $NiBr_2.4(Ph_3AsO).8H_2O$ (green) and $NiBr_2.4(Ph_3AsO).3/2(C_6H_5CH_3).H_2O$ (orange) obtained from the title compound (blue) by recrystalli-

* Lists of structure factors, anisotropic thermal parameters, a complete list of C-atom parameters and H-atom parameters have been deposited with the British Library Document Supply Centre as Supplementary Publication No. SUP 53493 (16 pp.). Copies may be obtained through The Technical Editor, International Union of Crystallography, 5 Abbey Square, Chester CH1 2HU, England

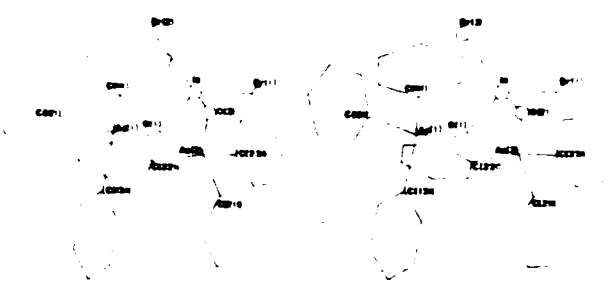

Fig. 1. Stereoscopic projection of the complex.

0108-2701/91/030654-02$03.00

© 1991 International Union of Crystallography

Table 1. *Crystallographic summary for* $NiBr_2(Ph_3AsO)_2$

Data collection[a,b]	
Mode	θ–2θ
Scan rate (° min^{-1})	1·9–6·7
θ range (°)	0–22
Range of hkl	$0 \le h \le 19$, $0 \le k \le 11$, $0 \le l \le 18$
Unique reflections	2209
Crystal dimensions approx. (mm)	0·08 × 0·18 × 0·30
Structure refinement[c,d]	
Reflections used [$I > 2\sigma(I)$]	724
Number of variables	126
R, wR	0·059, 0·061
S	0·75
Max. shift e.s.d.	0·1
Max., min. density in difference map (e Å^{-3})	0·55, −0·53

(*a*) Unit-cell parameters by least-squares refinement of the setting angles of 23 reflections with $10 < \theta < 22°$.

(*b*) Enraf–Nonius CAD-4 diffractometer with graphite monochromator was used. Standard reflections showed no significant variation.

(*c*) The intensities were corrected for Lp and for absorption, min. and max. values 0·85–1·02 (Walker & Stuart, 1983).

(*d*) Function minimized was $\sum w(|F_o| - |F_c|)^2$, where $w^{-1} = \sigma^2(F_o) + 0{\cdot}0075F_o^2$.

Table 2. *Fractional atomic coordinates and isotropic temperature factors* (Å^2) (*only two C atoms for each rigid phenyl ring are given*)

	x	y	z	B_{iso}
Br(1)	0·4470 (3)	0·6576 (5)	0·4263 (7)	5·8 (2)
Br(2)	0·4620 (3)	1·0272 (5)	0·3441 (7)	5·1 (2)
Ni	0·4762 (3)	0·8070 (6)	0·3285 (7)	3·7 (2)
As(1)	0·6208 (2)	0·7067 (5)	0·2423 (7)	3·7 (2)
As(2)	0·3572 (2)	0·8114 (5)	0·1875 (7)	3·3 (2)
O(1)	0·577 (2)	0·783 (3)	0·310 (2)	5·0 (8)
O(2)	0·430 (2)	0·756 (3)	0·230 (2)	5·7 (9)
C(111)	0·281 (1)	0·840 (3)	0·256 (2)	4 (1)
C(112)	0·221 (1)	0·908 (3)	0·231 (2)	5 (1)
C(121)	0·371 (1)	0·963 (2)	0·133 (2)	2·4 (9)
C(122)	0·365 (1)	1·081 (2)	0·168 (2)	6 (1)
C(131)	0·333 (2)	0·682 (3)	0·115 (2)	5 (1)
C(132)	0·264 (2)	0·665 (3)	0·087 (2)	5 (1)
C(211)	0·583 (1)	0·546 (2)	0·226 (2)	6 (1)
C(212)	0·561 (1)	0·475 (2)	0·289 (2)	7 (1)
C(221)	0·630 (2)	0·803 (3)	0·152 (2)	4 (1)
C(222)	0·692 (2)	0·803 (3)	0·108 (2)	5 (1)
C(231)	0·713 (1)	0·673 (3)	0·277 (2)	4 (1)
C(232)	0·752 (1)	0·565 (3)	0·261 (2)	5 (1)

Table 3. *Selected interatomic distances* (Å) *and angles* (°)

Br(1)—Ni	2·39 (1)	As(1)—C(221)	1·80 (3)
Br(2)—Ni	2·364 (8)	As(1)—C(231)	1·87 (2)
Ni—O(1)	1·94 (3)	As(2)—O(2)	1·66 (3)
Ni—O(2)	2·00 (3)	As(2)—C(111)	1·89 (3)
As(1)—O(1)	1·65 (3)	As(2)—C(121)	1·88 (3)
As(1)—C(211)	1·87 (3)	As(2)—C(131)	1·92 (3)
Br(1)—Ni—Br(2)	123·1 (5)	C(211)—As(1)—C(231)	103 (1)
Br(1)—Ni—O(1)	105 (1)	C(221)—As(1)—C(231)	107 (1)
Br(1)—Ni—O(2)	109 (1)	O(2)—As(2)—C(111)	114 (1)
Br(2)—Ni—O(1)	105 (1)	O(2)—As(2)—C(121)	114 (1)
Br(2)—Ni—O(2)	108 (1)	O(2)—As(2)—C(131)	104 (1)
O(1)—Ni—O(2)	104 (1)	C(111)—As(2)—C(121)	107 (1)
O(1)—As(1)—C(211)	111 (1)	C(111)—As(2)—C(131)	110 (1)
O(1)—As(1)—C(221)	112 (1)	C(121)—As(2)—C(131)	108 (1)
O(1)—As(1)—C(231)	109 (1)	Ni—O(1)—As(1)	132 (1)
C(211)—As(1)—C(221)	114 (1)	Ni—O(2)—As(2)	130 (1)

zation were reported. At that time it was not possible to produce single crystals of the blue complex. The present crystals were of poor diffracting quality and did not allow measurements of data with a resolution good enough to perform anisotropic refinements for all the non-H atoms and for accurate calculation of distances and angles. Nevertheless, the main aim of the present study could still be achieved, namely the unambiguous determination of the (somewhat distorted) tetrahedral coordination around the Ni ion.

This work has received partial support from CAPES, CNPq, FAPESP and FINEP.

References

CROMER, D. T. & LIBERMAN, D. (1970). *J. Chem. Phys.* **53**, 1891–1898.

CROMER, D. T. & MANN, J. B. (1968). *Acta Cryst.* A**24**, 321–324.

JOHNSON, C. K. (1965). *ORTEP*. Report ORNL-3794. Oak Ridge National Laboratory, Tennessee, USA.

OLIVA, G., CASTELLANO, E. E., ZUKERMAN-SCHPECTOR, J. & MASSABNI, A. C. (1984). *Inorg. Chim. Acta*, **89**, 9–17.

SHELDRICK, G. M. (1976). *SHELX76*. Program for crystal structure determination. Univ. of Cambridge, England.

STEWART, R. F., DAVIDSON, E. R. & SIMPSON, W. T. (1965). *J. Chem. Phys.* **42**, 3175–3187.

WALKER, N. & STUART, D. (1983). *Acta Cryst.* A**39**, 158–166.

Acta Cryst. (1991). C**47**, 655–657

Structure of a Bis{[(2,3-η,$\kappa P'$)-1,2-diphospha-2-propene]nickel}

BY MARTIN NIEGER, GREGOR BRUDER AND ROLF APPEL

Institut für Anorganische Chemie der Universität, Gerhard-Domagk-Straße 1, D-5300 Bonn, Germany

(*Received* 30 *July* 1990, *accepted* 31 *August* 1990)

Abstract. Bis[μ-(3,4-η,κP^5)-5-chloro-2,2,6,6-tetramethyl-3-phenyl-4,5-diphospha-2-silahept-3-ene]bis[carbonylnickel(0)], $C_{30}H_{46}Cl_2Ni_2O_2P_4Si_2$, M_r = 807·0, monoclinic, $P2_1/c$, a = 18·418 (4), b = 10·697 (3), c = 21·080 (7) Å, β = 102·32 (2)°, V = 4057 Å^3, Z = 4, D_x = 1·32 Mg m^{-3}, λ(Mo $K\alpha$) =

0108-2701/91/030655-03$03.00

© 1991 International Union of Crystallography

Acta Cryst. (1991). C47, 358-360

Structure of Methyl (1*R*,2*R*,9*R*)-12-Isopropyl-9-methyl-10,13-dioxo-7-phenylthiotricyclo[7.4.0.0^{2,6}]trideca-6,11-diene-1-carboxylate

BY J. ZUKERMAN-SCHPECTOR, E. E. CASTELLANO AND G. OLIVA

Instituto de Física e Química de São Carlos, Universidade de São Paulo, Caixa Postal 369, 13560 *São Carlos, SP, Brazil*

AND TIMOTHY J. BROCKSOM AND V. CATANI

Departamento de Química, Universidade Federal de São Carlos, Caixa Postal 676, 13560 *São Carlos, SP, Brazil*

(*Received* 14 *March* 1990, *accepted* 30 *April* 1990)

Abstract. $C_{24}H_{28}O_4S$, M_r = 424·56, monoclinic, $P2_1/n$, a = 10·338 (2), b = 14·538 (3), c = 15·829 (2) Å, β = 106·54 (1)°, V = 2281 (1) Å^3, Z = 4, D_x = 1·236 g cm^{-3}, λ(Mo $K\alpha$) = 0·71073 Å, μ = 1·61 cm^{-1}, $F(000)$ = 904, T = 298 K, R = 0·050 for 2029 observed reflections. The five-membered ring is in an envelope conformation with C(3) out of the plane, the cyclohexene ring in a half-chair conformation with C(1) and C(9) out of the plane, and the cyclohexenedione is in a sofa conformation with C(1) out of the plane. The basic tricyclic system adopts an overall hemispherical conformation.

Introduction. The title compound (I) was prepared by a Diels–Alder reaction (Catani & Brocksom, 1989). The crystal structure determination was carried out in order to investigate the influence of the bulky —S—Ph substituent on the overall conformation of the molecule; in particular we were interested in a comparison between (I) and (II) (Zukerman-Schpector, Castellano, De Simone, Brocksom & Catani, 1990). Knowledge of the molecular conformation helps in the prediction of the steric course of subsequent reactions (Trost, 1983) and in the prediction of the orientation of similar Diels–Alder reactions (Woodward & Hoffman, 1970).

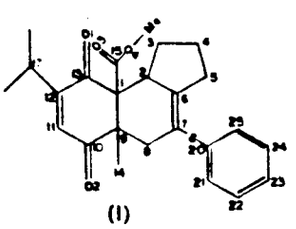

(I)

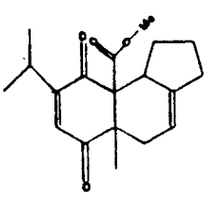

(II)

Experimental. A single colourless crystal of (I) with approximate dimensions 0·15 × 0·28 × 0·30 mm was used for data collection and cell determination on an Enraf–Nonius CAD-4 diffractometer with graphite-monochromatized Mo $K\alpha$ radiation. Unit-cell parameters were obtained from a least-squares refinement of the setting angles of 25 reflections in the θ range 8 to 24°. Intensity data were collected in the $\theta/2\theta$ scan mode up to θ_{max} = 25°; 4087 reflections were measured of which 3935 were independent (R_{int} = 0·016; $-12 < h < 11$, $0 < k < 17$, $0 < l < 18$) and 2029 with $I > 3\sigma(I)$ were employed in the refinement procedure. Data were corrected for Lorentz and polarization effects. The intensities of two standard reflections (800 and 080) were essentially constant throughout the experiment.

The structure was solved using standard direct methods and difference Fourier techniques. In the final cycles of full-matrix least-squares refinement (Q = 7·46), all non-H atoms were treated anisotropically. H atoms were included at positions found in difference synthesis, all with a common isotropic temperature factor that refined to U = 0·12 Å^2. The function minimized was $\sum w(|F_o| - |F_c|)^2$, where $w^{-1} = \sigma^2(F_o) + 0{\cdot}0005F_o^2$ resulting in R = 0·050, wR = 0·053 and S = 1·63. Maximum shift to e.s.d. ratio 0·001 and maximum and minimum electron density in final difference map 0·28 and −0·19 e Å^{-3}. Scattering factors for non-H atoms were taken from Cromer & Mann (1968) with corrections for anomalous dispersion from Cromer & Liberman (1970); for H atoms from Stewart, Davidson & Simpson (1965). Programs used: *SHELX*76 (Sheldrick, 1976) and *ORTEP* (Johnson, 1965).

Discussion. The final atomic parameters are given in Table 1,* bond distances and angles in Table 2. A

* Lists of H-atom positions, anisotropic thermal parameters and structure factors have been deposited with the British Library Document Supply Centre as Supplementary Publication No. SUP 53222 (23 pp.). Copies may be obtained through The Technical Editor, International Union of Crystallography, 5 Abbey Square, Chester CH1 2HU, England.

0108-2701/91/020358-03$03.00

© 1991 International Union of Crystallography

Table 1. *Final atomic coordinates and isotropic temperature factors* (Å²)

	x	*y*	*z*	B_{iso}*
S	0·4189 (1)	0·1287 (1)	−0·0835 (1)	5·27 (4)
O(1)	0·1445 (3)	0·1790 (2)	0·0961 (2)	5·0 (1)
O(2)	0·1237 (3)	0·4770 (2)	−0·0909 (2)	5·3 (1)
O(3)	0·2368 (3)	0·4813 (2)	0·1392 (2)	5·0 (1)
O(4)	0·1990 (3)	0·3646 (2)	0·2198 (2)	5·9 (1)
C(1)	0·2580 (4)	0·3238 (3)	0·0925 (3)	3·4 (1)
C(2)	0·3939 (4)	0·2764 (3)	0·1343 (3)	3·9 (1)
C(3)	0·4225 (5)	0·2227 (3)	0·2231 (3)	5·5 (2)
C(4)	0·5468 (5)	0·1666 (3)	0·2214 (3)	6·0 (2)
C(5)	0·5167 (4)	0·1337 (3)	0·1262 (3)	5·1 (2)
C(6)	0·4268 (4)	0·2072 (3)	0·0729 (3)	3·6 (1)
C(7)	0·3731 (4)	0·2107 (3)	−0·0144 (3)	3·7 (1)
C(8)	0·2720 (4)	0·2820 (3)	−0·0594 (3)	3·9 (1)
C(9)	0·2623 (4)	0·3637 (3)	0·0018 (2)	3·4 (1)
C(10)	0·1296 (4)	0·4121 (3)	−0·0414 (3)	3·9 (1)
C(11)	0·0063 (4)	0·3732 (3)	−0·0280 (3)	4·6 (1)
C(12)	0·0050 (4)	0·3010 (3)	0·0243 (3)	4·3 (1)
C(13)	0·1365 (4)	0·2590 (3)	0·0737 (3)	3·8 (1)
C(14)	0·3830 (4)	0·4283 (3)	0·0086 (3)	4·5 (1)
C(15)	0·2312 (4)	0·4004 (3)	0·1515 (3)	4·0 (1)
C(16)	0·1652 (6)	0·4299 (4)	0·2797 (3)	7·4 (2)
C(17)	−0·1205 (5)	0·2564 (3)	0·0350 (4)	6·5 (2)
C(18)	−0·1348 (7)	0·2786 (4)	0·1248 (5)	10·0 (3)
C(19)	−0·2466 (6)	0·2855 (5)	−0·0355 (6)	10·7 (3)
C(20)	0·2652 (4)	0·0702 (3)	−0·1294 (3)	4·0 (1)
C(21)	0·1785 (5)	0·0484 (3)	−0·0798 (3)	5·0 (2)
C(22)	0·0618 (5)	−0·0017 (3)	−0·1175 (4)	6·2 (2)
C(23)	0·0318 (6)	−0·0311 (4)	−0·2017 (4)	6·6 (2)
C(24)	0·1174 (6)	−0·0107 (4)	−0·2515 (3)	6·6 (2)
C(25)	0·2334 (5)	0·0411 (3)	−0·2166 (3)	5·4 (2)

*$B_{iso} = 4/3\sum_i\sum_j B_{ij}\mathbf{a}_i\mathbf{a}_j$

Table 2. *Interatomic bond distances* (Å) *and angles* (°)

S—C(7)	1·771 (4)	S—C(20)	1·766 (4)
O(1)—C(13)	1·212 (5)	O(2)—C(10)	1·217 (5)
O(3)—C(15)	1·196 (5)	O(4)—C(15)	1·325 (5)
O(4)—C(16)	1·453 (6)	C(1)—C(2)	1·535 (6)
C(1)—C(9)	1·561 (5)	C(1)—C(13)	1·530 (6)
C(1)—C(15)	1·529 (6)	C(2)—C(3)	1·561 (6)
C(2)—C(6)	1·504 (6)	C(3)—C(4)	1·529 (7)
C(4)—C(5)	1·526 (7)	C(5)—C(6)	1·507 (6)
C(6)—C(7)	1·335 (6)	C(7)—C(8)	1·500 (6)
C(8)—C(9)	1·554 (5)	C(9)—C(10)	1·520 (6)
C(9)—C(14)	1·541 (6)	C(10)—C(11)	1·464 (6)
C(11)—C(12)	1·339 (6)	C(12)—C(13)	1·492 (6)
C(12)—C(17)	1·503 (7)	C(17)—C(18)	1·51 (1)
C(17)—C(19)	1·51 (1)	C(20)—C(21)	1·386 (7)
C(20)—C(25)	1·391 (6)	C(21)—C(22)	1·390 (7)
C(22)—C(23)	1·349 (8)	C(23)—C(24)	1·375 (9)
C(24)—C(25)	1·390 (8)		

C(7)—S—C(20)	102·2 (2)	C(15)—O(4)—C(16)	116·0 (4)
C(2)—C(1)—C(9)	107·5 (3)	C(2)—C(1)—C(13)	114·0 (3)
C(2)—C(1)—C(15)	111·5 (3)	C(9)—C(1)—C(13)	106·7 (3)
C(9)—C(1)—C(15)	110·4 (3)	C(13)—C(1)—C(15)	106·6 (3)
C(1)—C(2)—C(3)	121·9 (3)	C(1)—C(2)—C(6)	111·7 (3)
C(3)—C(2)—C(6)	103·2 (3)	C(2)—C(3)—C(4)	101·3 (4)
C(3)—C(4)—C(5)	104·4 (4)	C(4)—C(5)—C(6)	104·5 (4)
C(2)—C(6)—C(5)	109·2 (3)	C(2)—C(6)—C(7)	122·6 (4)
C(5)—C(6)—C(7)	127·9 (4)	S—C(7)—C(6)	120·5 (3)
S—C(7)—C(8)	116·4 (3)	C(6)—C(7)—C(8)	123·1 (4)
C(7)—C(8)—C(9)	113·1 (3)	C(1)—C(9)—C(8)	108·2 (3)
C(1)—C(9)—C(10)	109·1 (3)	C(1)—C(9)—C(14)	113·4 (3)
C(8)—C(9)—C(10)	106·5 (3)	C(8)—C(9)—C(14)	108·3 (3)
C(10)—C(9)—C(14)	111·0 (3)	O(2)—C(10)—C(9)	121·5 (4)
O(2)—C(10)—C(11)	120·4 (4)	C(9)—C(10)—C(11)	117·9 (4)
C(10)—C(11)—C(12)	123·7 (4)	C(11)—C(12)—C(13)	118·5 (4)
C(11)—C(12)—C(17)	124·7 (4)	C(13)—C(12)—C(17)	116·8 (4)
O(1)—C(13)—C(1)	123·4 (4)	O(1)—C(13)—C(12)	121·5 (4)
C(1)—C(13)—C(12)	115·1 (4)	O(3)—C(15)—O(4)	123·6 (4)
O(3)—C(15)—C(1)	126·2 (4)	O(4)—C(15)—C(1)	110·1 (3)
C(12)—C(17)—C(18)	109·5 (5)	C(12)—C(17)—C(19)	112·7 (5)
C(18)—C(17)—C(19)	109·9 (5)	S—C(10)—C(21)	121·9 (3)
S—C(20)—C(25)	119·1 (3)	C(21)—C(20)—C(25)	119·0 (4)
C(20)—C(21)—C(22)	119·9 (4)	C(21)—C(22)—C(23)	121·2 (5)
C(22)—C(23)—C(24)	119·6 (5)	C(23)—C(24)—C(25)	120·8 (5)
C(20)—C(25)—C(24)	119·5 (5)		

stereoscopic projection of compound (I) is shown in Fig. 1 where the phenyl ring has been omitted for clarity.

The main result of the present communication is that the basic tricyclic system adopts, as in the case of (II), an overall hemispherical conformation: a least-squares fit (Kabsch, 1976) between equivalent atoms of the tricyclic systems gives a mean deviation of 0·044 Å and a root-mean-square deviation of 0·051 Å, showing that the —S—Ph substituent has virtually no conformational influence.

The five-membered ring is in an envelope conformation with C(3) 0·624 (5) Å out of the plane defined by the other four atoms. The cyclohexenedione ring conformation is close to that of a sofa with C(1) 0·709 (4) Å out of the plane defined by the other five atoms. The cyclohexene ring is in an essentially half-chair conformation with C(1) 0·517 (4) Å above and C(9) 0·308 (4) Å below the plane defined by the other four atoms. The phenyl ring is planar to within experimental accuracy (σ_{av} = 0·007 Å).

The C(15)—O(3) carbonyl bond length of 1·196 (5) Å is in the range normally observed in esters (Allen, Kennard, Watson, Brammer, Orpen & Taylor, 1987).

The intermolecular distances are in the expected range for non-bonded contacts: C(6)···O(2)($-x$, $1-y$, $-z$) = 3·396 (5), C(6)···O(3)($-x$, $1-y$, $-z$) = 3·372 (5) Å.

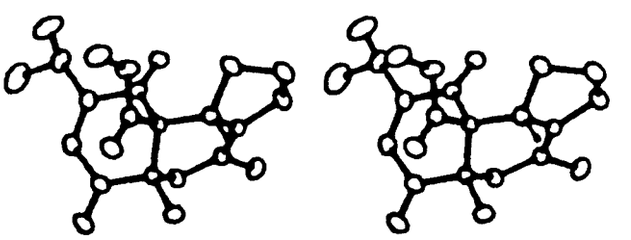

Fig. 1. Stereoscopic projection of the molecule; the phenyl ring has been omitted for clarity.

This work has received partial support from CNPq, CAPES, FAPESP and FINEP. One of us (JZS) would like to thank the Departamento de Química Inorgánica, Facultad de Farmacia,

Universidad de Santiago de Compostela, Spain, for providing X-ray diffraction facilities.

References

ALLEN, F. H., KENNARD, O., WATSON, D. G., BRAMMER, L., ORPEN, A. G. & TAYLOR, R. (1987). *J. Chem. Soc. Perkin Trans. 2*, pp. S1-S19

CATANI, V. & BROCKSOM, T. J. (1989). 3rd. Braz. Meet. Org Synth. São Carlos, Brazil

CROMER, D. T. & LIBERMAN, D. (1970). *J. Chem. Phys.* 1891-1898

CROMER, D. T. & MANN, J. B. (1968). *Acta Cryst.* A24, 321-324.

JOHNSON, C. K. (1965). *ORTEP*. Report ORNL-3794. Oak Ridge National Laboratory, Tennessee, USA.

KABSCH, W. (1976). *Acta Cryst.* A32, 922-923.

SHELDRICK, G. M. (1976) *SHELX76*. Program for crystal structure determination. Univ. of Cambridge, England.

STEWART, R. F., DAVIDSON, E. R. & SIMPSON, W. T. (1965). *J. Chem. Phys.* 42, 3175-3187.

TROST, B. M. (1983). *Science*, 219, 245-250

WOODWARD, R. B & HOFFMAN, R. (1970) *The Conservation of Orbital Symmetry*. Weinheim: Verlag Chemie.

ZUKERMAN-SCHPECTOR, J., CASTELLANO, E. E., DE SIMONE, C. A., BROCKSOM, T. J. & CATANI, V. (1990). *Acta Cryst.* C46, 1971-1973.

Acta Cryst. (1991). C47, 360-362

Structure of a Modified β-Lactam Antibiotic

BY SAMPA PAIN, GOUTAM BISWAS AND ASOK BANERJEE*

Department of Biophysics, Bose Institute, Calcutta-700 054, India

AMITABHA DE

Department of Physics, University College of Science, 92 Acharya Prafulla Chandra Road, Calcutta-700 009, India

A. MATHUR AND AJOY BOSE

Department of Chemistry, Stevens Institute of Technology, New Jersey, USA

AND Y. IITAKA

Tokyo University, Laboratory of Biophysics School of Medicine, Tokyo 192-03, Japan

(*Received* 17 *January* 1990; *accepted* 25 *April* 1990)

Abstract. 1-Phenoxy-9b-phenyl-1,4,5,9b-tetrahydro-2*H*-azeto[1,2-*a*]isoquinolin-2-one, $C_{25}H_{19}NO_2$, is a carbocyclic analogue of cephalosporin. The crystals are monoclinic, $M_r = 341$, $C2/c$, $a = 23{\cdot}054$ (1), $b = 7{\cdot}315$ (2), $c = 23{\cdot}713$ (4) Å, $\beta = 115{\cdot}08$ (6)°, $V = 3621{\cdot}9$ Å^3, $Z = 8$, $D_m = 1{\cdot}24$, $D_x = 1{\cdot}25$ g cm^{-3}, λ(Cu $K\alpha$) = 1·5418 Å, $\mu = 5{\cdot}96$ cm^{-1}, $F(000) = 1440$, $T = 288$ K, final $R = 0{\cdot}071$ for 2450 observed reflections. The β-lactam N atom, N(7), is 0·229 Å away from mean plane containing C(11), C(5) and C(25). From the plane N(7)–C(5)–C(11)–C(3), atoms O(2) and O(1) are in the *trans* position whereas O(1) and C(8) are in the *cis* position. The crystal structure is stabilized by base–base interactions about the center of inversion.

Introduction. A large family of antibiotics is known whose single common structural feature is a β-lactam ring. As a class, they consist of penicillins, the cephalosporins and non-classical β-lactam antibiotics. The penicillins and cephalosporins show bactericidal reactions by interfering with bacterial cell-wall synthesis and inhibiting the enzymes that catalyse the cross-linking reaction of D-alanyl peptides on peptidoglycan strands of the growing cell wall (Blumberg & Strominger, 1974). Several penicillins and cephalosporin antibiotics inhibit the synthesis of bacterial cell walls.

Since the β-lactam ring plays a key role in the biological activity of β-lactam antibiotics, its activity can be influenced by substituents or fused rings (Takasuka, Nishikawa & Tori, 1982).

The compound reported here is a carbocyclic analogue of cephalosporin (Sharma, Mehra & Gupta, 1978; Bose, Amin, Kapur & Manhas, 1976) the structure of which was sought as a part of an investigation into the geometrical features which provide significant stereochemical information on the lability of the β-lactam amide bonds and on the conformation of the antibiotic in the region of the

* To whom correspondence should be addressed.

0108-2701/91/020360-03$03.00 © 1991 International Union of Crystallography

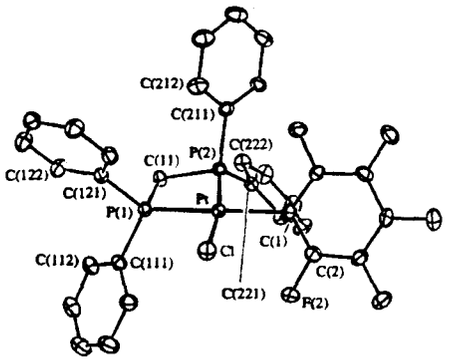

Fig. 1. Molecular structure and crystallographic numbering scheme employed for [PtCl(dppm)C_6F_5] (Johnson, 1971).

atom, a C atom from the pentafluoroaryl group and two P atoms from a bidentate dppm ligand. The deviations from the least-squares plane through the four donor atoms are significant: Cl −0·025 (1), P(1) 0·023 (1). P(2) −0·024 (1) and C(1) 0·346 (4) Å; the Pt atom lies 0·1099 (2) Å out of this plane. The distortion from ideal square-planar geometry may be related to the restricted bite distance of the bidentate ligand which imposes a P—Pt—P angle of 73·9 (1)°. As a consequence, the two angles P(1)—Pt—Cl and P(2)—Pt—C(1) are each opened up to approximately 99°. In the related complex, $Pt(C_6H_5)_2$(dppm), there is also a deviation from square-planar geometry [P—Pt—P 73 (1)°], but the Pt atom and the four donor atoms are coplanar (Braterman, Cross, Manojlovic-Muir, Muir & Young, 1975) by contrast with the present complex.

The Pt—P bond distances, Pt—P(1) 2·295 (1) and Pt—P(2) 2·224 (1) Å, are not equivalent with the shorter bond distance being *trans* to the Cl atom reflecting the greater *trans*-influence of the aryl C atom over that of the Cl atom; this effect has been reported previously for a related complex PtCl(dcy)-C_6F_5 (dcy = dicyclopentadiene) (Deacon *et al.*, 1989). The longer Pt—P bond distance is comparable to the Pt—P bond distances of 2·30 (1) Å found in $Pt(C_6H_5)_2$(dppm) (Braterman *et al.*, 1975). In order to relieve possible steric interactions between the phenyl groups bound to the dppm ligand and the C_6F_5 group, the latter is oriented such that the dihedral angle between it and the square plane about the Pt atom is 60·4°; the C_6F_5 group is perpendicular to the coordination plane in PtCl(dcy)C_6F_5 (Deacon *et al.*, 1989), where steric interactions are greater.

This study was carried out during the tenure of grants from the Australian Research Council and the Anticancer Council of Victoria. This support and the loan of platinum from Johnson Matthey are gratefully acknowledged.

References

BOER, J. L. DE & DUISENBERG, A. J. M. (1984). Enraf–Nonius CAD-4F diffractometer software update. February 1984. Groningen and Utrecht, The Netherlands.

BRATERMAN, P. S., CROSS, R. J., MANOJLOVIC-MUIR, L., MUIR, K. W. & YOUNG, G. B. (1975). *J. Organomet. Chem.* **84**, C40–C42.

DEACON, G. B., GATEHOUSE, B. M. & NELSON-REED, K. T. (1989). *J. Organomet. Chem.* **359**, 267–283.

DEACON, G. B. & NELSON, K. T. (1990). Unpublished results.

JOHNSON, C. K. (1971). *ORTEPII*. Report ORNL-3794. Oak Ridge National Laboratory, Tennessee, USA.

SHELDRICK, G. M. (1976). *SHELX76*. Program for crystal structure determination. Univ. of Cambridge, England.

USÓN, R. & FORNIÉS, J. (1988). *Adv. Organomet. Chem.* **28**, 219–297.

Acta Cryst. (1991). C47, 957–959

Structure of Di-μ-cyanato-bis[cyanato(*N*,*N*-diethylethylenediamine)copper(II)], $[Cu(NCO)_2(diEten)]_2$

BY J. ZUKERMAN-SCHPECTOR, E. E. CASTELLANO, C. A. DE SIMONE AND G. OLIVA

Instituto de Física e Química de São Carlos, Universidade de São Paulo, Caixa Postal 369, 13560 *São Carlos SP, Brazil*

AND A. E. MAURO

Instituto de Química de Araraquara, UNESP, Caixa Postal 355, 14800 *Araraquara SP, Brazil*

(*Received* 15 *August* 1990; *accepted* 11 *October* 1990)

Abstract. $[Cu_2(NCO)_4(C_6N_2H_{16})_2]$, $M_r = 527{\cdot}56$, monoclinic, $P2_1/c$, $a = 11{\cdot}586$ (2), $b = 7{\cdot}279$ (1), $c = 13{\cdot}742$ (2) Å, $\beta = 96{\cdot}02$ (2)°, $V = 1152{\cdot}5$ (6) Å^3, $Z = 2$, $D_x = 1{\cdot}520$ g cm^{-3}, λ(Mo $K\alpha$) = 0·71073 Å, $\mu = 18{\cdot}87$ cm^{-1}, $F(000) = 548$, $T = 296$ *K*, $R = 0{\cdot}033$ for 1393 observed reflections. The compound is in a

0108-2701/91/050957-03$03.00 © 1991 International Union of Crystallography

dimeric form. Each metal atom is coordinated to five N atoms: two from one diEten group [Cu—N = 2·102 (3), 1·974 (3) Å], one from a terminal cyanate group [Cu—N = 1·938 (4) Å] and two belonging to bridging cyanate groups [Cu—N = 2·017 (3), 2·450 (4) Å], giving rise to a distorted, elongated square-pyramidal configuration. The Cu···Cu distance is 3·236 (1) Å. Dimers are linked through H bonds involving the O of the bridging cyanate and the NH_2 end of diEten [N(4)···O(1)($-x$, $-1-y$, $1-z$) = 2·943 (5) Å, N(4)—H(4)···O(1) = 165·2 (2)°].

Introduction. One of our research interests has been the solid-state structural characterization of copper compounds with nitrogen-based ligands (Zukerman-Schpector, Castellano, Oliva, Mauro & Roveri, 1985; Zukerman-Schpector, Castellano, Mauro & Roveri, 1986), because structural parameters from copper amine complexes may be related to those of biological systems such as copper-containing proteins (Chaudhuri, Oder, Wieghardt, Nuber & Weiss, 1986). As part of this study the title compound was synthesized and its structure determination carried out.

Experimental. To a solution 2·82 mmol of $Cu(NO_3)_2.3H_2O$ in methanol was added a 2·82 mmol solution of diEten, followed by a dropwise addition of a 6·47 mmol water solution of KCNO. The mixture was stirred for 15 min at room temperature and the compound obtained was filtered off, washed with Et_2O and dried in vacuo. Recrystallization from methanol yielded prismatic blue crystals.

A single crystal with approximate dimensions 0·13 × 0·30 × 0·35 mm was used for data collection and cell determination on an Enraf–Nonius CAD-4 diffractometer with graphite-monochromatized Mo $K\alpha$ radiation. Unit-cell parameters were obtained from a least-squares refinement of the setting angles of 25 reflections in the θ range 12 to 24°. Intensity data were collected in the $\omega/2\theta$ scan mode up to θ_{max} = 25°; 2106 reflections were measured, of which 2002 were independent (R_{int} = 0·013, $-13 \le h \le 13$, $0 \le k \le 8$, $0 \le l \le 16$) and 1393 with $I \ge 4\sigma(I)$ were employed in the refinement procedure (137 parameters refined). Data were corrected for Lp and absorption, maximum and minimum transmission factors were 1·16, 0·81 (Walker & Stuart, 1983). The intensities of two standard reflections (029, 606) were essentially constant throughout the experiment.

The structure was solved using the heavy-atom Patterson method and difference Fourier techniques. In the final cycles of least-squares refinement, on F's, all non-H atoms were treated anisotropically. H atoms were included as fixed contributors at positions found in a difference synthesis, slightly modified, when possible, on stereochemical grounds, all with a common isotropic temperature factor that refined to U = 0·073 Å^2. The function minimized was $\sum w(|F_o| - |F_c|)^2$, where $w^{-1} = \sigma^2(F_o) + 0{\cdot}003F_o^2$, resulting in R = 0·033, wR = 0·036 and S = 0·63. The maximum shift/e.s.d. ratio was 0·001 and the maximum and minimum electron densities in the final difference map were 0·8 and −0·46 e Å^{-3} respectively. Scattering factors for non-H atoms were taken from Cromer & Mann (1968) with corrections for anomalous dispersion from Cromer & Liberman (1970); scattering factors for H atoms were from Stewart, Davidson & Simpson (1965). Programs used: *SHELX*76 (Sheldrick, 1976) and *ORTEP* (Johnson, 1965).

The infrared (IR) spectrum was recorded as a Nujol mull between CsI plates on a Nicolet 720-FT spectrophotomer.

Table 1. *Final fractional atomic coordinates and isotropic temperature factors* (Å^2) *with e.s.d.'s in parentheses*

$^*B_{iso} = \frac{4}{3}\sum_i\sum_j B_{ij}(\mathbf{a}_i.\mathbf{a}_j)$.

	x	y	z	B_{iso}*
Cu	0·1259 (1)	−0·0935 (1)	0·5274 (1)	2·53 (1)
N(1)	−0·0205 (3)	−0·1940 (5)	0·4541 (3)	3·6 (1)
N(2)	0·1882 (3)	−0·0104 (6)	0·4095 (3)	4·0 (1)
N(3)	0·2890 (3)	−0·0939 (5)	0·6103 (2)	2·78 (9)
N(4)	0·0677 (3)	−0·1639 (5)	0·6521 (2)	2·90 (9)
O(1)	−0·0868 (3)	−0·4329 (5)	0·3478 (3)	5·9 (1)
O(2)	0·3011 (5)	0·1976 (9)	0·3340 (4)	10·2 (2)
C(1)	−0·0513 (3)	−0·3141 (5)	0·4036 (3)	3·1 (1)
C(2)	0·2437 (4)	0·0922 (7)	0·3724 (3)	4·3 (1)
C(3)	0·1528 (3)	−0·1144 (7)	0·7345 (3)	3·5 (1)
C(4)	0·2697 (3)	−0·1720 (7)	0·7068 (3)	3·9 (1)
C(5)	0·3729 (4)	−0·2077 (7)	0·5608 (3)	4·1 (1)
C(6)	0·3291 (3)	0·1002 (6)	0·6191 (3)	3·7 (1)
C(7)	0·4479 (4)	0·1318 (8)	0·6750 (4)	5·3 (2)
C(8)	0·3239 (5)	−0·3880 (8)	0·5234 (5)	5·9 (2)

Table 2. *Interatomic distances* (Å) *and angles* (°)

Cu—N(1)	2·017 (3)	Cu—N(2)	1·938 (4)
Cu—N(3)	2·102 (3)	Cu—N(4)	1·974 (3)
Cu—N(1′)	2·450 (4)	Cu—Cu′	3·236 (1)
N(1)—C(1)	1·149 (5)	N(2)—C(2)	1·140 (6)
N(3)—C(4)	1·481 (5)	N(3)—C(5)	1·494 (6)
N(3)—C(6)	1·488 (6)	N(4)—C(3)	1·466 (5)
C(1)—O(1)	1·199 (6)	C(2)—O(2)	1·176 (8)
C(3)—C(4)	1·504 (6)	C(5)—C(8)	1·499 (8)
C(6)—C(7)	1·522 (7)		

N(1)—Cu—N(2)	93·6 (2)	N(1)—Cu—N(3)	158·7 (1)
N(1)—Cu—N(4)	89·6 (1)	N(1)—Cu—N(1′)	87·7 (1)
N(2)—Cu—N(3)	93·5 (1)	N(2)—Cu—N(4)	176·1 (1)
N(2)—Cu—N(1′)	93·1 (1)	N(3)—Cu—N(4)	84·2 (1)
N(3)—Cu—N(1′)	112·0 (1)	N(4)—Cu—N(1′)	85·0 (1)
Cu—N(1)—C(1)	140·3 (3)	Cu—N(1)—Cu′	92·3 (1)
C(1)—N(1)—Cu′	125·9 (3)	Cu—N(2)—C(2)	148·8 (4)
Cu—N(3)—C(4)	105·9 (2)	Cu—N(3)—C(5)	110·2 (2)
Cu—N(3)—C(6)	107·3 (2)	C(4)—N(3)—C(5)	111·2 (3)
C(4)—N(3)—C(6)	111·5 (3)	C(5)—N(3)—C(6)	110·5 (3)
Cu—N(4)—C(3)	110·1 (2)	N(1)—C(1)—O(1)	176·5 (5)
N(2)—C(2)—O(2)	179·8 (6)	N(4)—C(3)—C(4)	106·6 (3)
N(3)—C(4)—C(3)	110·1 (3)	N(3)—C(5)—C(8)	113·6 (4)
N(3)—C(6)—C(7)	116·3 (4)		

Symmetry operation: (′) $-x$, $-y$, $1-z$.

Discussion. The final atomic parameters are given in Table 1* and bond distances and angles in Table 2. A projection of the dimer is shown in Fig. 1.

The compound is in a dimeric form with the two halves related by a center of symmetry; the Cu···Cu distance of 3·236 (1) Å is sufficiently long to preclude any significant interaction. The dimers are H bonded through the NH_2 end of the diEten group and the O of the bridging cyanate group: N(4)···O(1)-($-x$, $-1-y$, $1-z$) = 2·943 (5), N(4)—H(N4) = 0·941 (3) Å, N(4)—H(N4)···O(1) = 165·2 (2)°.

The Cu atom exhibits a distorted square-pyramidal coordination. The equatorial positions are occupied by four N atoms: two from the diEten group, one from the terminal and one from a bridging cyanate; the apical position is occupied by the N atom of the symmetry-related bridging cyanate group. As a result of the steric constraints imposed by the bite of the diEten residue the equatorial plane is distorted. The Cu atom lies out of the basal plane by 0·158 (1) Å towards the apical N atom.

As in other Cu(diEten) and Cu(diMeen) (diMeen = *N,N*-dimethylethylenediamine) complexes (Casagrande, Klein, Mauro & Tomita, 1989; Mauro, Klein, Saldaña, De Simone, Zukerman-Schpector & Castellano, 1990), the longest Cu—N bond length involves the most substituted N atom. The Cu—N(1) distance of 2·017 (3) Å is essentially equal to those found in other cyanate-bridged binuclear copper(II) complexes (Valach, Dunaj-Jurco, Garaj & Hvastijová, 1975; Boillot, Kahn, O'Connor, Gouteron, Jeannin & Jeannin, 1985).

The coordination chemistry of the cyanate anion has been extensively considered (Kepert, Kucharski & White, 1980) and a list of cyanate dimensions of structurally characterized cyanate-containing molecules can be found in Cortés, Arriortua, Rojo, Mesa, Solans & Beltran (1988). In agreement with the general aspects found for coordinated cyanate groups, both terminal and bridging cyanates are essentially linear [N(1)—C(1)—O(1) = 176·5 (5), N(2)—C(2)—O(2) = 179·8 (6)°]. They are, however, asymmetric, the longest N—C and C—O bonds being those of the bridging cyanate. Cortés *et al.* (1988) suggest that in agreement with the shorter N(2)—C(2) bond length, the shortening of the Cu—N(2) bond length, which is 0·079 Å shorter than that of the Cu—N(1), can be ascribed to a larger π-donor character in the Cu—N(2) bond.

The IR spectrum shows the absorption bands corresponding to N-bonded NCO ions (Nelson & Nelson, 1969; Burmeister & O'Sullivan, 1969): at 2206(*w*), 2187(*s*) cm^{-1}, νCN; 1214(*m*) cm^{-1}, νCO; 646(*m*), 618(*m*) cm^{-1}, δ(NCO).

This work has received partial support from CAPES, CNPq, FINEP and FAPESP which are hereby gratefully acknowledged.

* Lists of H-atom positions, anisotropic thermal parameters and structure factors have been deposited with the British Library Document Supply Centre as Supplementary Publication No. SUP 53651 (13 pp.). Copies may be obtained through The Technical Editor, International Union of Crystallography, 5 Abbey Square, Chester CH1 2HU, England.

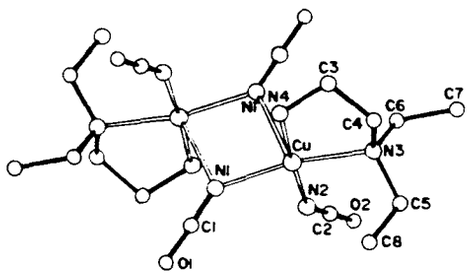

Fig. 1. Projection of a dimer showing the atom labeling. N(1′) = N(1)($-x$, $-y$, $1-z$).

References

BOILLOT, M. L., KAHN, O., O'CONNOR, C. J., GOUTERON, J., JEANNIN, S. & JEANNIN, Y. (1985). *J. Chem. Soc. Chem. Commun.* pp. 178–180.

BURMEISTER, J. L. & O'SULLIVAN, T. P. (1969). *Inorg. Chim. Acta*, **3**, 479–486.

CASAGRANDE, O. L., KLEIN, S., MAURO, A. E. & TOMITA, K. (1989). *Transition Met. Chem.* **14**, 45–47.

CHAUDHURI, P., ODER, K., WIEGHARDT, K., NUBER, B. & WEISS, J. (1986). *Inorg. Chem.* **25**, 2818–2824.

CORTÉS, R., ARRIORTUA, M. I., ROJO, T., MESA, J. L., SOLANS, X. & BELTRAN, D. (1988). *Acta Cryst.* C**44**, 986–990.

CROMER, D. T. & LIBERMAN, D. (1970). *J. Chem. Phys.* **53**, 1891–1898.

CROMER, D. T. & MANN, J. B. (1968). *Acta Cryst.* A**24**, 321–324.

JOHNSON, C. K. (1965). *ORTEP*. Report ORNL-3794. Oak Ridge National Laboratory, Tennessee, USA.

KEPERT, D. L., KUCHARSKI, E. S. & WHITE, A. H. (1980). *J. Chem. Soc. Dalton Trans.* pp. 1932–1938.

MAURO, A. E., KLEIN, S. I., SALDAÑA, J. S., DE SIMONE, C. A., ZUKERMAN-SCHPECTOR, J. & CASTELLANO, E. E. (1990). *Polyhedron*. Submitted.

NELSON, J. & NELSON, S. M. (1969). *J. Chem. Soc.* pp. 1597–1603.

SHELDRICK, G. M. (1976). *SHELX*76. Program for crystal structure determination. Univ. of Cambridge, England.

STEWART, R. F., DAVIDSON, E. R. & SIMPSON, W. T. (1965). *J. Chem. Phys.* **42**, 3175–3187.

VALACH, F., DUNAJ-JURCO, M., GARAJ, J. & HVASTIJOVÁ, M. (1975). *Collect. Czech. Chem. Commun.* **39**, 380–386.

WALKER, N. & STUART, D. (1983). *Acta Cryst.* A**39**, 158–166.

ZUKERMAN-SCHPECTOR, J., CASTELLANO, E. E., MAURO, A. E. & ROVERI, M. R. (1986). *Acta Cryst.* C**42**, 302–303.

ZUKERMAN-SCHPECTOR, J., CASTELLANO, E. E., OLIVA, G., MAURO, A. E. & ROVERI, M. R. (1985). *Acta Cryst.* C**41**, 204–206.

Acta Cryst. (1991). C47, 960–962

Structure of Dichloro[(*Z*)-2-chloro-2-*p*-tolylvinyl](*p*-methoxyphenyl)tellurium(IV)

BY J. ZUKERMAN-SCHPECTOR, E. E. CASTELLANO AND G. OLIVA

Instituto de Física e Química de São Carlos, Universidade de São Paulo, Caixa Postal 369, 13560 *São Carlos SP, Brazil*

AND J. V. COMASSETO AND H. A. STEFANI

Instituto de Química, Universidade de São Paulo, Caixa Postal, 20780, 01498 *São Paulo SP, Brazil*

(*Received* 3 *September* 1990; *accepted* 30 *October* 1990)

Abstract. $[TeCl_2(C_9H_8Cl)(C_7H_7O)]$, $M_r = 457{\cdot}26$, orthorhombic, *Pbcn*, $a = 18{\cdot}829\ (3)$, $b = 8{\cdot}809\ (3)$, $c = 20{\cdot}969\ (3)$ Å, $V = 3478\ (2)$ Å^3, $Z = 8$, $D_x = 1{\cdot}747$ g cm^{-3}, λ(Mo $K\alpha$) = 0·71073 Å, $\mu = 21{\cdot}75$ cm^{-1}, $F(000) = 1776$, $T = 296$ K, final $R = 0{\cdot}034$ for 1958 independent observed reflections. The Te^{IV} ion is in a trigonal bipyramidal configuration with the lone pair of electrons at one of the equatorial positions. Distances and angles are: Te—Cl = 2·478 (2), 2·521 (2); Te—C = 2·085 (6), 2·117 (5) (aryl) Å; Cl—Te—Cl = 177·65 (6); Cl—Te—C = 90·8 (2), 90·2 (1), 86·8 (2), 90·1 (1); C—Te—C = 94·1 (2)°.

Introduction. Vinylic tellurides are emerging as important intermediates in the synthesis of vinyllithium compounds (Barros, Comasseto & Berriel, 1989) which are, in turn, important intermediates in organic synthesis, either as nucleophiles leading to products of chain elongation by reaction with many electrophiles or as precursors of the widely used vinyl cuprate compounds (Lipshutz, 1989; Comasseto & Berriel, 1990).

The crystal structure determination of compound (I) was undertaken because the knowledge of its stereochemistry is needed, both to predict successive reaction pathways (it is supposed that transformations occur with retention of the olefin geometry) and to postulate the structure of the intermediate compound in its synthesis.

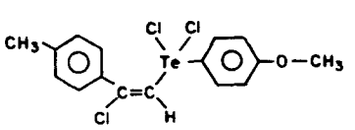

(I)

Experimental. The synthesis of the title compound is being published elsewhere (Comasseto, Stefani & Chieffi, 1990).

A single colorless crystal with approximate dimensions 0·20 × 0·40 × 0·45 mm was used for data collection and cell determination on an Enraf–Nonius CAD-4 diffractometer with graphite-monochromatized Mo $K\alpha$ radiation. Unit-cell parameters were obtained from a least-squares refinement of the setting angles of 25 reflections in the θ range 9 to 19°. Intensity data were collected in the ω–2θ scan mode up to $\theta_{max} = 25°$; 3173 reflections were measured, of which 2789 were independent ($R_{int} = 0{\cdot}025$, $0 \le h \le 22$, $0 \le k \le 10$, $0 \le l \le 24$), and 1958 with $I > 3\sigma(I)$ were employed in the refinement procedure (191 parameters refined). Data were corrected for Lp and absorption, max. and min. transmission factors 1·16, 0·76 (Walker & Stuart, 1983). The intensities of two standard reflections (0,0,16, 0,16,0) were essentially constant throughout the experiment.

The structure was solved using the heavy-atom method and difference Fourier techniques. In the final cycles of least-squares refinement on F, all non-H atoms were treated anisotropically. H atoms were included as fixed contributors at positions found in a difference synthesis, slightly modified when possible on stereochemical grounds, all with a common isotropic temperature factor that refined to $U = 0{\cdot}086$ Å^2. The function minimized was $\sum w(|F_o| - |F_c|)^2$, where $w^{-1} = \sigma^2(F_o) + 0{\cdot}0005F_o^2$ resulting in $R = 0{\cdot}034$, $wR = 0{\cdot}036$ and $S = 1{\cdot}34$. Maximum shift-to-e.s.d. ratio was 0·001 and the maximum and minimum electron densities in the final difference map were 0·77 and −0·74 e Å^{-3}, respectively. Scattering factors for non-H atoms were taken from Cromer & Mann (1968) with corrections for anomalous dispersion from Cromer & Liberman (1970); for H atoms from Stewart, Davidson & Simpson (1965). Programs used: *SHELX*76 (Sheldrick, 1976) and *ORTEP* (Johnson, 1965).

Discussion. Final atomic parameters for non-H atoms are given in Table 1,* interatomic distances

* Lists of H-atom positions, anisotropic thermal parameters and structure factors have been deposited with the British Library Document Supply Centre as Supplementary Publication No. SUP 53713 (18 pp.). Copies may be obtained through The Technical Editor, International Union of Crystallography, 5 Abbey Square, Chester CH1 2HU, England.

0108-2701/91/050960-03$03.00

© 1991 International Union of Crystallography

Table 1. *Final atomic coordinates and equivalent isotropic temperature factors* (Å^2)

	x	y	z	B_{eq}
Te	0·6878 (1)	0·1080 (1)	0·4049 (1)	4·01 (1)
Cl(1)	0·5674 (1)	0·1862 (2)	0·4395 (1)	5·66 (6)
Cl(2)	0·8080 (1)	0·0215 (2)	0·3663 (1)	5·85 (6)
Cl(3)	0·6163 (2)	0·1922 (2)	0·2667 (1)	9·2 (1)
O(1)	0·6866 (2)	−0·3582 (5)	0·6282 (2)	5·3 (2)
C(1)	0·6445 (3)	−0·0420 (6)	0·3385 (3)	4·2 (2)
C(2)	0·6185 (3)	0·0000 (6)	0·2825 (3)	4·1 (2)
C(3)	0·5918 (3)	−0·0987 (7)	0·2327 (2)	3·9 (2)
C(4)	0·5652 (3)	−0·0449 (7)	0·1761 (3)	4·4 (2)
C(5)	0·5423 (3)	−0·1469 (8)	0·1293 (3)	5·1 (2)
C(6)	0·5445 (3)	−0·3004 (8)	0·1377 (3)	4·8 (2)
C(7)	0·5716 (3)	−0·3552 (7)	0·1941 (3)	5·1 (2)
C(8)	0·5958 (3)	−0·2573 (7)	0·2410 (3)	4·7 (2)
C(9)	0·5167 (4)	−0·4094 (9)	0·0879 (3)	7·1 (3)
C(10)	0·6913 (3)	−0·0553 (6)	0·4789 (2)	3·8 (2)
C(11)	0·7542 (3)	−0·0882 (6)	0·5092 (3)	4·3 (2)
C(12)	0·7550 (3)	−0·1922 (7)	0·5600 (3)	4·5 (2)
C(13)	0·6927 (3)	−0·2596 (7)	0·5795 (3)	4·1 (2)
C(14)	0·6303 (3)	−0·2284 (7)	0·5476 (3)	4·8 (2)
C(15)	0·6292 (3)	−0·1264 (7)	0·4974 (3)	4·4 (2)
C(16)	0·7481 (3)	−0·3861 (8)	0·6664 (3)	6·6 (3)

Table 2. *Interatomic distances* (Å) *and angles* (°)

Te—Cl(1)	2·478 (2)	Te—Cl(2)	2·521 (2)
Te—C(1)	2·085 (6)	Te—C(10)	2·117 (5)
Cl(3)—C(2)	1·726 (6)	O(1)—C(13)	1·345 (7)
O(1)—C(16)	1·429 (8)	C(1)—C(2)	1·325 (8)
C(2)—C(3)	1·449 (8)	C(3)—C(4)	1·373 (8)
C(3)—C(8)	1·410 (9)	C(4)—C(5)	1·399 (9)
C(5)—C(6)	1·36 (1)	C(6)—C(7)	1·375 (9)
C(6)—C(9)	1·51 (1)	C(7)—C(8)	1·385 (9)
C(10)—C(11)	1·375 (7)	C(10)—C(15)	1·382 (7)
C(11)—C(12)	1·405 (8)	C(12)—C(13)	1·377 (8)
C(13)—C(14)	1·379 (8)	C(14)—C(15)	1·384 (8)

Cl(1)—Te—Cl(2)	177·65 (6)	Cl(1)—Te—C(1)	90·8 (2)
Cl(1)—Te—C(10)	90·2 (1)	Cl(2)—Te—C(1)	86·8 (2)
Cl(2)—Te—C(10)	90·1 (1)	C(1)—Te—C(10)	94·1 (2)
C(13)—O(1)—C(16)	117·9 (5)	Te—C(1)—C(2)	124·0 (4)
Cl(3)—C(2)—C(1)	116·9 (4)	Cl(3)—C(2)—C(3)	116·2 (4)
C(1)—C(2)—C(3)	126·8 (5)	C(2)—C(3)—C(4)	122·9 (5)
C(2)—C(3)—C(8)	119·2 (5)	C(4)—C(3)—C(8)	117·9 (5)
C(3)—C(4)—C(5)	119·8 (5)	C(4)—C(5)—C(6)	122·5 (6)
C(5)—C(6)—C(7)	118·0 (6)	C(5)—C(6)—C(9)	122·0 (6)
C(7)—C(6)—C(9)	120·0 (6)	C(6)—C(7)—C(8)	120·9 (6)
C(3)—C(8)—C(7)	120·8 (5)	Te—C(10)—C(11)	120·6 (4)
Te—C(10)—C(15)	119·2 (4)	C(11)—C(10)—C(15)	120·2 (5)
C(10)—C(11)—C(12)	119·8 (5)	C(11)—C(12)—C(13)	119·8 (5)
O(1)—C(13)—C(12)	125·2 (5)	O(1)—C(13)—C(14)	115·1 (5)
C(12)—C(13)—C(14)	119·7 (5)	C(13)—C(14)—C(15)	120·7 (5)
C(10)—C(15)—C(14)	119·7 (5)		

and angles are in Table 2. Fig. 1 is a projection of the molecule showing the atom numbering.

The Te^{IV} ion presents a typical trigonal bipyramidal configuration formed from four bonds to the ligands (two Cl and two C atoms) and one lone pair of electrons. The lone pair invariably occupies one of the equatorial sites, together with C(1) and C(10) in this compound, while the Cl atoms occupy the axial positions. This configuration is in complete agreement with the valence-shell electron-pair-repulsion model (VSEPR) (Gillespie, 1972). The quadruple average angle of the lone pair, α_4^E, is 112·1° and is a typical value found in TeX_4E configurations (Hargittai & Rozsondai, 1986). The Te—Cl bond lengths of 2·478 (2) and 2·521 (2) Å and the Cl—Te—Cl angle of 177·65 (6)° are in good agreement, within experimental accuracy, with the values found in other $TeCl_2RR'$ compounds (Castellano, Zukerman-Schpector, Ferreira & Comasseto, 1986; Zukerman-Schpector, Castellano, Comasseto & Stefani, 1988) and, as expected for trigonal bipyramidal coordination, the axial bonds are 0·12 and 0·16 Å longer than the sum of the normal covalent radii, 2·36 Å (Ziolo & Troup, 1983). On the other hand, the C—Te—C angle of 94·1 (2)° is smaller than the average value of 99° found in the these species. The Te—C(10) bond of 2·117 (5) Å is in good agreement with the values found for most Te^{IV}—C(aryl) bonds (Zukerman-Schpector, Castellano, Comasseto & Stefani, 1988, and references therein). Using the empirical value proposed by Lide (1962) for the radius of the trigonal C atom and the Pauling (1960) radius for the Te atom, the predicted Te—C distance is (0·74 + 1·37) = 2·11 Å, in good agreement with the values observed, Te—C(1) = 2·085 (6), Te—C(10) = 2·117 (5) Å.

Both phenyl rings are planar to within experimental accuracy [σ_{av} defined as $(\sum_i d_i^2/N-3)^{1/2}$ are σ_{av}C(3)–C(8) = 0·009 and σ_{av}C(10)–C(15) = 0·012]; the average C—C distance, uncorrected for thermal motion, is 1·384 (3) Å, which is in good agreement with the values found elsewhere (Domenicano, Murray-Rust & Vaciago, 1983). The dihedral angle between the planes defined by atoms O(1), C(13), C(13), C(16) and C(10)–C(15) inclusive is 5 (1)°. The C(1)—C(2) double-bond distance, 1·325 (8) Å, is in the expected range. The distances C(2)—C(3) = 1·449 (8) and O(1)—C(13) = 1·345 (7) Å are both shorter than the sum of the corresponding single-bond radii (Pauling, 1960), presumably due to conjugation with the phenyl rings to which they are attached.

The C(1)···C(3) distance of 2·481 (7) Å is in good agreement with the value of 2·50 Å predicted from the 1···3 non-bonded radius, also called the 'one angle' atomic radius, for C atoms of 1·25 Å (O'Keeffe & Hyde, 1981). From the Te···C(2) distance of 3·035 (5) Å, the non-bonded radius for

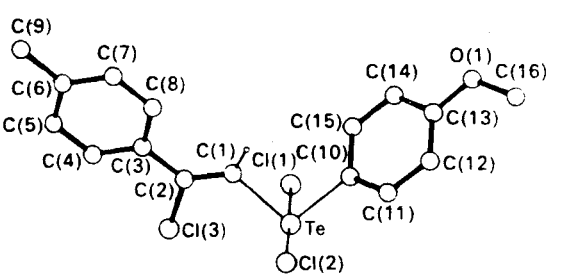

Fig. 1. Perspective view of the molecule showing the atom labelling.

Te may be estimated to be 1·79 Å; a value of 1·78 Å is found in $TeCl_2(C_7H_7O)(C_7H_{11}O_2)$ (Castellano, Zukerman-Schpector, Ferreira & Comasseto, 1986).

The fact that the title compound is in a *Z* configuration is consistent with a four-member transition state (II) and not with a telluronium intermediate which should lead to the *E* isomer.

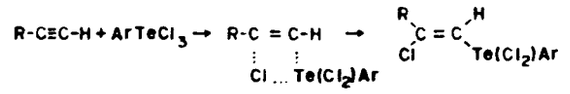

(II)

This work has received partial support from CNPq, FAPESP, CAPES and FINEP, which are hereby gratefully acknowledged.

References

BARROS, S. M., COMASSETO, J. V. & BERRIEL, J. (1989). *Tetrahedron Lett.* **30**, 7353–7356.

CASTELLANO, E. E., ZUKERMAN-SCHPECTOR, J., FERREIRA, J. T. B. & COMASSETO, J. V. (1986). *Acta Cryst.* C**42**, 44–46.

COMASSETO, J. V. & BERRIEL, J. (1990). *Synth. Commun.* In the press.

COMASSETO, J. V., STEFANI, H. A. & CHIEFFI, A. (1990). *Tetrahedron Lett.* Submitted.

CROMER, D. T. & LIBERMAN, D. (1970). *J. Chem. Phys.* **53**, 1891–1898.

CROMER, D. T. & MANN, J. B. (1968). *Acta Cryst.* A**24**, 321–324.

DOMENICANO, A., MURRAY-RUST, P. & VACIAGO, A. (1983). *Acta Cryst.* B**39**, 457–468.

GILLESPIE, R. J. (1972). *Molecular Geometry*. London: Van Nostrand Reinhold.

HARGITTAI, I. & ROZSONDAI, B. (1986). In *The Chemistry of Organic Selenium and Tellurium Compounds*, Vol. 1, edited by S. PATAI & Z. RAPPOPORT, pp. 63–155. New York: John Wiley.

JOHNSON, C. K. (1965). *ORTEP*. Report ORNL-3794. Oak Ridge National Laboratory, Tennessee, USA.

LIDE, D. L. (1962). *Tetrahedron*, **17**, 125–134.

LIPSHUTZ, B. H. ED. (1989). *Tetrahedron*, **45**(2), 349–578.

O'KEEFFE, M. & HYDE, B. G. (1981). *Structure and Bonding in Crystals*, Vol. 1, edited by M. O'KEEFFE & A. NAVROTSKY, pp. 227–254. New York: Academic Press.

PAULING, L. (1960). *The Nature of the Chemical Bond*, 3rd ed. Ithaca, NY: Cornell Univ. Press.

SHELDRICK, G. M. (1976). *SHELX76*. Program for crystal structure determination. Univ. of Cambridge, England.

STEWART, R. F., DAVIDSON, E. R. & SIMPSON, W. T. (1965). *J. Chem. Phys.* **42**, 3175–3187.

WALKER, N. & STUART, D. (1983). *Acta Cryst.* A**39**, 158–166.

ZIOLO, R. F. & TROUP, J. M. (1983). *J. Am. Chem. Soc.* **105**, 229–235.

ZUKERMAN-SCHPECTOR, J., CASTELLANO, E. E., COMASSETO, J. V. & STEFANI, H. A. (1988). *Acta Cryst.* C**44**, 2182–2184.

Acta Cryst. (1991). C**47**, 962–966

Structure of Wolffram's Salt Analogues $[M(-chxn)_2Br]Br_2$ [*M* = Pd, Pt; −chxn = (−)-1,2-cyclohexanediamine]

BY ALAN HAZELL

Institute of Chemistry, Aarhus University, DK-8000 Århus C., Denmark

(*Received* 22 *June* 1990; *accepted* 7 *November* 1990)

Abstract. *trans*-Dibromobis[(−)-1(*R*),2(*R*)-cyclohexanediamine]palladium(IV)-bis[(−)-1(*R*),2(*R*)-cyclohexanediamine]palladium(II) tetrabromide, $[Pd(C_6H_{14}N_2)_2Br_2][Pd(C_6H_{14}N_2)_2]Br_4$, M_r = 936·2, MDO1: monoclinic, a = 24·464 (3), b = 7·073 (1), c = 10·586 (2) Å, β = 102·504 (6)°, V = 1788·4 (4) Å^3, Z = 2; superposition structure: orthorhombic, *I*222, a = 23·884 (3), b = 7·073 (1), c = 5·293 (1) Å, V = 894·2 (2) Å^3, Z = 1, D_x = 1·783 g cm^{-3}, $F(000)$ = 558, Ag $K\alpha$ (λ = 0·56087 Å), μ = 36·3 cm^{-1}, T = 295 K, $R(F)$ = 0·032 for 1390 observed unique reflexions [$I > 3\sigma(I)$]. *trans*-Dibromobis[(−)-1(*R*),2(*R*)-cyclohexanediamine]platinum(IV)-bis[(−)-1(*R*),2(*R*)-cyclohexanediamine]platinum(II) tetrabromide, $[Pt(C_6H_{14}N_2)_2Br_2][Pt(C_6H_{14}N_2)_2]Br_4$, M_r = 1326·4, MDO1: monoclinic, a = 24·478 (3), b = 7·022 (1), c = 10·747 (1) Å, β = 102·668 (7)°, V = 1802·4 (3) Å^3, Z = 2; superposition structure: orthorhombic, *I*222, a = 23·884 (3), b = 7·022 (1), c = 5·374 (1) Å, V = 901·3 (2) Å^3, Z = 1, D_x = 2·443 g cm^{-3}, $F(000)$ = 622, Mo $K\alpha$ (λ = 0·71073 Å), μ = 144·5 cm^{-1}, T = 295 K, $R(F)$ = 0·036 for 2697 reflexions [$I > 3\sigma(I)$]. $[Pt(C_6H_{14}N_2)_2Cl_2][Pt(C_6H_{14}N_2)_2]Cl_4$, M_r = 1059·6, MDO1: monoclinic, a = 24·810 (4), b = 6·820 (1), c = 10·316 (2) Å, β = 101·999 (3)°, V = 853·7 (3) Å^3, Z = 2. The superposition structures are isomorphous with the platinum chloride compound [Larsen & Toftlund (1977). *Acta Chem. Scand. Ser. A*, **31**, 182–186]. They are built up of M^{IV}—X···M^{II} chains parallel to the c axis, but with two half-weight halide ions indicating disorder. Pd^{IV}—Br = 2·521 (4), Pd^{II}—Br = 2·782 (4) and Pd—N = 2·058 (3) Å. PdN_4 is tetrahedrally distorted with N—Pd—N = 177·6 (8)°. Pt^{IV}—Br =

0108-2701/91/050962-05$03.00 © 1991 International Union of Crystallography

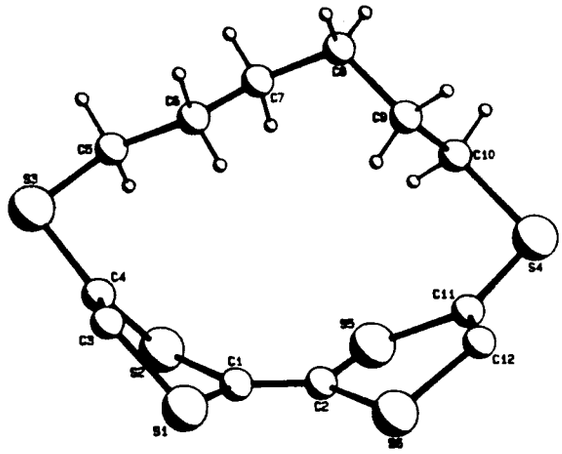

Fig. 2. Side view of the molecule (*PLUTO*; Motherwell & Clegg, 1978). The *p*-tolyl substituents have been omitted for clarity.

in the TTF molecule [1·729 (2) to 1·732 Å] (Cooper, Kenny, Edmonds, Nagel, Wudl & Coppens, 1971). The average S—C_{sp^2} bond length of 1·821 (4) Å is in agreement with the sum of single-bond radii (1·812 Å) (Pauling, 1960) as well as with the previously reported value [1·802 (4) Å] for 3,4′-dimethyl-3′4-bis(methylthio)-2,2′,5,5′-tetrathiafulvalene (Ouahab & Batail, 1985).

References

BERTHO, F., ROBERT, A., BATAIL, P. & ROBIN, P. (1990). *Tetrahedron*, **46**, 433–444.

BERTHO-THORAVAL, F. (1988). Thèse Doctorat, Univ. Rennes 1, France.

COOPER, W. F., KENNY, N. C., EDMOND, W. J., NAGEL, A., WUDL, F. & COPPENS, P. (1971). *J. Chem. Soc. Chem. Commun.* pp. 889–890.

FRENZ, B. A. (1983). *Enraf–Nonius Structure Determination Package; SDP Users Guide*. Version of 6 January 1983. Enraf–Nonius, Delft, The Netherlands.

JOHNSON, C. K. (1976). *ORTEPII*. Report ORNL-5138. Oak Ridge National Laboratory, Tennessee, USA.

MAIN, P., FISKE, S. J., HULL, S. E., LESSINGER, L., GERMAIN, G., DECLERCQ, J.-P. & WOOLFSON, M. M. (1982). *MULTAN11/82. A System of Computer Programs for the Automatic Solution of Crystal Structures from X-ray Diffraction Data*. Univs. of York, England, and Louvain, Belgium.

MOTHERWELL, W. D. S. & CLEGG, W. (1978). *PLUTO*. Program for plotting molecular and crystal structures. Univ. of Cambridge, England.

OUAHAB, L. & BATAIL, P. (1985). *Acta Cryst.* C**41**, 928–929.

PAULING, L. (1960). *The Nature of the Chemical Bond*. Ithaca: Cornell Univ. Press.

STAAB, H. A., IPPEN, J., TAO-PEN, C., KRIEGER, C. & STARKER, B. (1980). *Angew. Chem. Int. Ed. Engl.* **19**, 66–67.

Acta Cryst. (1991). C**47**, 1111–1113

Structure of 6,7-Dimethoxy-2,2-dimethyl-2*H*-chromene, a Natural Precocene

BY J. ZUKERMAN-SCHPECTOR, C. A. DE SIMONE, E. E. CASTELLANO AND G. OLIVA

Instituto de Física e Química de São Carlos, Universidade de São Paulo, Caixa Postal 369, 13560 *São Carlos – SP, Brazil*

AND J. TERCIO, B. FERREIRA AND V. CATANI

Departamento de Química, Universidade Federal de São Carlos, Caixa Postal 676, 13560 *São Carlos – SP, Brazil*

(*Received* 1 *October* 1990; *accepted* 23 *October* 1990)

Abstract. $C_{13}H_{16}O_3$, $M_r = 220·3$, orthorhombic, $Pca2_1$, $a = 14·358$ (2), $b = 9·297$ (1), $c = 9·011$ (1) Å, $V = 1202·9$ (4) Å^3, $Z = 4$, $D_x = 1·216$ g cm^{-3}, λ(Mo $K\alpha$) = 0·71073 Å, $\mu = 0·80$ mm^{-1}, $F(000) = 472$, $T = 298$ K, $R = 0·036$ for 866 observed reflections. The heterocyclic ring is in a distorted sofa conformation, and the C—O bonds are inequivalent: C(2)—O(1) = 1·463 (4) Å and C(9)—O(1) = 1·379 (4) Å.

Experimental. Crystals of compound (I) were obtained from *n*-hexane at 277 K. The data collection and refinement parameters are summarized in Table 1.

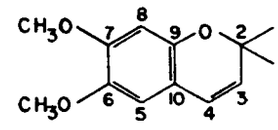

(I)

The structure was solved using standard direct methods and difference Fourier synthesis techniques. In the final cycles of full-matrix least-squares

0108-2701/91/051111-03$03.00

© 1991 International Union of Crystallography

Table 1. *Crystallographic summary for* (I)

Data collection[a]	
Mode	ω–2θ
Scan rate (° min^{-1})	2·8–10·0
θ range (°)	0–25
Range of *hkl*	$0 \le h \le 10$, $0 \le k \le 11$, $-2 \le l \le 17$
Total reflections measured	1304
Unique reflections	1113
R_{int}	0·013
Crystal dimensions approx. (mm)	0·40 × 0·38 × 0·35
Structure determination[b]	
Reflections used [$I > 3\sigma(I)$]	866
Number of variables	145
R, wR	0·036, 0·041
Max. shift/e.s.d.	0·004
Max., min. density in final difference map (e Å^{-3})	0·12, −0·12
S	1·62

Notes: (i) Unit-cell parameters by least-squares refinement of the setting angles of 25 reflections with $11 < \theta < 24°$. (ii) Enraf–Nonius CAD-4 diffractometer with a graphite monochromator. Two standard reflections (006, 0012), measured every hour, showed no significant variation. (iii) Function minimized was $\sum w(|F_o| - |F_c|)^2$, where $w^{-1} = [\sigma^2(F_o) + 0{\cdot}0005F_o^2]$.

refinement on F's all non-H atoms were treated anisotropically. H atoms included, as fixed contributors, at positions found in difference synthesis, all with a common isotropic temperature factor that refined to $U = 0{\cdot}078$ (3) Å^2. Scattering factors for non-H atoms were taken from Cromer & Mann (1968) with corrections for anomalous dispersion taken from Cromer & Liberman (1970), for H atoms were taken from Stewart, Davidson & Simpson (1965). Programs used: *SHELX*76 (Sheldrick, 1976) and *ORTEP* (Johnson, 1965). Most of the calculations were performed on a VAX 11/780 computer of the Instituto de Física e Química de São Carlos.

Atomic coordinates are listed in Table 2,* bond lengths and angles are listed in Table 3. The shortest intermolecular distance is O(3)···C(13)($\frac{1}{2}-x$, y, $\frac{1}{2}+z$) = 3·131 (5) Å. Fig. 1 is a stereoscopic projection of the molecule.

Related literature. The C—O bonds in the heterocyclic ring are different [C(2)—O(1) = 1·463 (4), C(9)—O(1) = 1·379 (4) Å] owing to the effect of conjugation on the C(9) side. The conformation of the heterocycle is a distorted sofa; C(3) and C(4) are coplanar, to within experimental accuracy, with the C(5)—C(10) benzene ring, whereas C(2) is 0·418 (3) Å above and O(1) is only 0·116 (2) Å below that plane. The C(9)—O(1)—C(2)—C(3) torsion angle is −40·8 (3)°. The O(1)—C(2)—C(3) angle of 109·9 (3)° is closely similar to those found by Flippen, Karle & Karle (1970), Spek, Kojić-Prodić & Labadie (1984), Rao, Seshadri & Rao (1987) and Valente, Eggleston & Schomaker (1987).

This work has received partial support from CAPES, CNPq, FAPESP and FINEP.

* Lists of structure factors, anisotropic thermal parameters and H-atom parameters have been deposited with the British Library Document Supply Centre as Supplementary Publication No. SUP 53679 (10 pp.). Copies may be obtained through The Technical Editor, International Union of Crystallography, 5 Abbey Square, Chester CH1 2HU, England.

Table 2. *Final atomic coordinates and equivalent isotropic temperature factors* (Å^2) *with e.s.d.'s in parentheses*

$B_{eq} = (4/3)\sum_i\sum_j \beta_{ij}\mathbf{a}_i.\mathbf{a}_j$.

	x	y	z	B_{eq}
O(1)	−0·1292 (1)	0·8597 (2)	0·5	4·60 (8)
O(2)	0·2036 (1)	0·6349 (2)	0·6991 (3)	4·94 (8)
O(3)	0·0581 (1)	0·6278 (2)	0·8675 (3)	4·93 (8)
C(2)	−0·1505 (2)	0·8673 (3)	0·3414 (4)	4·2 (1)
C(3)	−0·0647 (3)	0·9096 (3)	0·2562 (4)	4·4 (1)
C(4)	0·0199 (2)	0·8783 (3)	0·3042 (4)	4·2 (1)
C(5)	0·1163 (2)	0·7491 (3)	0·4987 (3)	3·64 (9)
C(6)	0·1236 (2)	0·6920 (3)	0·6382 (4)	3·6 (1)
C(7)	0·0450 (2)	0·6882 (3)	0·7310 (4)	3·8 (1)
C(8)	−0·0391 (2)	0·7410 (3)	0·6807 (4)	3·7 (1)
C(9)	−0·0450 (2)	0·7993 (3)	0·5391 (4)	3·7 (1)
C(10)	0·0312 (2)	0·8041 (3)	0·4470 (3)	3·5 (1)
C(11)	−0·1843 (2)	0·7214 (3)	0·2940 (4)	5·2 (1)
C(12)	−0·2267 (3)	0·9759 (3)	0·3289 (5)	6·1 (1)
C(13)	0·2826 (2)	0·6248 (4)	0·6048 (5)	5·8 (1)
C(14)	−0·0190 (3)	0·6192 (4)	0·9635 (4)	5·8 (1)

Table 3. *Interatomic bond distances* (Å) *and angles* (°)

O(1)—C(2)	1·463 (4)	O(1)—C(9)	1·379 (4)
O(2)—C(6)	1·379 (4)	O(2)—C(13)	1·420 (4)
O(3)—C(7)	1·365 (4)	O(3)—C(14)	1·407 (5)
C(2)—C(3)	1·504 (5)	C(2)—C(11)	1·503 (5)
C(2)—C(12)	1·493 (5)	C(3)—C(4)	1·322 (5)
C(4)—C(10)	1·469 (5)	C(5)—C(6)	1·369 (5)
C(5)—C(10)	1·404 (4)	C(6)—C(7)	1·405 (4)
C(7)—C(8)	1·380 (4)	C(8)—C(9)	1·389 (5)
C(9)—C(10)	1·374 (4)		

C(2)—O(1)—C(9)	116·9 (2)	C(6)—O(2)—C(13)	116·9 (2)
C(7)—O(3)—C(14)	118·0 (3)	O(1)—C(2)—C(3)	109·9 (3)
O(1)—C(2)—C(11)	107·6 (3)	O(1)—C(2)—C(12)	105·0 (3)
C(3)—C(2)—C(11)	110·8 (3)	C(3)—C(2)—C(12)	112·6 (3)
C(11)—C(2)—C(12)	110·6 (3)	C(2)—C(3)—C(4)	121·9 (3)
C(3)—C(4)—C(10)	119·4 (3)	C(6)—C(5)—C(10)	120·8 (3)
O(2)—C(6)—C(5)	125·3 (3)	O(2)—C(6)—C(7)	115·0 (3)
C(5)—C(6)—C(7)	119·7 (3)	O(3)—C(7)—C(6)	115·8 (3)
O(3)—C(7)—C(8)	124·2 (3)	C(6)—C(7)—C(8)	119·9 (3)
C(7)—C(8)—C(9)	119·6 (3)	O(1)—C(9)—C(8)	116·6 (3)
O(1)—C(9)—C(10)	122·0 (3)	C(8)—C(9)—C(10)	121·3 (3)
C(4)—C(10)—C(5)	123·9 (3)	C(4)—C(10)—C(9)	117·2 (3)
C(5)—C(10)—C(9)	118·7 (3)		

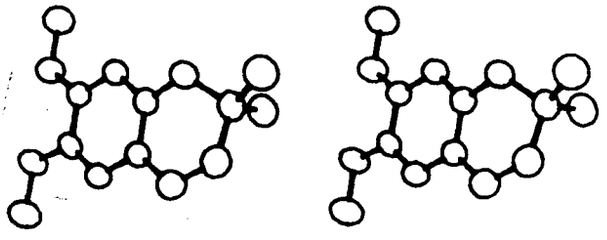

Fig. 1. Stereoscopic projection of the molecule.

References

CROMER, D. T. & LIBERMAN, D. (1970). *J. Chem. Phys.* **53**, 1891–1898.

CROMER, D. T. & MANN, J. B. (1968). *Acta Cryst.* A**24**, 321–324.

FLIPPEN, J. L., KARLE, J. & KARLE, I. L. (1970). *J. Am. Chem. Soc.* **92**, 3749–3754.

JOHNSON, C. K. (1965). *ORTEP*. Report ORNL-3794. Oak Ridge National Laboratory, Tennessee, USA.

RAO, B. H. L., SESHADRI, T. P. & RAO, L. M. (1987). *Acta Cryst.* C**43**, 495–497.

SHELDRICK, G. M. (1976). *SHELX76*. Program for crystal structure determination. Univ. of Cambridge, England.

SPEK, A. L., KOJIĆ-PRODIĆ, B. & LABADIE, R. P. (1984). *Acta Cryst.* C**40**, 2068–2071.

STEWART, R. F., DAVIDSON, E. R. & SIMPSON, W. T. (1965). *J. Chem. Phys.* **42**, 3175–3187.

VALENTE, E. J., EGGLESTON, D. S. & SCHOMAKER, V. (1987). *Acta Cryst.* C**43**, 533–536.

Acta Cryst. (1991). C**47**, 1113–1114

Structure of Phenazine

BY K. WOŹNIAK

Department of Chemistry, Warsaw University, Pasteura 1, 02-093 *Warszawa, Poland*

AND B. KARIUKI AND W. JONES

Department of Chemistry, Cambridge University, Lensfield Road, Cambridge CB2 1*EW, England*

(*Received* 28 *August* 1990; *accepted* 23 *October* 1990)

Abstract. $C_{12}H_8N_2$, $M_r = 180{\cdot}21$, monoclinic, $P2_1/n$, $a = 7{\cdot}083\ (1)$, $b = 5{\cdot}072\ (1)$, $c = 12{\cdot}794\ (8)$ Å, $\beta = 102{\cdot}34\ (2)^\circ$, $V = 449{\cdot}01\ (3)$ Å^3, $Z = 2$, $D_x = 1{\cdot}333$ g cm^{-3}, λ(Mo $K\alpha$) = 0·71069 Å, $\mu = 0{\cdot}756$ cm^{-1}, $F(000) = 188$, $T = 291$ K, $R = 0{\cdot}0532$ for 2005 observed reflections. The structure consists of phenazine molecules oriented about a centre of symmetry. The molecule is planar within experimental error, and a pseudo C_{2v} axis is observed in the molecule.

Experimental. Crystals of phenazine were crystallized from acetonitrile. An Enraf–Nonius CAD-4 diffractometer was used with graphite-monochromatized Mo $K\alpha$ radiation. Crystal size was 0·25 × 0·30 × 0·35 mm. Unit-cell parameters were obtained by least-squares fit of the setting angles of 25 reflections in the range $3 \le 2\theta \le 18^\circ$. The intensities of 2702 reflections were measured ($\sin\theta/\lambda \le 0{\cdot}704$ Å^{-1}, $-9 \le h \le 9$, $0 \le k \le 7$, $0 \le l \le 18$, ω–2θ scan mode). No significant variation (< 3%) was found in the intensities of the intensity control reflections $3\bar{1}\bar{1}$ and 103. The data were corrected for Lorentz and polarization effects but no absorption correction was applied. 2005 reflections with $|F| \ge 34\sigma(F)$ were used in the calculations. The structure was solved with multisolution direct methods (*SHELXS*86; Sheldrick, 1990) and refined using full-matrix least-squares refinement (*SHELX*76; Sheldrick, 1976), minimizing $\sum w(|F_o| - |F_c|)^2$, $w = \{2{\cdot}7955/[\sigma^2(F) + 0{\cdot}000553F^2]\}$. The C and N atoms were refined with anisotropic, and H atoms with isotropic temperature factors, 81 parameters were varied. The refinement converged to $R = 0{\cdot}0532$, $wR = 0{\cdot}061$, $(\Delta/\sigma)_{max} = 0{\cdot}002$, $(\Delta/\sigma)_{mean} = 0{\cdot}001$, $\Delta\rho_{max} = 0{\cdot}52$, $\Delta\rho_{min} = -0{\cdot}35$ e Å^{-3}. The

Table 1. *Fractional coordinates* (× 10^4) *and equivalent isotropic temperature coefficients* (× 10^4) *for non*-H *atoms*

$U_{eq} = (1/3)\sum_i\sum_j U_{ij}a_i^*a_j^*\mathbf{a}_i.\mathbf{a}_j$.

	x	y	z	U_{eq}(Å^2)
N1	8035 (1)	550 (1)	9523 (1)	461 (3)
C2	9491 (1)	1851 (2)	9233 (1)	423 (2)
C3	8523 (1)	−1293 (2)	10284 (1)	415 (2)
C4	7050 (1)	−2758 (2)	10629 (1)	522 (3)
C5	9077 (1)	3834 (2)	8429 (1)	551 (3)
C6	7519 (1)	−4624 (2)	11395 (1)	572 (4)
C7	10525 (2)	5155 (2)	8124 (1)	590 (4)

Table 2. *Bond lengths* (Å) *and bond angles* (°)

C2—N1	1·342 (1)	C4—C3	1·426 (1)
C3—N1	1·341 (1)	C6—C4	1·352 (2)
C3—C2^i	1·438 (1)	C7—C5	1·351 (2)
C5—C2	1·424 (2)	C7—C6	1·416 (1)

N1—C2—C3^i	121·56 (10)	C3^i—C2—C5	118·75 (9)
N1—C2—C5	119·70 (7)	C2—C5—C7	120·49 (8)
C2—N1—C3	116·72 (7)	C3—C4—C6	120·44 (7)
N1—C3—C2^i	121·73 (9)	C4—C6—C7^i	120·94 (9)
N1—C3—C4	119·74 (7)	C5—C7—C6^i	120·85 (10)
C2^i—C3—C4	118·53 (10)		

Symmetry code: (i) $2 - x, -y, 2 - z$.

0108-2701/91/051113-02$03.00 © 1991 International Union of Crystallography

Acta Cryst. (1991). C47, 2699–2700

Structure of 1,4-Bis(diphenylphosphinoyl)butane

BY M. R. M. FONTES, G. OLIVA AND J. ZUKERMAN-SCHPECTOR

Instituto de Física e Química de São Carlos, Universidade de São Paulo, Caixa Postal 369, 13560 São Carlos – SP, Brazil

AND S. L. QUEIROZ AND A. A. BATISTA

Departamento de Química, Universidade Federal de São Carlos, Rod. Washington Luiz km235, 13560 São Carlos – SP, Brazil

(*Received* 20 *May* 1991; *accepted* 18 *June* 1991)

Abstract. $C_{28}H_{28}O_2P_2$, M_r = 458·48, triclinic, $P\bar{1}$, a = 5·826 (1), b = 8·862 (1), c = 12·517 (2) Å, α = 100·29 (1), β = 102·67 (1), γ = 104·22 (1)°, V = 592·5 (3) Å^3, Z = 1, D_x = 1·285 g cm^{-3}, λ(Mo $K\alpha$) = 0·71073 Å, μ = 2·00 cm^{-1}, $F(000)$ = 242, T = 296 K, final R = 0·031 for 1390 independent observed reflections. The —$(CH_2)_4$— group is essentially planar with the P atoms 0·126 (1) Å away from its calculated mean plane. Both phenyl rings are planar to within experimental accuracy. The P atom has a distorted tetrahedral configuration.

Experimental. During our studies, using {$RuCl_2$[1,4-bis(diphenylphosphino)]butane} as a starting material for reactions with bulky ligands like triethylphosphite, the title compound was obtained. Single colorless crystals were obtained from CH_2Cl_2/ether by slow evaporation at 293 K. The data collection and refinement parameters are summarized in Table 1. The structure was solved using standard direct methods and difference Fourier techniques. In final cycles of least-squares refinement, all non-H atoms were treated anisotropically, H atoms were refined isotropically. Scattering factors for non-H atoms were taken from Cromer & Mann (1968) with corrections for anomalous dispersion from Cromer & Liberman (1970); for H atoms from Stewart, Davidson & Simpson (1965). Programs used: *SHELX*76 (Sheldrick, 1976) and *ORTEP* (Johnson, 1965).

Atomic coordinates for non-H atoms are given in Table 2,* interatomic distances and angles are listed in Table 3. Fig. 1 is a projection of the title compound showing the atom-numbering scheme.

* Lists of H-atom positions, anisotropic thermal parameters and structure factors have been deposited with the British Library Document Supply Centre as Supplementary Publication No. SUP 54361 (12 pp.). Copies may be obtained through The Technical Editor, International Union of Crystallography, 5 Abbey Square, Chester CH1 2HU, England.

Table 1. *Crystallographic summary*

Data collection[a]	
Mode	ω–2θ
Scan rate (° min^{-1})	1·8, 5·5
θ range (°)	0–23
Range of hkl	$-6 \le h \le 6$, $-9 \le k \le 9$, $0 \le l \le 13$
Total reflections measured	1848
Unique reflections	1647
R_{int}	0·01
Standard reflections (h^{-1})	1
Variation	None significant
Crystal dimensions approx. (mm)	0·20 × 0·20 × 0·20
Diffractometer	Enraf-Nonius CAD-4, graphite monochromator
Structure determination and refinement[a, b]	
Reflections used [$I > 3\sigma(I)$]	1390
No. of variables	202
R, wR	0·031, 0·030
w	$1/[\sigma^2(F_o) + 0·0001F_o^2]$
Max. shift/e.s.d.	0·02
Max., min. density in final difference map (e Å^{-3})	0·20, −0·22
S	1·77

Notes: (i) Unit-cell parameters by least-squares refinement of the setting angles of 25 reflections with $12 < \theta < 20°$. (ii) A secondary-extinction correction was applied [$F_{corr} = F_c(1·0 \times 10^{-4}\chi F_c^2/\sin\theta)$] where χ refined to 0·009. No correction for absorption. (iii) Function minimized was $\sum w(|F_o| - |F_c|)^2$.

Table 2. *Final atomic coordinates and isotropic temperature factors* (Å^2)

$B_{eq} = (4/3)\sum_i\sum_j \beta_{ij}\mathbf{a}_i.\mathbf{a}_j$

	x	y	z	B_{eq}
P	0·5041 (1)	0·6540 (1)	0·8270 (1)	2·60 (2)
O	0·7736 (3)	0·6842 (2)	0·8476 (1)	3·66 (4)
C(1)	0·4130 (4)	0·7703 (2)	0·9337 (2)	2·64 (6)
C(2)	0·5457 (4)	0·9493 (2)	0·9585 (2)	2·77 (6)
C(11)	0·3718 (4)	0·6998 (2)	0·6960 (2)	2·72 (5)
C(12)	0·1218 (5)	0·6681 (3)	0·6498 (2)	4·06 (7)
C(13)	0·0353 (6)	0·7013 (4)	0·5478 (2)	5·11 (8)
C(14)	0·1929 (7)	0·7678 (3)	0·4916 (2)	5·29 (9)
C(15)	0·4395 (7)	0·8018 (3)	0·5365 (2)	5·23 (9)
C(16)	0·5301 (5)	0·7678 (3)	0·6383 (2)	4·02 (7)
C(21)	0·3439 (4)	0·4456 (2)	0·8115 (2)	2·77 (5)
C(22)	0·1451 (5)	0·3960 (3)	0·8533 (2)	3·83 (7)
C(23)	0·0353 (5)	0·2344 (3)	0·8405 (3)	4·72 (8)
C(24)	0·1202 (6)	0·1216 (3)	0·7850 (2)	4·69 (7)
C(25)	0·3147 (6)	0·1684 (3)	0·7417 (2)	4·52 (7)
C(26)	0·4272 (5)	0·3297 (3)	0·7552 (2)	3·66 (7)

0108-2701/91/122699-02$03.00

© 1991 International Union of Crystallography

Table 3. *Interatomic distances* (Å) *and angles* (°)

P—O	1·482 (2)	P—C(1)	1·793 (2)
P—C(11)	1·812 (2)	P—C(21)	1·807 (2)
C(1)—C(2)	1·525 (3)	C(2)—C(2')	1·521 (3)
C(11)—C(12)	1·381 (4)	C(11)—C(16)	1·382 (4)
C(12)—C(13)	1·377 (4)	C(13)—C(14)	1·361 (5)
C(14)—C(15)	1·358 (5)	C(15)—C(16)	1·383 (4)
C(21)—C(22)	1·381 (4)	C(21)—C(26)	1·387 (3)
C(22)—C(23)	1·382 (4)	C(23)—C(24)	1·368 (4)
C(24)—C(25)	1·367 (5)	C(25)—C(26)	1·381 (4)
O—P—C(1)	114·9 (1)	O—P—C(11)	111·00 (9)
O—P—C(21)	112·45 (9)	C(1)—P—C(11)	105·6 (1)
C(1)—P—C(21)	106·9 (1)	C(11)—P—C(21)	105·3 (1)
P—C(1)—C(2)	112·0 (2)	C(1)—C(2)—C(2')	113·1 (2)
P—C(11)—C(12)	123·7 (2)	P—C(11)—C(16)	118·1 (2)
C(12)—C(11)—C(16)	118·3 (2)	C(11)—C(12)—C(13)	120·1 (2)
C(12)—C(13)—C(14)	121·1 (3)	C(13)—C(14)—C(15)	119·6 (3)
C(14)—C(15)—C(16)	120·2 (3)	C(11)—C(16)—C(15)	120·7 (3)
P—C(21)—C(22)	123·6 (2)	P—C(21)—C(26)	117·9 (2)
C(22)—C(21)—C(26)	118·5 (2)	C(21)—C(22)—C(23)	120·4 (2)
C(22)—C(23)—C(24)	120·4 (3)	C(23)—C(24)—C(25)	120·0 (3)
C(24)—C(25)—C(26)	119·9 (3)	C(21)—C(26)—C(25)	120·8 (2)

Related literature. The molecule is sited on a crystallographic center of symmetry which relates one half of the molecule to the other. Related structures have been described by Oliva, Castellano & De Carvalho (1981) and Rivera, Gómez C, Rodulfo de Gil & Suarez (1988).

This work has received partial support from CNPq, FAPESP, CAPES and FINEP, which are hereby gratefully acknowledged.

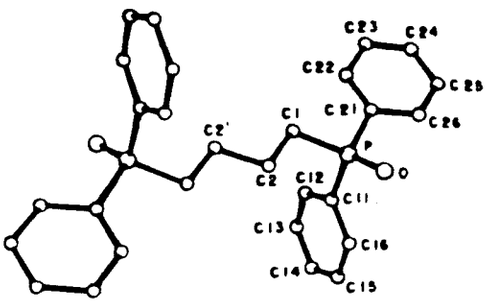

Fig. 1. Perspective view of the molecule showing the atom labeling

References

CROMER, D. T. & LIBERMAN, D. (1970). *J. Chem. Phys.* **53**, 1891–1898.

CROMER, D. T. & MANN, J. B. (1968). *Acta Cryst.* A**24**, 321–324.

JOHNSON, C. K. (1965). *ORTEP*. Report ORNL-3794. Oak Ridge National Laboratory, Tennessee, USA.

OLIVA, G., CASTELLANO, E. E. & DE CARVALHO, L. R. F. (1981). *Acta Cryst.* B**37**, 474–475.

RIVERA, A. V., GÓMEZ C, D., RODULFO DE GIL, E. E. & SUAREZ, T. (1988). *Acta Cryst.* C**44**, 277–279.

SHELDRICK, G. M. (1976). *SHELX76*. Program for crystal structure determination. Univ. of Cambridge, England.

STEWART, R. F., DAVIDSON, E. R. & SIMPSON, W. T. (1965). *J. Chem. Phys.* **42**, 3175–3187.

Acta Cryst. (1991). C**47**, 2700–2702

Structure of *endo*-(5*R**,6*R**,11*R**,12*S**)-5,6,11,12-Tetrahydro-4,11,12-trimethoxy-9,13,13-trimethyl-5-(triethylsiloxy)-6,10-methano-8(7*H*)-benzocyclodecenone

BY YOSHII SAKAI, YUKO KOJIMA, YUJI OHASHI,* KOICHIRO MORIHIRA, TAKASHI FURUKAWA, YOSHIAKI HORIGUCHI AND ISAO KUWAJIMA*

Department of Chemistry, Faculty of Science, Tokyo Institute of Technology, O-okayama, Meguro-ku, Tokyo 152, *Japan*

(*Received* 20 *May* 1991, *accepted* 1 *July* 1991)

Abstract. $C_{27}H_{42}O_5Si$, $M_r = 474.71$, monoclinic, $P2_1/n$, $a = 9.389$ (5), $b = 35.542$ (7), $c = 8.899$ (4) Å, $\beta = 114.25$ (3)°, $V = 2707$ (2) Å^3, $Z = 4$, $D_x = 1.164$ g cm^{-3}, λ(Mo $K\alpha$) = 0.71069 Å, $\mu = 1.14$ cm^{-1}, $F(000) = 1032$, $T = 298$ K, final $R = 0.049$ for 2926 unique reflections [$I > 3.0\sigma(I)$]. This C-aromatic taxane-like compound contains a C=C double bond [C(9)=C(10)] at the bridgehead site [C(10)] and, consequently, atoms C(8), C(11), C(13) and C(16) bonded to this C=C bond are twisted from coplanarity. The largest torsion angle, C(8)—C(9)—C(10)—C(11), is −158.3 (3)°.

Experimental. Colorless plate-like crystals grown from hexane. Crystal size 0.40 × 0.40 × 0.50 mm, Rigaku AFC-5R diffractometer, graphite-monochromated Mo $K\alpha$ radiation, ω scan with scan speed 16° min^{-1} in ω, scan width $(1.34 + 0.35\tan\theta)$°. Range of indices, $0 < h < 11$, $0 < k < 42$, $-9 < l < 9$ ($2\theta < 50$°). Three standard reflections ($\bar{3}33$, $50\bar{5}$, $\bar{4},\bar{1}6,2$) monitored every 100 reflections with random variation of 2.7% over data collection. Lattice-

* To whom correspondence should be addressed.

0108-2701/91/122700-03$03.00

© 1991 International Union of Crystallography

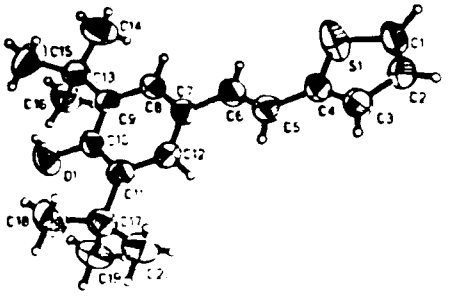

Fig. 1. Structure of the title compound. The ellipsoids are shown at 50% probability level.

Plus. The calculations of geometrical data and crystal packing were computed using the program *PARST* (Nardelli, 1983). All computations were carried out on a VAX 3100 work station. Table 1 gives the atomic coordinates and equivalent isotropic thermal parameters* and Table 2 lists bond distances and angles. Fig. 1 shows a perspective view of the molecule with the adopted numbering scheme and Fig. 2 gives a view of the unit cell along the *c* axis.

Related literature. The 2,6-di-*tert*-butylphenol derivatives appear to represent a new class of non-steroidal anti-inflammatory drugs with antioxidant properties (Ikuta, Shirota, Kobayashi, Yamagishi, Yamada, Yamatsu & Katayama, 1987). The title compound is one of a series of related compounds prepared by Lazer, Wong, Possanza, Graham & Farina (1989) that have anti-inflammatory activity. In all essential details the geometry of the molecule in terms of bond lengths and angles shows normal values (Tenon, Ebby, Voglozin, Degny, N'Guessan, Baldy, Pierrot & Bodot, 1989; Bernstein, 1975; Tirado-Rives, Fronczek & Gandour, 1985).

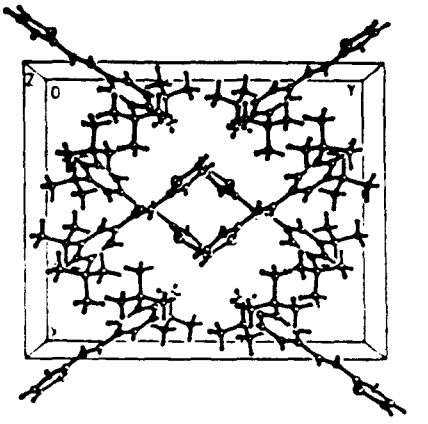

Fig. 2. The unit cell viewed down the *c* axis.

The assistance of Miss Madhavi Bhogaraju is gratefully acknowledged.

* Lists of structure factors, anisotropic thermal parameters and H-atom parameters have been deposited with the British Library Document Supply Centre as Supplementary Publication No. SUP 54789 (9 pp.). Copies may be obtained through The Technical Editor, International Union of Crystallography, 5 Abbey Square, Chester CH1 2HU, England.

References

BERNSTEIN, J. (1975). *Acta Cryst.* B31, 1268–1271.

IKUTA, S., SHIROTA, H., KOBAYASHI, S., YAMAGISHI, Y., YAMADA, K., YAMATSU, I. & KATAYAMA, K. (1987). *J. Med. Chem.* 30, 1995–1998.

LAZER, E. S., WONG, H. C., POSSANZA, G. J., GRAHAM, A. & FARINA, P. R. (1989). *J. Med. Chem.* 32, 100–104.

NARDELLI, M. (1983). *Comput. Chem.* 7, 95–98.

SHELDRICK, G. M. (1990). *SHELXTL-Plus*. Revision 4.11/*V*. Siemens Analytical X-ray Instruments, Inc., Application Laboratory, Single Crystal, Siemens AG, AUT V353, Karlsruhe, Germany.

TENON, A. J., EBBY, N., VOGLOZIN, A., DEGNY, E., N'GUESSAN, T. Y., BALDY, A., PIERROT, M. & BODOT, H. (1989). *Acta Cryst.* C45, 622–625.

TIRADO-RIVES, J., FRONCZEK, F. R. & GANDOUR, R. D. (1985). *Acta Cryst.* C41, 1327–1329.

Acta Cryst. (1992). C48, 953–955

Structure of (3*R*,6*S*,12b*R*)-6-Cyanomethyl-3-ethyl-2-oxo-1,2,3,4,7,7a,12a,12b-octahydro-6*H*-indolo[2,3-*a*]quinolizine

BY L. F. DELBONI AND G. OLIVA

Instituto de Física e Química de São Carlos, Universidade de São Paulo, Caixa Postal 369, 13560 – *São Carlos, SP, Brazil*

(*Received* 12 *August* 1991; *accepted* 2 *October* 1991)

Abstract. $C_{19}H_{21}N_3O$, $M_r = 307.40$, monoclinic, $P2_1/c$, $a = 12.200$ (7), $b = 16.795$ (2), $c = 15.655$ (1) Å, $\beta = 104.18$ (3)°, $V = 3308$ (3) Å^3, $Z = 8$, $D_x = 1.234$ g cm^{-3}, λ(Mo $K\alpha$) = 0.71073 Å, $\mu = 0.73$ cm^{-1}, $F(000) = 1312$, $T = 296$ K, final $R = 0.051$ for 2227 independent observed reflections. The two

0108-2701/92/050953-03$06.00

© 1992 International Union of Crystallography

Table 1. *Data-collection and refinement summary*

Data collection[a,b]	
Mode	ω–2θ
Scan rate (° min^{-1})	1.56–5.49
θ range (°)	0–23
Range of hkl	$-13 \le h \le 12$, $0 \le k \le 18$, $0 \le l \le 18$
Total reflections measured	4980
Unique reflections	4590
R_{int}	0.035
Approximate crystal dimensions (mm)	0.30 × 0.45 × 0.45
Structure determination and refinement[a,c]	
Reflections used [$I > 3\sigma(I)$]	2227
No. of variables	417
R, wR	0.051, 0.048
Maximum, minimum density in final difference map (e Å^{-3})	0.16, −0.19
S	2.24

Notes: (i) Unit-cell parameters by least-squares refinement of the setting angles of 16 reflections with $10 < \theta < 15$°. (ii) Enraf–Nonius CAD-4 diffractometer with graphite monochromator. One standard reflection measured every hour showed no significant variation. (iii) Function minimized was $\sum w(|F_o| - |F_c|)^2$, where $w^{-1} = \sigma^2(F_o) + 0.0002F_o^2$.

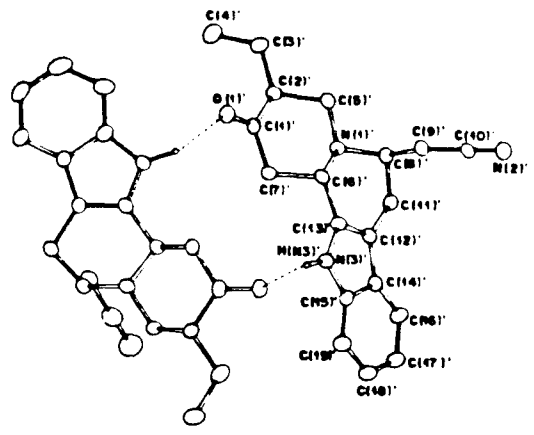

Fig. 1. Perspective view of the molecules showing the crystallographic atom labelling of one of the independent molecules and the hydrogen-bonding scheme.

independent enantiomeric molecules in the asymmetric unit are hydrogen bonded through N(3)···O(1′) [2.868 (4) Å] and N(3′)···O(1) [2.969 (4) Å]. The junction N(1)—C(6) is *trans* and the group CH_2CN is axial.

Experimental. Crystals were obtained from ethanol by slow evaporation at 293 K. Details of data collection and refinement parameters are summarized in Table 1. The structure was solved using standard direct methods and difference Fourier techniques. In the final cycles of least-squares refinement all non-H atoms were treated anisotropically. H atoms were included as fixed contributors, with overall isotropic temperature factors: for methyl H atoms $U = 0.077$ (2) Å^2, and for all others $U = 0.130$ (7) Å^2. Absorption corrections were not considered necessary. The maximum value of Δ/σ in the final refinement cycle was 0.09. Scattering factors for

Table 2. *Final atomic coordinates and equivalent isotropic temperature factors* (Å^2)

$B_{eq} = (4/3)\sum_i\sum_j \beta_{ij} \mathbf{a}_i.\mathbf{a}_j$

	x	y	z	B_{eq}
N(1)	0.1138 (3)	0.5982 (2)	0.2042 (2)	3.6 (1)
N(2)	−0.1028 (4)	0.5796 (3)	−0.0145 (3)	8.0 (2)
N(3)	0.4133 (3)	0.5712 (2)	0.1945 (2)	3.7 (1)
O(1)	0.1328 (2)	0.3711 (2)	0.2680 (2)	5.3 (1)
C(1)	0.1327 (4)	0.4436 (3)	0.2731 (2)	4.1 (2)
C(2)	0.0294 (3)	0.4922 (2)	0.2737 (2)	3.9 (2)
C(3)	−0.0755 (4)	0.4407 (3)	0.2697 (2)	5.2 (2)
C(4)	−0.1719 (4)	0.4867 (3)	0.2920 (3)	7.0 (2)
C(5)	0.0119 (3)	0.5508 (2)	0.2010 (2)	4.2 (2)
C(6)	0.2099 (3)	0.5470 (2)	0.1974 (2)	3.4 (2)
C(7)	0.2363 (3)	0.4911 (2)	0.2738 (2)	3.7 (1)
C(8)	0.0959 (3)	0.6694 (2)	0.1515 (3)	4.1 (2)
C(9)	0.0801 (3)	0.6550 (2)	0.0578 (3)	4.7 (2)
C(10)	−0.0231 (5)	0.6122 (3)	0.0176 (3)	5.6 (2)
C(11)	0.1964 (3)	0.7260 (2)	0.1813 (2)	4.2 (2)
C(12)	0.3039 (4)	0.6800 (3)	0.1864 (2)	3.6 (2)
C(13)	0.3066 (3)	0.5998 (3)	0.1949 (2)	3.6 (2)
C(14)	0.4136 (4)	0.7051 (3)	0.1798 (2)	3.7 (2)
C(15)	0.4791 (4)	0.6360 (3)	0.1846 (2)	3.7 (2)
C(16)	0.4617 (4)	0.7787 (3)	0.1696 (2)	4.7 (2)
C(17)	0.5717 (5)	0.7806 (3)	0.1645 (3)	5.4 (2)
C(18)	0.6362 (4)	0.7114 (4)	0.1680 (3)	5.6 (2)
C(19)	0.5916 (4)	0.6377 (3)	0.1790 (2)	4.8 (2)
N(1′)	0.4048 (3)	0.2262 (2)	0.0480 (2)	3.3 (1)
N(2′)	0.4004 (3)	−0.0599 (2)	0.0429 (3)	7.6 (2)
N(3′)	0.1625 (3)	0.2519 (2)	0.1434 (2)	3.7 (1)
O(1′)	0.5241 (2)	0.4262 (2)	0.1688 (2)	5.0 (1)
C(1′)	0.4797 (4)	0.3757 (2)	0.1183 (3)	4.1 (2)
C(2′)	0.5387 (3)	0.3368 (2)	0.0585 (2)	3.9 (2)
C(3′)	0.6618 (4)	0.3623 (3)	0.0710 (3)	5.4 (2)
C(4′)	0.6766 (4)	0.4458 (3)	0.0393 (3)	6.5 (2)
C(5′)	0.5252 (3)	0.2458 (2)	0.0644 (2)	3.9 (2)
C(6′)	0.3563 (3)	0.2566 (2)	0.1146 (2)	3.2 (1)
C(7′)	0.3614 (3)	0.3476 (2)	0.1128 (2)	4.0 (2)
C(8′)	0.3803 (3)	0.1427 (2)	0.0254 (2)	3.5 (2)
C(9′)	0.4221 (3)	0.0845 (3)	0.0996 (2)	4.4 (2)
C(10′)	0.4106 (4)	0.0021 (3)	0.0692 (3)	5.1 (2)
C(11′)	0.2529 (3)	0.1332 (2)	−0.0139 (2)	3.7 (1)
C(12′)	0.1900 (3)	0.1723 (2)	0.0420 (2)	3.2 (1)
C(13′)	0.2378 (3)	0.2269 (2)	0.0993 (2)	3.3 (2)
C(14′)	0.0758 (4)	0.1624 (2)	0.0470 (3)	3.5 (2)
C(15′)	0.0600 (4)	0.2134 (2)	0.1110 (3)	3.4 (2)
C(16′)	−0.0163 (4)	0.1171 (2)	0.0046 (3)	4.3 (2)
C(17′)	−0.1181 (4)	0.1235 (3)	0.0260 (3)	5.5 (2)
C(18′)	−0.1308 (4)	0.1749 (3)	0.0891 (3)	5.3 (2)
C(19′)	−0.0423 (4)	0.2202 (3)	0.1333 (3)	4.6 (2)

non-H atoms were taken from Cromer & Mann (1968) with corrections for anomalous dispersion from Cromer & Liberman (1970); for H atoms from Stewart, Davidson & Simpson (1965). Programs used: *SHELX76* (Sheldrick, 1976) and *ORTEP* (Johnson, 1965).

Atomic coordinates for non-H atoms are given in Table 2,* interatomic distances and angles are given in Table 3. Fig. 1 is a projection of the title compound showing the atom-numbering scheme for one of the independent molecules.

Related literature. The title compound is a key intermediate in the reaction pathway for the synthesis of sarpagines (Braga, 1989). The knowledge of its

* Lists of H-atom positions, anisotropic thermal parameters and structure factors have been deposited with the British Library Document Supply Centre as Supplementary Publication No. SUP 54710 (25 pp.). Copies may be obtained through The Technical Editor, International Union of Crystallography, 5 Abbey Square, Chester CH1 2HU, England. [CIF reference: LI0101]

Table 3. *Interatomic distances* (Å) *and angles* (°)

N(1)—C(5)	1.466 (5)	N(1')—C(5')	1.464 (5)
N(1)—C(6)	1.481 (5)	N(1')—C(6')	1.471 (5)
N(1)—C(8)	1.468 (5)	N(1')—C(8')	1.464 (5)
N(2)—C(10)	1.130 (7)	N(2')—C(10')	1.125 (7)
N(3)—C(13)	1.389 (6)	N(3')—C(13')	1.375 (5)
N(3)—C(15)	1.386 (6)	N(3')—C(15')	1.394 (5)
O(1)—C(1)	1.221 (6)	O(1')—C(1')	1.224 (5)
O(1)—C(2)	1.504 (6)	O(1')—C(2')	1.513 (6)
O(1)—C(7)	1.492 (6)	O(1')—C(7')	1.500 (6)
C(2)—C(3)	1.533 (6)	C(2')—C(3')	1.526 (6)
C(2)—C(5)	1.534 (5)	C(2')—C(5')	1.543 (6)
C(3)—C(4)	1.527 (7)	C(3')—C(4')	1.525 (6)
C(6)—C(7)	1.550 (5)	C(6')—C(7')	1.530 (5)
C(6)—C(13)	1.485 (6)	C(6')—C(13')	1.491 (6)
C(8)—C(9)	1.544 (6)	C(8')—C(9')	1.560 (5)
C(8)—C(11)	1.535 (6)	C(8')—C(11')	1.540 (6)
C(9)—C(10)	1.462 (7)	C(9')—C(10')	1.468 (7)
C(11)—C(12)	1.506 (6)	C(11')—C(12')	1.496 (6)
C(12)—C(13)	1.354 (6)	C(12')—C(13')	1.349 (6)
C(12)—C(14)	1.433 (7)	C(12')—C(14')	1.426 (6)
C(14)—C(15)	1.400 (7)	C(14')—C(15')	1.417 (6)
C(14)—C(16)	1.396 (7)	C(14')—C(16')	1.397 (6)
C(15)—C(19)	1.399 (7)	C(15')—C(19')	1.391 (7)
C(16)—C(17)	1.366 (8)	C(16')—C(17')	1.378 (7)
C(17)—C(18)	1.397 (8)	C(17')—C(18')	1.398 (7)
C(18)—C(19)	1.382 (8)	C(18')—C(19')	1.377 (7)

C(5)—N(1)—C(6)	111.2 (3)	C(5')—N(1')—C(6')	110.6 (3)
C(5)—N(1)—C(8)	114.8 (3)	C(5')—N(1')—C(8')	113.3 (3)
C(6)—N(1)—C(8)	115.6 (3)	C(6')—N(1')—C(8')	115.6 (3)
C(13)—N(3)—C(15)	107.4 (3)	C(13')—N(3')—C(15')	107.8 (3)
O(1)—C(1)—C(2)	123.9 (4)	O(1')—C(1')—C(2')	123.4 (4)
O(1)—C(1)—C(7)	121.2 (4)	O(1')—C(1')—C(7')	121.2 (4)
C(2)—C(1)—C(7)	114.8 (4)	C(2')—C(1')—C(7')	115.5 (3)
C(1)—C(2)—C(3)	112.7 (3)	C(1')—C(2')—C(3')	113.6 (3)
C(1)—C(2)—C(5)	107.3 (3)	C(1')—C(2')—C(5')	108.1 (3)
C(3)—C(2)—C(5)	112.0 (3)	C(3')—C(2')—C(5')	112.7 (3)
C(2)—C(3)—C(4)	112.9 (4)	C(2')—C(3')—C(4')	114.0 (4)
N(1)—C(5)—C(2)	111.5 (3)	N(1')—C(5')—C(2')	109.2 (3)
N(1)—C(6)—C(7)	107.3 (3)	N(1')—C(6')—C(7')	107.8 (3)
N(1)—C(6)—C(13)	107.7 (3)	N(1')—C(6')—C(13')	107.9 (3)
C(7)—C(6)—C(13)	112.2 (3)	C(7')—C(6')—C(13')	111.9 (3)
O(1)—C(7)—C(6)	108.2 (3)	O(1')—C(7')—C(6')	110.9 (3)
N(1)—C(8)—C(9)	116.1 (3)	N(1')—C(8')—C(9')	113.0 (3)
N(1)—C(8)—C(11)	108.7 (3)	N(1')—C(8')—C(11')	109.3 (3)
C(9)—C(8)—C(11)	108.4 (3)	C(9')—C(8')—C(11')	111.8 (3)
C(8)—C(9)—C(10)	114.8 (4)	C(8')—C(9')—C(10')	109.4 (3)
N(2)—C(10)—C(9)	179.0 (6)	N(2')—C(10')—C(9')	177.3 (5)
C(8)—C(11)—C(12)	108.4 (3)	C(8')—C(11')—C(12')	108.0 (3)
C(11)—C(12)—C(13)	121.0 (4)	C(11')—C(12')—C(13')	122.7 (4)
C(11)—C(12)—C(14)	131.4 (4)	C(11')—C(12')—C(14')	130.0 (4)
C(13)—C(12)—C(14)	107.5 (4)	C(13')—C(12')—C(14')	107.3 (4)

Table 3 (*cont.*)

N(3)—C(13)—C(6)	123.1 (4)	N(3')—C(13')—C(6')	123.6 (3)
N(3)—C(13)—C(12)	110.0 (4)	N(3')—C(13')—C(12')	110.9 (3)
C(6)—C(13)—C(12)	126.7 (4)	C(6')—C(13')—C(12')	125.6 (4)
C(12)—C(14)—C(15)	106.4 (4)	C(12')—C(14')—C(15')	106.8 (4)
C(12)—C(14)—C(16)	134.3 (4)	C(12')—C(14')—C(16')	135.3 (4)
C(15)—C(14)—C(16)	119.3 (4)	C(15')—C(14')—C(16')	118.0 (4)
N(3)—C(15)—C(14)	108.6 (4)	N(3')—C(15')—C(14')	107.3 (3)
N(3)—C(15)—C(19)	129.1 (4)	N(3')—C(15')—C(19')	129.6 (4)
C(14)—C(15)—C(19)	122.3 (4)	C(14')—C(15')—C(19')	123.1 (4)
C(14)—C(16)—C(17)	118.5 (4)	C(14')—C(16')—C(17')	119.4 (4)
C(16)—C(17)—C(18)	122.0 (5)	C(16')—C(17')—C(18')	121.0 (5)
C(17)—C(18)—C(19)	121.0 (5)	C(17')—C(18')—C(19')	121.8 (5)
C(15)—C(19)—C(18)	116.9 (4)	C(15')—C(19')—C(18')	116.7 (4)

molecular conformation may help in the prediction of the steric course of subsequent reactions. The two independent molecules are approximately related by an inversion centre, the main difference being the relative conformation of the nitrile and methyl groups. Superposition of the ring core of the two molecules gives a root-mean-square deviation between equivalent atoms of 0.11 Å (Kabsch, 1976).

This work received partial support from CNPq, FAPESP, CAPES and FINEP, which are hereby gratefully acknowledged.

References

BRAGA, R. M. (1989). PhD thesis. Unicamp, Campinas, Brazil

CROMER, D. T. & LIBERMAN, D. (1970). *J. Chem. Phys.* **53**, 1891–1898.

CROMER, D. T. & MANN, J. B. (1968). *Acta Cryst.* A**24**, 321–324.

JOHNSON, C. K. (1965). *ORTEP*. Report ORNL-3794. Oak Ridge National Laboratory, Tennessee, USA.

KABSCH, W. (1976). *Acta Cryst.* A**32**, 922–923.

SHELDRICK, G. M. (1976). *SHELX76*. Program for crystal structure determination. Univ. of Cambridge, England.

STEWART, R. F., DAVIDSON, E. R. & SIMPSON, W. T. (1965). *J. Chem. Phys.* **42**, 3175–3187.

Acta Cryst. (1992). C**48**, 955–957

Structure of Di-*O*-methylscandenin: a Complex 4-Hydroxy-3-phenylcoumarin Derivative

BY SAFIA MEHDI AND K. RAVIKUMAR

Laboratory of Crystallography, Indian Institute of Chemical Technology, Hyderabad-500 007, India

(*Received* 23 *July* 1991; *accepted* 14 *October* 1991)

Abstract. 4,5-Dimethoxy-3-(4-methoxyphenyl)-8,8-dimethyl-6-(3-methyl-2-butenyl)-2*H*,8*H*-benzo[1,2-*b*:3,4-*b*']dipyran-2-one, $C_{28}H_{30}O_6$, $M_r = 462.54$, monoclinic, $P2_1/c$, $a = 11.728$ (3), $b = 8.956$ (3), $c = 24.262$ (8) Å, $\beta = 103.98$ (1)°, $V = 2473$ (1) Å^3, $Z = 4$, D_m(flotation) = 1.239 (5), $D_x = 1.242$ g cm^{-3}, Mo $K\alpha$ radiation, $\lambda = 0.71069$ Å, $\mu = 0.809$ cm^{-1}, $F(000) = 984$, $T = 294$ K, final $R = 0.079$ for 1197 reflections [$I \geq 3\sigma(I)$]. The coumarin ring system is nearly planar. The phenyl ring attached to this system is also planar and the dihedral angle between the phenyl and coumarin rings is 47.5 (3)°. The mean plane of the isoprenyl side chain makes an angle of 79.5 (4)° with the mean plane of the coumarin ring system. The angularly fused pyran ring is in a half-chair conformation.

0108-2701/92/050955-03$06.00

© 1992 International Union of Crystallography

Synthesis, Characterization and Crystal Structure of the $UO_6N_2C_{20}H_{22}.2H_2O$ Complex.

O. Signorini, E.R. Dockal*, G. Castellano and G. Oliva* Departamento de Química, Universidade Federal de São Carlos, Caixa Postal 676, 13560, São Carlos, SP, Brazil and Instituto de Física e Química de São Carlos, Universidade de São Paulo, Caixa Postal 369, 13560, São Carlos, SP, Brazil.

Abstract

The complex $[UO_2(3\text{-EtOSalen})(H_2O)].H_2O$, where (3-EtOSalen) $\bar{2}$ N,N'--Ethylenebis(3-ethoxysalicylidieniminato), $C_{20}O_4H_{22}$, was synthesized and crystallized in space group $P\bar{1}$, with a=10.250(2), b=10.274(2), c=10.829(3) Å, α=91.66(2), β=102.18(1), γ=94.48(2)°, V=1110.2(4)Å^3 and Z=2. The structure was solved from 3562 independent reflections with $I>3\sigma(I)$ by Patterson and difference Fourier techniques and refined to R=0.022. The UO_2^{2+} ion is coordinated to two nitrogen and two oxygen atoms of the ligand, with a water molecule completing the seven-coordinate, pentagonal-bipryamidal geometry. Another water molecule completes the crystal structure and is involved in several intra-and intermolecular hydrogen bonds. In the infrared spectrum three bands appearing at 3318, 3444 and 3584 cm^{-1} are assigned as O-H stetching frequencies of the water of crystallization and the coordenated water respectively. Four bands at 455, 396, 341 and 267 nm are observed for the complex in acetonitrile. The weak band at 455 nm is assigned to the $^1E^* \longrightarrow {}^2\pi\mu$ transition.

Introduction

The Shiff base ligands obtained by condensation of diamines with substituted salicylaldehydes are a class of ligands widely studied [1-14]. Most studies are focused on complexes of the d-block elements especially

*Authors to whom correspondence should be addressed.

SYNTHESIS, CHARACTERIZATION AND MOLECULAR STRUCTURE OF THE $VO_5N_2C_{20}\cdot H_2O$ COMPLEX

J.R. Zamian, E.R. Dockal*, G. Castellano and G. Oliva* Departamento de Química, Universidade Federal de São Carlos, Caixa Postal 676, 13560 São Carlos, SP, Brazil and Instituto de Física e Química de São Carlos, Universidade de São Paulo, Caixa Postal 369, 13560 São Carlos, SP, Brazil.

Abstract

The complex $VO_5N_2C_{20}H_{22}H_2O$, MW=439.36, was synthesized and crystallized in the monoclinic space group $P2_1/c$, with a=9.423(1), b=17.005(4), c=12.773(2)Å, β=98.23(1)°, V=2026(1)Å^3, z=4, D_x=1.441 g cm^{-3}, λ (MoKα)=0.71073Å, μ=4.77cm^{-1}, F(000)=916, T=298K. The structure was solved from 2566 independent reflections with $I>3\sigma(I)$ by Patterson and difference Fourier techniques and refined to a final R=0.039. The coordination around the V atom is in the form of a squared base pyramid, with the base formed by two nitrogen and two oxygen atoms of the ligand, and the vanadyl oxygen at the apical position. A crystallization water molecule, strongly hydrogen bonded to two independent pairs of ligand oxygen atoms completes the structure. In the infrared spectrum two sharp bands appearing at 3524 and 3577 cm^{-1} are assigned as O-H stretching frequencies of the water of crystallization. The Gaussian analysis of the visible spectrum of the complex yields four peaks assigned as the four d-d transitions.

Introduction

The most important V(IV) compounds are those containing the VO^{2+} unit. Numerous complexes of oxovanadium (IV) ion, vanadyl ion, have been prepared and studied. Almost all compounds contaning the VO^{2+} unit are blue or green and have a strong V=O stretching band in the ir in the range 950 to

*Authors to whom correspondence should be addressed.